Biomechanics of bone transport: *in vivo*, *ex vivo* and numerical characterization

A dissertation presented by

Juan Mora Macías

Advisors:

PhD Jaime Domínguez Abascal

and

PhD Esther Reina Romo

UNIVERSITY OF SEVILLE, 2016

Esta Tesis se presenta como un compendio de artículos previamente publicados para optar al título de Doctor por la Universidad de Sevilla.

Los artículos que forman parte de la Tesis y que han sido publicados son los siguientes:

- J Mora-Macías, E Reina-Romo, J Morgaz and J Domínguez. *In vivo* gait analysis during bone transport. *Annals of Biomedical Engineering*, 43(9):2090-100, 2015 (capítulo 9).
- J Mora-Macías, E Reina-Romo and J Domínguez. Distraction osteogenesis device to estimate the axial stiffness of the callus *in vivo*. *Medical Engineering & Physics*, 37(10):969-78, 2015 (capítulo 4).
- J Mora-Macías, E Reina-Romo, M López-Pliego, MA Giráldez-Sánchez and J Domínguez. *In vivo* mechanical characterization of the distraction callus during bone consolidation. *Annals of Biomedical Engineering*, 43(11):2663-74, 2015 (capítulo 6).
- J Mora-Macías, E Reina-Romo and J Domínguez. Model of the distraction callus tissue behavior during bone transport based in experiments *in vivo*. *Journal of the Mechanical Behavior of Biomedical Materials*, 15(61):419-430, 2016 (capítulo 5).

Además de los artículos anteriores hay tres artículos que, aunque todavía no han sido publicados, también son parte importante de la Tesis:

- J Mora-Macías, A Pajares, P Miranda, J Domínguez and E Reina-Romo. Spatial and temporal variations of the mechanical properties of the woven bone during bone transport (capítulo 7).
- J Mora-Macías, M López, J Domínguez and E Reina-Romo. Finite element versus experimental mechanical characterization of the distraction callus (capítulo 8).
- J Mora-Macías, A Pajares, P Miranda, J Domínguez and E Reina-Romo. Time-dependence of nanoscale mechanical properties of cortical and woven bone (Apéndice A).

A mis padres

Acknowledgements

Esta Tesis se ha desarrollado en el departamento de Ingeniería Mecánica y de Fabricación de la Universidad de Sevilla durante el periodo 2011-2016. Su desarrollo ha sido posible gracias a la financiación del programa de Formación de Profesorado Universitario del Ministerio de Educación, Cultura y Deporte (AP2010-5061) y de la Consejería de Innovación, Ciencia y Empresa de la Junta de Andalucía (P09-TEP-5195). En menor medida, también contribuyeron a la financiación de esta Tesis el Ministerio de Economía y Competitividad (DPI2014-58233-P), el 7º Programa Marco de la Unión Europea (FP7/2007-2013, beca nº 604036) y fondos FEDER del Gobierno de Extremadura (IB13007).

Sin todas las personas que han contribuido directa o indirectamente hubiera sido imposible realizar este trabajo. Quisiera agradecerles todo el apoyo prestado y el tiempo que les he robado, tanto en lo profesional como en lo personal.

En primer lugar, a mis directores de Tesis, Jaime y Esther, les agradezco sus consejos, la atención y el rigor en el seguimiento de esta Tesis. Agradezco a Jaime que desde que comencé con el proyecto fin de carrera haya creído en mis posibilidades. Valoro mucho lo que he aprendido de él en todos los aspectos, desde cualquier concepto de ingeniería hasta la forma de entender y abordar diferentes situaciones de la vida. Gracias a Esther, por su total disposición, colaboración y cercanía. Has sabido ser amiga y al mismo tiempo analizar con ojo crítico el trabajo, nada fácil.

A Miguel Ángel y Macarena les agradezco su trabajo, su buen hacer y el esfuerzo que han estado realizando durante el proyecto para sacar tiempo de su complicada agenda en el hospital. Esta Tesis ha supuesto casi 50.000 km de viaje y muchos los he compartido con ellos, especialmente con Macarena. Gracias por tu amistad y por mantener el buen humor durante tantas horas.

Gracias a todo el Departamento de Medicina y Cirugía Animal de la Facultad de Veterinaria de Córdoba por su buena disposición y colaboración con el proyecto. Quisiera agradecer especialmente a Juan Morgaz y Sergio Ventura el gran trabajo y sacrificio que realizaron en el cuidado de los animales.

A Antonia Pajares por su amabilidad, el buen trato que siempre mostró y por poner a nuestra disposición su trabajo y los equipos del departamento de Ingeniería Mecánica, Energética y Materiales de la Universidad de Extremadura. A Pedro Miranda, por su implicación junto con Antonia en los ensayos. Gracias también a Consuelo Cerrillos, que también estuvo dispuesta a ayudar y a sacrificarse por este trabajo.

Furthermore, I would like to express my gratitude to Dr Sandra Shefelbine, who let me take part of her Lab in the Northeastern University in Boston during three months. It was a reward-

ing internship during which I had the chance of learn a lot thanks also to the collaboration of all the people of the lab. Moreover, I acknowledge Dr Liesbet Geris the opportunity of working in her research group in the University of Liege and I regret not spending more time with them.

Muchas gracias a Manuel y a Antonio del taller de mecanizado del departamento de Ingeniería Mecánica y de Fabricación, por sus consejos y por su implicación en la fabricación de los dispositivos utilizados en esta Tesis.

También quiero agradecer el buen ambiente de trabajo del que he disfrutado estos años en el departamento de Ingeniería Mecánica y de Fabricación de la Universidad de Sevilla. Muchas gracias a todos los que lo han hecho posible. Especialmente a Jesús por iniciarme en la investigación y por tantas reflexiones de viaje. A Dani por compartir espacio, filosofía y aficiones. Y a Joselu, Javi Aceituno, Javi González, Guido y Jorge por ser amigos además de compañeros.

Durante estos años ha sido imprescindible el apoyo de mis familiares y amigos. A mis amigos les agradezco que siempre hayan estado ahí cada vez que he parado para disfrutar, pasar un buen rato y cargar las pilas para continuar con el trabajo. Mis padres me han enseñado lo que es el sacrificio y el esfuerzo, y a disfrutar de lo que uno hace. Tanto ellos como mi hermano me han apoyado en todo lo que he hecho y se lo agradeceré siempre.

Por último, estoy muy agradecido a mi mujer. Inma me ha apoyado y animado durante todos estos años, incluso acompañándome en congresos y estancias. Además, ha soportado mis quejas y ha sabido comprenderme aun cuando ni yo era capaz de hacerlo conmigo mismo. Gracias por aguantarme.

Abstract

The work carried out in this Thesis was motivated by the need of providing experimental data about distraction osteogenesis to improve and validate *in silico* models of the process. Computational models of distraction osteogenesis allow understanding the mechanobiology and improving the clinical applications of the process. In the last years, numerical models were proposed based on different hypothesis [59, 85, 140, 141, 145]. Although experimental studies which evaluated mechanical, biological or both aspects of distraction osteogenesis may be found in literature [3, 8, 11, 20, 31, 32, 49, 72, 78, 79], the differences existing in the conditions of the experiments carried out make difficult to compare among these studies and to make conclusions. Therefore, more experimental data are demanded to validate computational models and to improve the clinical applications.

The aim of this Thesis was to relate quantifiable biological parameters (the bone tissue volume and its distribution in the distraction callus, proportion of different tissue types...) with mechanical parameters (the force through the fixator and through the callus, the mechanical properties of the callus tissue during the process...) during the complete distraction osteogenesis process. *In vivo* and *ex vivo* experiments were carried out in the same specimens and conditions with the objective of providing results in multiple directions of analysis. These results can be connected and related, directly or using numerical analysis techniques which have also been developed.

Bone transport experiments were carried out in 11 sheep by an interdisciplinary team of mechanical engineers, orthopaedics surgeons and veterinarians. The experiments consisted of the implantation of the distractor in animals which followed the same distraction protocol: 7 days of latency after surgery, 15 days of distraction with a rate of 1 mm per day, the consolidation phase until the distraction callus was completely ossified and the remodeling phase. Different mechanical parameters were monitored *in vivo* by means of the instrumentation of the fixator. Each animal was sacrificed at different time points (17, 22, 29, 35, 37, 51, 79, 98, 161 and 525 days after surgery) to obtain samples for *ex vivo* experiments along the process.

The distractor used was designed, calibrated and tested in preliminary *in vivo* experiments. This distractor allowed measuring callus stiffness *in vivo* during the experiments at any time under real load conditions during the distraction and consolidation phases of the bone transport process. *In vivo* measurements during the distraction phase provided the force relaxation of the callus tissue and the contribution of the callus traction and the docking-site compression to the distraction force. In addition, an experimental band was provided for the residual force value after each step of distraction from models of mechanical behavior of the callus tissue. During the consolidation phase, the callus stiffness, the force through the callus and the volume of the

callus were monitored. The period of maximum ossification took place from 20 to 70 days after surgery, where the maximum bone tissue production rate was achieved and the volume of the woven bone within the callus increased from zero to 80% of its maximum value (see Chapter 6). This period also coincided with the recovery of load sustained by the intervened limb (from 3 to 12% to 60 to 70%). However, this period of maximum ossification corresponded to low callus stiffness, which increased exponentially from the end of the distraction phase but did not achieved values above 10% of stiffness in healthy conditions. The ground reaction force was also monitored during gait along the complete process. Gait parameters were obtained from these measurements (peak force, mean force and impulse) and showed a decrease in the intervened limb and, most significantly, increases in the other limbs due to the intervention. During the consolidation, these gait parameter were approaching the normal values of healthy animals.

Nanoindentation experiments were carried out in the harvested samples completely ossified to assess the spatial and temporal evolution of the elastic modulus of the woven bone tissue generated during the bone transport process. The outcomes showed that the mean elastic modulus of the woven bone generated during the bone transport process in the distraction and the docking-site calluses increases with time (from 7 GPa, 35 days after surgery, to 14 GPa, 525 days after surgery approximately, which is 77% of the mean elastic modulus of the cortical bone). This increase was slower with time (0.5 GPa per week during the first week of consolidation to 0.05 GPa per week approximately from 161 days after surgery). Woven bone generated during the bone transport process presented lower increments of elastic modulus with time than values reported for fracture healing cases [109]. The period of time needed in fracture healing to reach 95% of the mean elastic modulus value of cortical bone is approximately 20% relative to the same magnitude in bone transport. Before these experiments were carried out, the elastic modulus and the hardness were measured in the same sample during 60 days to ensure that the duration of the experiments do not affect the mechanical properties of each sample. It was found that bone and woven bone elastic modulus and hardness do not present significant trends of variation during this period of time.

Finally, a numerical analysis of the experimental results was also carried out. It consisted of a finite element analysis based on the computed tomographies for predicting the stiffness of the distraction callus. Two methods were used to assign the mechanical properties: manual segmentation and segmentation according to the level of Hounsfield Units. Results using the level of Hounsfield Units to assign the mechanical properties showed more accurate results than using manual segmentation. The method predicted an increase of the distraction callus stiffness from 0.1 - 0.2 to 140 - 150 kN/mm (in the order of stiffness of the healthy metatarsus) after 250 days from bone transport surgery approximately.

Keywords: Distraction osteogenesis, bone transport, distractor, woven bone, nanoindentation, elastic modulus, callus stiffness, residual forces, gait analysis, finite element analysis.

Contents

Main abbreviations

BT	Bone transport
BL	Bone lengthening
BW	Body weight of animals
CT	Computerized tomography
C1$\cdots$C6	Load cell measurements
DO	Distraction osteogenesis
e	Relative error during the calibration of the distractor measurements
E_r	Reduced elastic modulus
f_a	Force through the distraction callus
f_b	Force through the docking-site
f_c	Force through the fixator (proximal Schanz screws)
f_d	Force through the fixator (distal Schanz screws)
f_h	Force through the Steinmann pins ($f_h = F$)
f_i	Force through the fixator (superior part of mobile bars)
f_j	Force through the fixator (inferior part of mobile bars)
f_l	Force through the fixator (guide bars)
F	Distraction force ($F = f_h$)
F_1	Axial force applied to the bone where the fixator is implanted
Fig	Figure
GRF	Ground reaction force
HU	Hounsfield Units
K_a	Axial stiffness of the distraction callus
K_b	Axial stiffness of the docking-site
K_c	Axial stiffness of the fixator (proximal Schanz screws)
K_d	Axial stiffness of the fixator (distal Schanz screws)
K_h	Axial stiffness of the Steinmann pins
K_i	Axial stiffness of the fixator (superior part of mobile bars)
K_j	Axial stiffness of the fixator (inferior part of mobile bars)
K_l	Axial stiffness of the fixator (guide bars)
p	Probability of no correlation of fits
R^2	Coefficient of determination of fits
U	Uncertainty during the calibration of the distractor measurements

Chapter 0

Resumen

Este capítulo es un resumen en castellano del contenido de la Tesis. En él se especifica la motivación de la misma, los objetivos y la estructura. También se incluyen los principales resultados que se han obtenido, así como la discusión y las principales conclusiones a las que dieron lugar. Además, se proponen algunas líneas futuras de investigación. Finalmente, se ofrece un listado de las principales contribuciones aportadas durante el desarrollo de la Tesis.

0.1 Motivación

La distracción osteogénica consiste en la generación de nuevo tejido óseo mediante la separación gradual de dos segmentos óseos a partir de una osteotomía inicial. Desde que la distracción osteogénica fue introducida por Ilizarov [76, 78, 79], la técnica ha sido aplicada tanto en huesos largos como en huesos planos. Algunas de las aplicaciones más importantes son: alargamiento de extremidades, [78, 79, 155] (Fig. 1), tratamiento de no uniones en fracturas, [25, 82, 83, 131], reconstrucción de pies [37, 60, 130], alargamiento y modificación de la forma de las mandíbulas [156], distracción de los huesos de la cara [44], distracción craneal [14, 106, 156] y tratamiento de defectos óseos en general. Esta última aplicación recibe el nombre de transporte óseo. El transporte óseo se usa frecuentemente en el tratamiento de defectos óseos en huesos largos mediante el desplazamiento de un segmento de hueso (segmento de transporte) relativo a los extremos de un hueso original. La separación del segmento de transporte con respecto a uno de los extremos del hueso original genera un callo de distracción a uno de los lados del segmento de transporte. Por el otro lado, la unión progresiva de éste con el otro extremo del hueso original, va rellenando el defecto inicial [20, 31, 72, 76, 131].

Hoy en día la distracción osteogénica se aplica en numerosos hospitales en todo el mundo. Por ejemplo, el equipo de reconstrucción de extremidades del Oxford University Hospital (Reino Unido) trata alrededor de 2000 pacientes al año y lleva a cabo 4 o 5 intervenciones con fijadores tipo Ilizarov semanalmente [70]. Se diagnostican hasta 100000 personas cada año en Estados Unidos con problemas de longitud de sus extremidades y se llevan a cabo unas 500 cirugías de alargamiento de extremidades anualmente en el Sinai Hospital, en Baltimore (Estados Unidos) [48]. Además, actualmente, la distracción osteogénica no solo se utiliza para abordar problemas de salud. Más de 30 hospitales privados en el mundo ofrecen tratamientos

de alargamiento de extremidades por motivos estéticos [71]. El alargamiento de extremidades por motivos estéticos se está convirtiendo en una importante actividad económica que puede reportar entre 10000 y 150000 dólares por cirugía o tratamiento [71].

El crecimiento del tejido óseo en un callo de distracción depende del ambiente mecánico [95, 150]. Se ha sugerido en diferentes trabajos [22, 23, 135, 136] que uno de los factores que influyen en la diferenciación del tejido granular a hueso maduro en una fractura es el estado de deformación del callo. Por lo tanto, en las últimas décadas, la distracción osteogénica ha sido estudiada por equipos interdisciplinares formados principalmente por médicos e ingenieros. Estos han llevado a cabo trabajos experimentales y computacionales con el objetivo de entender la mecanobiología del callo de distracción y mejorar las técnicas de aplicación de la distracción osteogénica. Algunos trabajos experimentales han utilizado fijadores instrumentados para tratar de obtener la evolución de algunos parámetros mecánicos (fuerza a través del callo, rigidez, movimientos interfragmentarios...) del proceso de distracción *in vivo* [4, 8, 20, 31, 43, 46, 55, 177]. Otros experimentos *ex vivo* evaluaron las propiedades mecánicas del callo [47, 123]. Los trabajos llevados a cabo también proporcionaron datos de tipo médico o biológico como histologías o radiografías [7, 9, 11, 38, 49, 78, 79, 92, 124]. Posteriormente, el desarrollo de las técnicas computacionales ha permitido a los ingenieros crear modelos numéricos del proceso de distracción osteogénica que han incluido diferentes teorías de diferenciación de los tejidos dependiendo del ambiente mecánico en el callo [15–17, 85, 140–145].

Sin embargo, aunque la técnica de distracción osteogénica es cada día más demandada y algunos estudios han sido publicados en este campo, actualmente, los cirujanos disponen de escasa información y protocolos de actuación. La mayoría de los cirujanos son autodidactas y las complicaciones durante las aplicaciones clínicas son todavía considerables [67, 170, 171] debido a diferentes razones. En primer lugar, los mecanismos mecanobiológicos que rigen la producción de tejido óseo y la osificación durante el proceso no son del todo conocidos. Por ejemplo, no existe consenso en la literatura sobre la diferenciación de los tejidos durante la distracción osteogénica. Algunos autores encontraron que la osificación intramembranosa es predominante en el callo de distracción [9, 39, 50, 51, 78, 79, 158, 160], mientras que otros demostraron la prevalencia de la osificación endocondral [92, 173, 178] o la presencia de ambos tipos de osificación [49] y, por lo tanto, la presencia de cartílago. En segundo lugar, la amplia variedad de trabajos experimentales hace difícil establecer comparaciones entre ellos y llegar a conclusiones. El proceso de distracción osteogénica tiene múltiples aplicaciones y puede ser llevado a cabo en diferentes huesos. Los resultados también dependen de la especie animal utilizada. Por ejemplo, la osificación es más rápida en pequeños animales como ratas o conejos [11, 148] que en cerdos u ovejas [20, 31], para los que el tiempo de osificación y las condiciones de carga en el callo de distracción son más parecidas a las que se dan en los humanos. Finalmente, hasta donde el autor conoce, ningún estudio ha relacionado resultados de trabajos *in vivo*, *ex vivo* y computacionales sobre un mismo espécimen. Los resultados de estudios *ex vivo* y computacionales son limitados ya que es complicado reproducir en estos trabajos las condiciones de carga reales. Además, con frecuencia los modelos computacionales se basan en parámetros mecánicos o proporcionan resultados no validados con estudios experimentales que reproduzcan las mismas condiciones. Sin embargo, las técnicas computacionales y *ex vivo* pueden proporcionar resultados que no son posibles de obtener *in vivo* y que son

complementarios entre ellos para condiciones similares.

Por lo tanto, la principal motivación de esta Tesis es llevar a cabo un estudio múltiple, que permita obtener, durante el proceso de distracción osteogénica y usando un mismo experimento animal: parámetros mecánicos *in vivo* (fuerza a través del callo de distracción, rigidez...), propiedades mecánicas locales del callo *ex vivo* (módulo elástico y dureza) y aspectos biológicos cuantificables (volumen del callo, tasa de producción de tejido óseo...). Los resultados obtenidos son también analizados mediante técnicas computacionales para obtener medidas *in silico* de los diferentes parámetros del modelo. Esto permite aumentar el conocimiento de la biomecánica del proceso de distracción osteogénica y mejorar las técnicas de aplicación en la práctica clínica.

Figura 1: Paciente durante la aplicación de la distracción osteogénica en alargamiento de extremidades, antes del tratamiento (izquierda) y después (derecha) [155].

0.2 Objetivos

El objetivo general de esta Tesis es cuantificar y relacionar, durante el proceso de distracción osteogénica, parámetros biológicos (el volumen de hueso y su distribución en el callo, la pro-

porción de los diferentes tipos de tejidos...) con parámetros mecánicos (fuerza a través del fijador, propiedades mecánicas de los tejidos del callo...). Se han llevado a cabo experimentos *in vivo* y *ex vivo* en los mismos especímenes y condiciones con el objetivo de proporcionar resultados en múltiples direcciones de análisis para ser conectados y relacionados entre ellos directamente o indirectamente, utilizando técnicas de análisis numérico. A continuación, se detallan los objetivos específicos de la Tesis:

- Proporcionar un nuevo dispositivo calibrado y probado en experimentos preliminares *in vivo* que permita medir la fuerza a través del callo y la rigidez del mismo *in vivo* en cualquier instante, bajo condiciones de carga reales, durante las fases de distracción y consolidación del proceso de transporte óseo. El dispositivo se diseñó para ser utilizado en experimentos de transporte óseo con ovejas y estudiar las propiedades mecánicas del callo de distracción. Podría ser usado en casos diferentes con algunas adaptaciones.

- Mejorar los datos experimentales de monitorización de fuerzas durante la fase de distracción en huesos largos. Se registraron medidas continuas de las fuerzas de relajación después del desplazamiento del segmento de transporte, mediante experimentos de transporte óseo y no elongación de extremidades, para minimizar los efectos de los tejidos blandos colindantes y de las fuerzas musculares sobre las medidas de fuerza a través del callo. Además, ajustando los datos experimentales, se proporcionó un modelo experimental del comportamiento mecánico del tejido del callo después de cada paso de distracción.

- Cuantificar y relacionar los siguientes parámetros durante el proceso de transporte óseo completo: el volumen de tejido óseo y su distribución en el callo de distracción, la tasa de producción de nuevo tejido óseo, la fuerza que actúa sobre el callo de distracción y sobre el fijador durante la marcha, y la rigidez del callo durante la fase de consolidación.

- Evaluar las variaciones espaciales y temporales de las propiedades mecánicas del tejido óseo inmaduro en el callo de distracción durante el proceso de transporte óseo. Se utiliza la técnica de nanoindentación que proporciona localmente el módulo elástico y la dureza del tejido óseo.

- Analizar cuantitativamente la relación entre los estados de osificación del callo de distracción durante el transporte óseo y las variaciones en las condiciones de marcha. Se trata de estudiar la posibilidad de usar el análisis de marcha como un método para evaluar el estado del proceso de distracción osteogénica.

- Llevar a cabo un análisis computacional para obtener una estimación de la rigidez del callo y de la distribución de los tejidos del callo con el tiempo. Este análisis computacional utiliza los datos experimentales anteriores que proporcionan la variación espacio-temporal de las propiedades mecánicas del tejido óseo del callo así como su geometría.

0.3 Estructura de la Tesis

Durante esta tesis se llevaron a cabo experimentos de transporte óseo en animales. Un equipo interdisciplinar se encargó de la planificación y realización de estos experimentos. El equipo lo formaban ingenieros del departamento de Ingeniería Mecánica de la Universidad de Sevilla, traumatólogos del Hospital Virgen del Rocío de Sevilla y veterinarios del Hospital Clínico Veterinario de Córdoba. La Tesis integra los trabajos de ingeniería realizados durante los experimentos (diseño y calibración de dispositivos, monitorización de fuerzas, etc) así como el análisis de los resultados que se basan en aspectos mecánicos del proceso (relajación de fuerzas en los tejidos del callo, evolución de la rigidez y el volumen del callo, variación espacio temporal de las propiedades mecánicas del tejido óseo inmaduro, análisis de marcha, etc). La mayoría de estos resultados han sido publicados o enviados para su publicación en diferentes revistas internacionales (ver la sección 0.9) y la mayoría de los capítulos de esta Tesis están basados en estos artículos como se detalla a continuación:

El capítulo 2 introduce el proceso de distracción osteogénica: en qué consiste el proceso, las diferentes fases del mismo, los mecanismos que rigen el crecimiento del callo de distracción, etc. También se tratan las diferentes aplicaciones del proceso de distracción osteogénica, especialmente la de transporte óseo ya que fue la técnica aplicada en los experimentos llevados a cabo en esta Tesis. Además, el capítulo 2 incluye el estado del arte de la investigación en distracción osteogénica, presentando los principales hallazgos sobre aspectos biológicos y mecánicos de la distracción osteogénica desde que la técnica fue introducida por Ilizarov [77–79].

En el capítulo 3se describen los experimentos de transporte óseo que se han realizado en animales. En este capítulo se explican la selección de animales, la cirugía y el protocolo de transporte óseo utilizado. Además, el capítulo 3 explica cómo fueron realizadas las medidas de los diferentes parámetros mecánicos *in vivo* y *ex vivo*. Por último, en este capítulo también se detalla el procedimiento de recolección de muestras para los experimentos *ex vivo* así como los diferentes instantes analizados para cada prueba a lo largo del proceso.

El capítulo 4 incluye el diseño del distractor. Además, en este capítulo se describe la instrumentación del fijador y el sistema de adquisición de datos utilizados para monitorizar la fuerza a través del callo y la rigidez del mismo. Por otro lado, se detalla el proceso de calibración del sistema y las medidas preliminares de fuerza y rigidez del callo. Este capítulo está basado en un artículo ya publicado [113]: **J Mora-Macías, E Reina-Romo, and J Domínguez. Distraction osteogenesis device to estimate the axial stiffness of the callus *in vivo*. *Medical Engineering & Physics*, 37(10):969-78, 2015**.

El capítulo 5 analiza las medidas *in vivo* de la fuerza de relajación de los tejidos del callo durante la fase de distracción. En este artículo se proporciona la contribución de la tracción sobre los tejidos del callo y la compresión del docking-site a la fuerza total de distracción. Se proponen dos modelos diferentes de comportamiento mecánico del callo que ofrecen una banda experimental para las fuerzas residuales después de cada paso de distracción. Estos resultados se incluyen en un artículo publicado [114]: **J Mora-Macías, E Reina-Romo and J Domínguez. Model of the distraction callus tissue behavior during bone transport based in experiments *in vivo*. *Journal of the Mechanical Behavior of Biomedical Materials*, 15(61):419-430, 2016**.

El capítulo 6 trata sobre la evolución durante la fase de consolidación de la fuerza a través del callo, la rigidez del callo y el volumen de tejido óseo en el callo. Estos datos fueron obtenidos a partir de la monitorización *in vivo* y las tomografías computarizadas. Los resultados de este capítulo relacionan aspectos biológicos (volumen del callo y tasa de producción de tejido óseo) con parámetros mecánicos (fuerza y rigidez del callo) del proceso de distracción osteogénica. Estos resultados, los métodos utilizados para obtenerlos así como la discusión de los mismos han sido publicados [115]: **J Mora-Macías, E Reina-Romo, M López-Pliego, MA Giráldez-Sánchez and J Domínguez. *In vivo* mechanical characterization of the distraction callus during bone consolidation. *Annals of Biomedical Engineering*, 43(11):2663-74, 2015**.

El capítulo 7 contiene los experimentos de nanoindentación llevados a cabo en muestras *ex vivo* para la caracterización de las propiedades mecánicas del tejido óseo inmaduro formado durante el proceso de transporte óseo. Se realizaron medidas de nanoindentación sobre muestras de tejido óseo inmaduro obtenidas en diferentes estadios del experimento de transporte óseo. Se mostraron las variaciones espacio temporales de módulo elástico y se compararon con la evolución temporal de otros parámetros mecánicos evaluados en capítulos anteriores como la rigidez o volumen del callo. Este capítulo está basado en un artículo enviado para publicación: **J Mora-Macías, A Pajares, P Miranda, J Domínguez and E Reina-Romo. Spatial and temporal variations of the mechanical properties of the woven bone during bone transport**.

El capítulo 8 presenta un método para evaluar la rigidez del callo de distracción mediante técnicas numéricas[161]. Este método consiste en un análisis usando un modelo de elementos finitos basado en tomografías computarizadas. Se compararon los resultados de dos enfoques diferentes para la asignación de las propiedades mecánicas de los tejidos del callo: segmentación manual o basada en el nivel de Hounsfield Units. Los contenidos de este capítulo están también incluidos en un artículo enviado para publicación: **J Mora-Macías, M López, J Domínguez and E Reina-Romo. Finite element versus experimental mechanical characterization of the distraction callus**.

En el capítulo 9 se analiza la evolución de las condiciones de marcha durante el proceso de transporte óseo mediante la medida de las fuerzas de reacción sobre el suelo desde el momento de la cirugía hasta más de un año después. Como aproximación preliminar que debe ser confirmada con más experimentos, los resultados mostraron que el análisis de las condiciones de marcha podría ser utilizado como un método alternativo para controlar los procesos de distracción osteogénica o fractura ósea. Estos resultados han sido publicados [116]: **J Mora-Macías, E Reina-Romo, J Morgaz and J Domínguez. *In vivo* gait analysis during bone transport. *Annals of Biomedical Engineering*, 43(9):2090-100, 2015**.

Las principales conclusiones de esta Tesis, junto a un breve resumen the las principales contribuciones realizadas por este trabajo y las líneas de investigación futuras se incluyen en el capítulo 10, así como en las siguientes secciones del presente capítulo en castellano.

Al final de la Tesis, se ha incluido un apéndice que añade información sobre los métodos utilizados en las medidas de nanoindentación del capítulo 7. Este apéndice A trata sobre la variación temporal de las medidas de módulo elástico en la misma muestra de hueso cortical o tejido óseo inmaduro. Los resultados incluidos en este apéndice han sido enviados para publicación: **J Mora-Macías, A Pajares, P Miranda, J Domínguez and E Reina-Romo.**

Time-dependence of nanoscale mechanical properties of cortical and woven bone.

0.4 Resumen de los principales resultados

Durante esta Tesis se ha llevado a cabo un experimento de transporte óseo en 11 ovejas por un equipo interdisciplinar de ingenieros, médicos y veterinarios. Estos experimentos consistieron en la implantación de un distractor en el metatarso de los animales, que siguieron un mismo protocolo de distracción: 7 días de latencia después de la cirugía, 15 días de distracción a razón de 1 mm por día, la fase de consolidación, hasta que el callo de distracción se osificó completamente, y la fase de remodelación.

Antes de realizar los experimentos, se diseñó un distractor instrumentado, se calibró y se probó en experimentos preliminares *in vivo*. Este equipo permitió medir la rigidez del callo, la fuerza a través del fijador y del callo *in vivo*, en diferentes momentos, bajo condiciones de carga reales, durante las fases de distracción y consolidación del proceso de transporte óseo (ver capítulo 4).

Las mediciones de fuerza *in vivo* durante la fase de distracción, proporcionaron la relajación diaria de los tejidos del callo durante el proceso. Se observó que la contribución de la compresión del docking site a la fuerza total de distracción es despreciable frente a la tracción ejercida sobre el callo. Se obtuvieron dos modelos experimentales para predecir la fuerza de relajación de los tejidos del callo después de aplicar 1 mm de desplazamiento: uno asumiendo la hipótesis de que la relajación de los tejidos era total y otro asumiendo la existencia de unas fuerzas residuales después de cada día de distracción. Estos modelos proporcionaron una cota experimental de las fuerzas durante la fase de distracción. A modo de ejemplo, las fuerzas pico, alcanzadas justo después de distraer se incrementan desde 7 - 34 N, el primer día de distracción, hasta 41 - 246 N, después de 15 días de distracción; y las fuerzas residuales están por debajo de 72 N, que es el máximo que pueden alcanzar el día 15 de distracción (ver capítulo 5).

Durante la fase de consolidación, se observó que el periodo de máxima osificación tiene lugar entre 20 y 70 días después de la cirugía (50 primeros días de consolidación). En este intervalo se alcanza el valor máximo de producción de tejido óseo inmaduro en el callo y se produce el mayor incremento de volumen de tejido óseo, pasando desde prácticamente cero al inicio de la consolidación, hasta el 80% del valor máximo (ver capítulo 6). Este periodo también coincidió con la recuperación de la capacidad portante en la extremidad intervenida (desde el 3 - 12 % hasta el 60 - 70%). Sin embargo, durante este tiempo el callo tiene una rigidez baja, que aunque se comprueba que se incrementa exponencialmente durante el proceso, 70 días después de la cirugía no supera el 10% de la rigidez del hueso original.

La fuerza de reacción sobre el suelo de la extremidad intervenida fue también monitorizada. Se obtuvieron los parámetros de marcha a partir de las mediciones de fuerza de reacción durante una pisada completa (fuerza pico, fuerza media e impulso). Se comprobó que todos estos parámetros disminuyen en la extremidad intervenida y, más significativamente, se aumentan en el resto de extremidades debido a la intervención quirúrgica. Tras la cirugía se observó como estos parámetros volvían a sus valores en condiciones normales más de un año después (ver capítulo 9).

Se realizaron experimentos de nanoindentación en las muestras *ex vivo* del callo que estaban completamente osificadas, para obtener la evolución espacial y temporal del módulo elástico del tejido óseo inmaduro generado durante el transporte óseo tanto en el callo de distracción como en el docking-site. Los resultados mostraron que el módulo elástico medio del tejido óseo inmaduro aumenta con el tiempo (desde 7 GPa 35 días después de la cirugía hasta 14 GPa 525 días después de la cirugía aproximadamente, el 77% del valor del módulo elástico medio para el hueso cortical). Este incremento de módulo elástico medio fue disminuyendo a lo largo del proceso (desde 0.5 GPa por semana entre 35 y 50 días después de la cirugía, hasta 0.05 GPa por semana entre 161 y 525 días después de la cirugía). Se comprobó que el tejido óseo inmaduro generado durante el transporte óseo presenta menores incrementos de módulo elástico que el tejido óseo inmaduro generado durante la consolidación de una fractura ósea [109]. El periodo de tiempo necesario para alcanzar el 95% del valor de módulo elástico medio para el hueso cortical en fractura es aproximadamente un 20% del tiempo necesario en el caso de transporte óseo (ver capítulo 7). Antes de llevar a cabo estos experimentos, se comprobó que para muestras de hueso cortical y tejido óseo inmaduro preparadas con el mismo método de embebido y pulido, el módulo elástico medio medido mediante nanoindentación no presenta tendencias significativas de variación durante el tiempo de duración de los experimentos para cada muestra (ver anexo A).

Finalmente, se realizó un análisis numérico de los resultados experimentales que consistió en la estimación de la rigidez del callo mediante un modelo de elementos finitos basado en tomografías computarizadas. Se utilizaron dos métodos para asignar las propiedades mecánicas: segmentación manual y segmentación según el nivel de Hounsfield Units. Los resultados de rigidez del callo usando segmentación según el nivel de Hounsfield Units resultaron ser más precisos que los obtenidos mediante el uso de la segmentación manual. Se estimó un aumento de rigidez del callo desde 0.1 - 0.2 hasta 140 - 150 kN/m (del orden de rigidez de un segmento de hueso original del mismo tamaño que el callo) después de 250 días desde la cirugía de transporte óseo (ver capítulo 8).

0.5 Discusión

En esta sección se incluye una comparativa entre la evolución con el tiempo de los diferentes parámetros mecánicos evaluados durante el proceso de transporte óseo en los diferentes capítulos de esta Tesis. La figura 2 muestra la medida *in vivo* de fuerza a través del callo y de la rigidez del callo, el volumen de tejido óseo del callo, la tasa de producción de tejido óseo (ver capítulo 6), el módulo elástico medio del tejido óseo en el callo (ver capítulo 7) y la simetría de la marcha basada en el valor pico de la fuerza de reacción (ver capítulo 9). La figura 2 también representa una correlación de los valores de rigidez del callo obtenidos usando el método de elementos finitos basado en tomografías computarizadas asignando las propiedades mecánicas del tejido según el nivel de Hounsfield Units (ver capítulo 8). Todos estos parámetros han sido normalizados para facilitar la comparación.

La figura 2 muestra que la fuerza a través del callo, la rigidez del callo y el módulo elástico del tejido óseo inmaduro en el callo aumentan a diferente ritmo después de la fase de distracción y alcanzan valores normales (carga en la extremidad no intervenida, rigidez y módulo

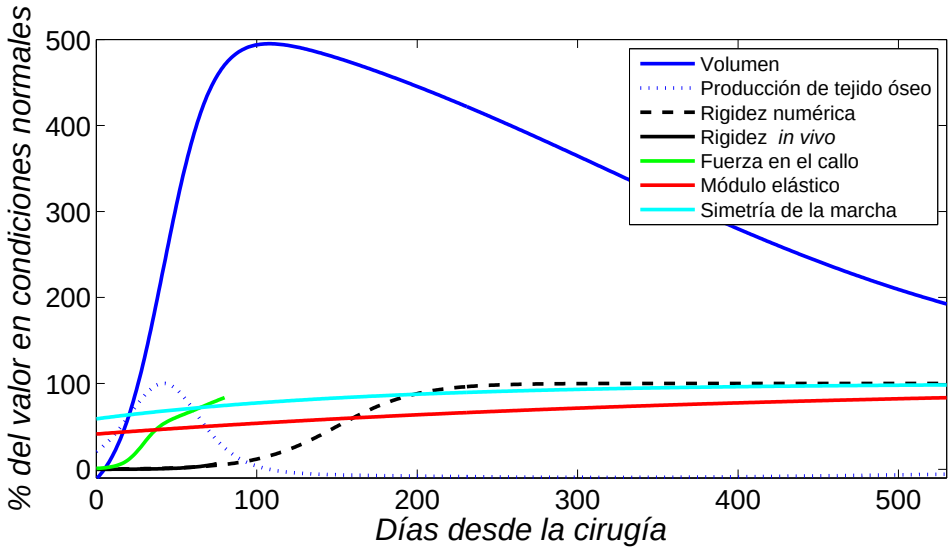

Figura 2: Evolución temporal de los valores normalizados de fuerza a través del callo, rigidez del callo (numérica e *in vivo*), volumen de tejido óseo del callo, tasa de producción de tejido óseo, módulo elástico medio del tejido óseo en el callo y simetría de la marcha basada en el valor pico de la fuerza de reacción. La fuerza fue normalizada con respecto al valor medio de la fuerza interna, que es la fuerza a través del metatarso (ver capítulo 6), es decir, la suma de fuerza a través del callo de distracción y del fijador. La rigidez axial del callo y el volumen de tejido óseo fueron normalizados con respecto a valores de un segmento del metatarso con la misma longitud (ver capítulo 6). La evolución con el tiempo del módulo elástico del tejido óseo del callo se normalizó con el módulo elástico medio del hueso cortical (18.2 GPa) (ver capítulo 7). Debido a que la tasa de producción de tejido óseo en condiciones normales es cero, los valores experimentales de producción de tejido óseo se normalizaron con respecto al valor máximo durante el proceso. Finalmente el índice de simetría de la marcha fue escalado considerando 100% como condiciones normales para ovejas sanas (ver capítulo 9). Las ecuaciones en las que se basan las curvas de esta figura, que son las normalizaciones de las mostradas en los diferentes capítulos de este trabajo, se incluyen en la tabla 1

.

elástico del hueso cortical respectivamente) después de 90, 250 y 500 días desde la cirugía respectivamente. El volumen del callo se incrementó alcanzando un valor máximo de aproximadamente 5 veces el volumen de un segmento de metatarso de la misma longitud 90 - 150 días después de la cirugía. El valor máximo de producción de tejido óseo inmaduro se alcanzó 50 días después de la cirugía. La recuperación de las condiciones de marcha se realizó de una forma más progresiva que el resto de parámetros analizados. Las condiciones de marcha alcanzaron valores cercanos a los observados en animales sanos 300 días después de la cirugía. El análisis de todos estos parámetros mecánicos simultáneamente permite obtener información adicional:

- Parece que el parámetro mecánico que está relacionado con la producción de tejido óseo

Tabla 1: Ecuaciones en las que se basan las curvas de la figura 2, que son las normalizaciones de las mostradas en los diferentes capítulos de este trabajo.

Volumen de tejido óseo del callo	$\frac{100}{1+e^{-0.065\cdot(t-42)}} - \frac{83.2}{1+e^{-0.007\cdot(t-320)}}$
Producción de tejido óseo	$\frac{416.7e^{-0.065\cdot(t-42)}}{(1+e^{-0.065\cdot(t-42)})^2} - \frac{37.0e^{-0.007\cdot(t-320)}}{(1+e^{-0.007\cdot(t-320)})^2}$
Rigidez del callo (resultados numéricos)	$\frac{100}{1+e^{-0.04\cdot(t-150)}}$
Rigidez del callo (resultados *in vivo*)	$0.054e^{0.064t}$
Fuerza a través del callo	$\frac{50}{1+e^{-0.170(t-28.99)}} + \frac{50}{1+e^{-0.062\cdot(t-68.70)}}$
Módulo elástico medio del tejido óseo inmaduro	$100 - 56.04e^{-0.0024\cdot(t-21)}$
Simetría de marcha	$100 - 41.23e^{-0.0059\cdot t}$

inmaduro durante la fase de consolidación es la fuerza a través del callo y no la rigidez del callo o el módulo elástico del tejido óseo del callo. Los valores máximos de la tasa de producción de tejido óseo en el callo se alcanzaron cuando los valores de fuerza a través del mismo eran menores que la fuerza total sobre el metatarso en condiciones normales. Además, el valor máximo de volumen del callo se alcanzó después de que la capacidad de carga de la extremidad intervenida se recuperara y después de este momento, el volumen del callo comenzó a decrecer. Sin embargo, para el instante de máximo volumen, la rigidez del callo estaba por debajo del 20 % y el módulo elástico del tejido del callo estaba lejos de los valores de módulo elástico del hueso cortical. Esto significa que la monitorización del callo de distracción mediante radiografías, que solo proporciona información del volumen de tejido óseo, debe ser utilizada con prudencia en las aplicaciones clínicas.

- La contribución del incremento de módulo elástico del tejido óseo inmaduro al incremento de la rigidez del callo es baja en comparación con el efecto del incremento de volumen. Se puede observar en la figura 2 que justo después de la recuperación de la rigidez en la extremidad intervenida el módulo elástico del tejido óseo del callo es

aproximadamente un 65% del módulo elástico en el hueso cortical, solo un 20% más que al principio del proceso. Sin embargo, durante el periodo de tiempo en el que la rigidez del callo alcanzó el 100% (0 - 200 días después de la cirugía), el volumen del callo se incrementó desde prácticamente cero hasta 4 o 5 veces el valor del volumen de un segmento de metatarso de la misma longitud.

- La reorganización de la estructura y la reducción de la porosidad del tejido óseo inmaduro juegan un papel importante en el incremento de la rigidez del callo, especialmente a partir de 100 días desde la cirugía. Una vez alcanzado el volumen máximo del callo, aproximadamente 100 días después de la cirugía, el volumen comenzó a decrecer. Sin embargo, la rigidez del callo continuó aumentando hasta 250 - 300 días después de la cirugía mientras el módulo elástico medio del tejido óseo del callo aumentó solo un 10%. Por otro lado, a partir de 205 - 300 días después de la cirugía, el volumen del callo disminuyó significativamente; sin embargo, la rigidez del callo se mantuvo aproximadamente constante y el módulo elástico medio aumentó solo un 20% en 200 días. Todo esto no puede ser justificado sin la reorganización de la estructura, la reducción de la porosidad y/o la variación de la heterogeneidad del tejido óseo inmaduro del callo. De hecho, se ha demostrado que la variación de la heterogeneidad del hueso afecta a las propiedades mecánicas del mismo [164].

- La recuperación de las condiciones de simetría durante la marcha se produjo tras alcanzar el 100% de rigidez. Esto refuerza la conclusión del capítulo 9 sobre la posibilidad de utilizar el análisis de la marcha como un método alternativo para controlar los procesos de distracción osteogénica o fractura ósea. Si las condiciones de marcha se recuperan se habrá recuperado la rigidez de la extremidad intervenida. Esto hace del análisis de marcha un criterio seguro para evaluar la distracción osteogénica en comparación con la evaluación radiográfica ya que se ha visto que el máximo volumen del callo se alcanza antes de que la rigidez de la extremidad se recupere.

0.6 Conclusiones

A continuación se incluyen las principales conclusiones de esta Tesis:

- El distractor instrumentado desarrollado y calibrado en el capítulo 4 ha permitido la caracterización mecánica del proceso de transporte óseo mediante los experimentos llevados a cabo en esta Tesis. Dispositivos con características similares proporcionan un exhaustivo control durante las aplicaciones del proceso de distracción osteogénica ya que permiten monitorizar la fuerza y la rigidez del callo durante el tiempo que el distractor está implantado en el paciente.

- Los modelos de comportamiento de los tejidos del callo desarrollados han proporcionado los límites experimentales para los valores de fuerza de relajación después de cada paso de distracción (ver capítulo 5). Según estos modelos, la fuerza residual 24 horas después de cada paso de distracción alcanzó un valor máximo de 71.6 N y el pico de fuerza de relajación aumentó desde 7 - 34 N hasta 41 - 246 N. Los valores máximos de fuerza

residual predichos por los modelos son mucho menores que los valores medidos durante aplicación de la distracción osteogénica en alargamiento de huesos [177]. Estos resultados pueden deberse a la diferente influencia de los tejidos blandos colindantes al callo de distracción durante el transporte óseo y el alargamiento óseo. Además, las medidas experimentales tomadas demostraron que, cuando se desplaza el segmento de transporte, la fuerza de distracción requerida debido a la compresión del docking-site es despreciable con respecto a la fuerza de tracción del callo de distracción.

- Durante la fase de consolidación del proceso de transporte óseo, el periodo de máxima osificación tuvo lugar entre 20 y 70 días después de la cirugía, cuando se alcanzó la mayor producción de tejido óseo inmaduro en el callo, aumentando el volumen de tejido mineralizado en el callo desde prácticamente cero hasta el 80% del máximo (ver capítulo 6). Este periodo también coincidió con el de recuperación de la carga soportada por la extremidad intervenida (del 3 - 12% al 60 - 70%). Sin embargo, este periodo de máxima osificación corresponde con valores bajos de rigidez. La rigidez del callo aumentó exponencialmente desde el final de la fase de distracción pero no pasó del 10 % de la rigidez de un segmento de hueso cortical de las mismas dimensiones hasta 70 días después de la cirugía.

  Por lo tanto, se puede concluir que el volumen de callo puede ser un buen indicador de la capacidad de carga de la extremidad intervenida pero no de la rigidez de la misma. Esto significa que el seguimiento mediante radiografía que se lleva a cabo normalmente en la práctica clínica puede predecir la capacidad de carga pero no la rigidez de la extremidad intervenida. El mayor incremento de rigidez se produce después de que el máximo volumen sea alcanzado y una vez se recupera la capacidad de carga de la extremidad intervenida (ver capítulo 8), es decir, durante la fase de remodelación.

- Las medidas de nanoindentación del capítulo 7 mostraron que el módulo elástico medio del tejido óseo inmaduro generado durante el proceso de transporte óseo en el callo de distracción y en el docking site, se incrementa con el tiempo (desde 7 GPa, 35 días después de la cirugía, hasta 14 GPa, 525 días después de la cirugía, aproximadamente el 77% del módulo elástico medio del hueso cortical). Este incremento fue menor con el tiempo tanto en el tejido óseo inmaduro del callo de distracción como en el docking-site (entre 0.5 GPa por semana al inicio del proceso, hasta 0.05 GPa por semana a partir de 161 días después de la cirugía). Se observó que el tejido óseo inmaduro generado durante el transporte óseo presenta menores incrementos de módulo elástico con el tiempo que el generado durante la consolidación de una fractura [109]. Durante la fractura, el periodo de tiempo necesario para que el nuevo tejido óseo alcance el 95% del valor medio de módulo elástico del hueso cortical es aproximadamente un 20% en relación a la misma magnitud en el caso de transporte óseo. Esto podría deberse a la ausencia de estímulo de tracción en el caso de fractura ósea. Además, en cuanto a la variación espacial de las propiedades mecánicas en la misma muestra, se observaron diferentes distribuciones del módulo elástico medio según el momento del proceso analizado.

- La rigidez del callo de distracción fue obtenida mediante análisis con elementos finitos basado en tomografías computarizadas (ver capítulo 8). Los resultados de aplicación

de esta técnica utilizando el nivel de Hounsfield Units para asignar las propiedades mecánicas de los tejidos del callo de distracción han mostrado resultados más precisos que utilizando segmentación manual. La segmentación manual trabaja con sets homogéneos de elementos y ha sido usada con frecuencia en estudios computacionales de distracción osteogénica y fractura ósea [59, 85, 140, 141, 145]. Por lo tanto, los modelos *in silico* combinados con imágenes de tomografías computarizadas pueden ser muy útiles para mejorar los actuales protocolos clínicos y los futuros trabajos computacionales. Los resultados de la aplicación de la técnica mostraron un incremento de la rigidez del callo de distracción entre 0.1 - 0.2 y 140 - 150 kN/mm (valor del orden de la rigidez de un segmento de metatarso de igual longitud) después de 250 días de la cirugía de transporte aproximadamente.

- El análisis de la marcha se podría utilizar como método alternativo en el control de la evolución de los procesos de distracción osteogénica o fractura ósea (ver capítulo 9). Los parámetros de la marcha obtenidos de la monitorización de la fuerza de reacción en la extremidad intervenida (pico de fuerza, fuerza media e impulso), disminuyeron en la pata intervenida y aumentaron más significativamente en el resto de extremidades debido a la cirugía de transporte óseo. Durante el proceso de consolidación, estos parámetros fueron recuperando los valores normales en animales sanos. Conociendo la evolución de estos parámetros en un paciente podría determinarse el estado de osificación del callo y estimarse el momento apropiado para retirar el fijador. Además, el análisis de la marcha presenta ventajas sobre otros métodos de control de la distracción osteogénica ya que proporciona datos cuantitativos, no requiere de distractores instrumentados y no es invasivo.

0.7 Aportaciones originales

A continuación se incluyen las principales aportaciones de esta Tesis:

- Diseño y calibración de un nuevo distractor instrumentado que permite la monitorización de la fuerza y la rigidez del callo de distracción durante el transporte óseo.

- Se han proporcionado dos modelos de comportamiento mecánico de los tejidos del callo durante la fase de distracción del proceso de transporte óseo basados en experimentos *in vivo*: asumiendo la relajación total de los tejidos y asumiendo la existencia de fuerzas residuales. Se obtuvieron los límites experimentales para la fuerza de relajación. Se ha observado experimentalmente que la fuerza de distracción empleada en comprimir el docking site es despreciable frente a la empleada en la elongación del callo de distracción.

- Medidas experimentales *in vivo* de fuerza, rigidez del callo y volumen del callo durante la fase de consolidación del proceso de transporte óseo.

- Variaciones espaciales y temporales del módulo elástico del tejido óseo inmaduro generado durante el transporte óseo en el callo de distracción y en el docking-site.

- Estimación de la rigidez del callo de distracción durante el transporte óseo mediante análisis con elementos finitos basado en tomografías computarizadas. La técnica se aplicó utilizando el nivel de Hounsfield Units para asignar las propiedades mecánicas de los tejidos del callo y usando segmentación manual.
- Monitorización de la recuperación de las condiciones de marcha (pico, media e impulso de las fuerzas de reacción sobre el suelo en la extremidad intervenida) durante el proceso de transporte óseo.
- Comparación de la evolución de los datos experimentales anteriores (fuerza de relajación, fuerza a través del callo, rigidez del callo, volumen del callo, tasa de producción de tejido óseo, módulo elástico del tejido óseo inmaduro y recuperación de las condiciones de marcha), todos ellos obtenidos del mismo experimento de transporte óseo.

0.8 Trabajos futuros

Las posibles mejoras y líneas de investigación en distracción osteogénica son innumerables ya que el proceso no está totalmente definido hoy en día desde el punto de vista mecanobiológico. Son necesarios nuevos hallazgos científicos para proporcionar instrucciones en aplicaciones clínicas adaptables a las particularidades de cada caso y no solo basadas en la experiencia clínica. Los modelos computacionales basados en datos experimentales pueden contribuir a hacer posible una herramienta capaz de predecir la evolución del proceso de distracción osteogénica en diferentes situaciones. Por lo tanto, se deben desarrollar tanto trabajos experimentales como computacionales en los próximos años y algunos de ellos podrían utilizar los datos aportados por esta Tesis como una extensión del trabajo realizado. Algunas de las líneas de investigación que podrían desarrollarse son las siguientes:

1. Trabajos experimentales futuros:
    - Este trabajo proporciona datos sobre la evolución local de las propiedades mecánicas del tejido óseo inmaduro durante la distracción osteogénica. Aunque la fuerza de relajación de los tejidos en el callo durante la fase de distracción ha sido obtenida, la evolución de las propiedades mecánicas locales de cada tipo de tejido en el callo de distracción no se ha estudiado. Se necesita una caracterización mecánica más exhaustiva del tejido blando en diferentes instantes del proceso para completar la base de datos experimentales sobre distracción osteogénica, especialmente durante la fase de distracción. Por ejemplo, podrían llevarse a cabo experimentos de nanoindentación del tejido blando similares a los realizados en esta Tesis para el tejido óseo.
    - Todos los parámetros mecánicos medidos experimentalmente en esta Tesis, especialmente el estudio de las fuerzas de relajación en cada paso de distracción, deberían ser evaluados durante el mismo experimento de distracción osteogénica pero con una fase de distracción de mayor duración (más longitud del callo). Los resultados de esta Tesis demostraron que los tejidos del callo de distracción aumentan sus propiedades mecánicas con el tiempo. Esto quiere decir que para una

duración diferente de la fase de distracción, los tejidos del callo tendrían diferentes propiedades mecánicas que las obtenidas en este trabajo y esto cambiaría las condiciones de contorno de fuerza en el callo. Esto podría tener consecuencias en una diferente evolución de la osificación durante la fase de consolidación.

- Aunque los resultados de este trabajo permitieron comparar algunos parámetros mecánicos medidos durante el proceso de transporte óseo con parámetros similares medidos durante la aplicación de la distracción osteogénica en el alargamiento de extremidades (e.g., el efecto de la elongación de los tejidos blandos colindantes en la fuerza sobre el callo), las diferentes condiciones de los experimentos en la literatura hace difícil obtener más conclusiones. Experimentos de alargamiento óseo que sigan las mismas condiciones mecánicas y usen el mismo tipo de animales que en esta Tesis podrían aportar información útil sobre las diferencias mecánicas entre ambas aplicaciones de la distracción osteogénica: transporte óseo y alargamiento de extremidades.
- Este trabajo y otros en la literatura se han centrado en las propiedades mecánicas elásticas del tejido óseo inmaduro; sin embargo, en ciertas condiciones, el comportamiento mecánico del tejido óseo inmaduro no se puede asumir elástico lineal. Por lo tanto, se necesitan trabajos futuros que evalúen las propiedades viscoelásticas del tejido óseo inmaduro.
- Es necesario monitorizar experimentalmente la angiogénesis con métodos que permitan obtener datos cuantitativos del proceso. Esto permitiría determinar como afecta la angiogénesis al aumento de rigidez del callo, el aumento de módulo elástico, la reducción de la porosidad y la reorganización del tejido óseo inmaduro observados en esta Tesis.

2. Trabajos computacionales futuros: Las conclusiones de esta Tesis y los datos experimentales obtenidos pueden aplicarse a la mejora de trabajos computacionales en distracción osteogénica [85, 86, 141–144, 146] o a la generación de nuevos modelos. Especialmente, los aspectos que podrían ser estudiados o añadidos en nuevos trabajos computacionales son los siguientes:

   - Los datos experimentales de fuerza de relajación obtenidos en el capítulo 5 podrían utilizarse en la mejora y desarrollo de modelos computacionales sobre la fase de distracción.
   - El capítulo 8 muestra que los resultados de modelos de elementos finitos que utilizan el nivel de Hounsfield Units para asignar las propiedades mecánicas de los elementos del callo de distracción son más precisos que los que utilizan segmentación manual. Los nuevos modelos computacionales sobre distracción osteogénica deberían tener en cuenta el nivel de escala de gris de los tejidos del callo medido experimentalmente mediante radiografías o tomografías computarizadas.
   - Además del incremento del volumen del callo y de las propiedades mecánicas de los tejidos, los resultados de esta Tesis han demostrado que la reorganización de

la estructura del tejido óseo inmaduro, la reducción de la porosidad y/o los cambios en la heterogeneidad del tejido óseo inmaduro contribuyen al incremento de la rigidez del callo. Los resultados de esta Tesis pueden utilizarse en la validación de modelos de la fase de consolidación de la distracción osteogénica que propongan diferentes hipótesis sobre la contribución de estos factores en el proceso de distracción osteogénica.

0.9 Publicaciones

0.9.1 Publicación de los resultados de esta Tesis

Los principales resultados de este trabajo han sido parcialmente publicados en revistas científicas, presentados en conferencias o forman parte de artículos en preparación:

Revistas

- J Mora-Macías, E Reina-Romo, J Morgaz y J Domínguez. *In vivo* gait analysis during bone transport. *Annals of Biomedical Engineering*, 43(9):2090-100, 2015.
- J Mora-Macías, E Reina-Romo y J Domínguez. Distraction osteogenesis device to estimate the axial stiffness of the callus *in vivo*. *Medical Engineering & Physics*, 37(10):969-78, 2015.
- J Mora-Macías, E Reina-Romo, M López-Pliego, MA Giráldez-Sánchez y J Domínguez. *In vivo* mechanical characterization of the distraction callus during bone consolidation. *Annals of Biomedical Engineering*, 43(11):2663-74, 2015.
- J Mora-Macías, E Reina-Romo y J Domínguez. Model of the distraction callus tissue behavior during bone transport based in experiments *in vivo*. *Journal of the Mechanical Behavior of Biomedical Materials*, 15(61):419-430, 2016.
- J Mora-Macías, A Pajares, P Miranda, J Domínguez y E Reina-Romo. Time-dependence of nanoscale mechanical properties of cortical and woven bone. Manuscrito enviado para publicación.
- J Mora-Macías, A Pajares, P Miranda, J Domínguez y E Reina-Romo. Spatial and temporal variations of the mechanical properties of the woven bone during bone transport. Manuscrito enviado para publicación.
- J Mora-Macías, M López, J Domínguez y E Reina-Romo. Finite element versus experimental mechanical characterization of the distraction callus. Manuscrito enviado para publicación.
- J Mora-Macías, M López, J Domínguez y E Reina-Romo. Mechanical characterization of the woven bone of the docking-site callus by means of finite element analysis. Manuscrito en preparación.

Conferencias

- J Mora-Macías, E Reina-Romo y J Domínguez. Diseño de dispositivos para el análisis del proceso de transporte óseo en ovejas. XXIX Encuentro del Grupo Español de Fractura. Bilbao, España, Marzo de 2012
- J Mora-Macías, E Reina-Romo y J Domínguez. Monitorización de fuerzas durante el proceso de transporte óseo en ovejas. II Reunión del Capítulo Español de la Sociedad Europea de Biomecánica. Sevilla, España, Octubre de 2012
- J Mora-Macías, M López-Pliego, MA Giráldez-Sánchez, J Morgaz, E Reina-Romo y J Domínguez. Bone stiffness during bone transport: device design. 19^{th} Congress of the European Society of Biomechanics. Patras, Grecia, Agosto de 2013
- J Mora-Macías, M López-Pliego, MA Giráldez-Sánchez, J Morgaz, E Reina-Romo y J Domínguez. Análisis experimental del proceso de transporte óseo en ovejas: mecanobiología del callo de distracción. III Reunión del Capítulo Español de la Sociedad Europea de Biomecánica. Barcelona, España, Octubre de 2013
- J Mora-Macías, E Reina-Romo, J Morgaz, M López-Pliego, MA Giráldez-Sánchez y J Domínguez. *In vivo* gait analysis during bone transport. 7^{th} World Congress of Biomechanics. Boston, Estados Unidos, Julio de 2014
- J Mora-Macías, E Reina-Romo, MA Giráldez-Sánchez, J Morgaz, M López-Pliego y J Domínguez. Monitorización 3D del callo en distracción osteogénica. IV Reunión del Capítulo Español de la Sociedad Europea de Biomecánica. Valencia, España, Noviembre de 2014
- J Mora-Macías , E Reina-Romo, M López-Pliego, MA Giráldez-Sánchez, J Morgaz y J Domínguez. Force relaxation in distraction callus during bone transport. 21^{th} Congress of the European Society of Biomechanics. Praga, República Checa, Julio de 2015
- J Mora-Macías, M López, J Domínguez y E Reina-Romo. Predicción numérica de la rigidez del callo de distracción en base a tomografías computarizadas. V Reunión del Capítulo Español de la Sociedad Europea de Biomecánica. Madrid, España, Noviembre de 2015
- J Mora-Macías, E Reina-Romo, A Pajares, P Miranda y J Domínguez. Variación espaciotemporal de las propiedades mecánicas del hueso inmaduro durante el transporte óseo. V Reunión del Capítulo Español de la Sociedad Europea de Biomecánica. Madrid, España, Noviembre de 2015

0.9.2 Otras aportaciones de esta Tesis

Además de las publicaciones sobre resultados obtenidos, esta Tesis ha contribuido a la generación de otros trabajos también publicados. Algunos de estos estudios se han centrado en aspectos biológicos de los resultados de los experimentos llevados a cabo que no fueron analizados en esta Tesis (histologías del callo, composición del tejido óseo inmaduro, medidas de

vascularización...). Otros han usado la experiencia en diseño de dispositivos médicos generada durante la realización de la Tesis:

Patentes

- C Pardo-Pardo, A Ordóñez, I Valverde-Pérez, SL Pardo-Prieto, J Mora-Macías, E Reina-Romo y J Domínguez. Dispositivo de control de flujo de sangre en un vaso sanguíneo. OEPM Madrid (España) P201630066, 20 de Enero de 2016

Revistas

- E Reina-Romo, MA Giráldez-Sánchez, J Mora-Macías, P Cano-Luis y J Domínguez. Biomechanical design of less invasive stabilization system femoral plates: computational evaluation of the fracture environment. *Proceedings of the Institution of Mechanical Engineers, Part H: Journal of Engineering in Medicine*, 228(10):1043-52, 2014.

- M López-Pliego, MA Giráldez-Sánchez, J Mora-Macías, E Reina-Romo y J Domínguez. Histological evolution of the regenerate during bone transport. Experimental study in sheep. Manuscrito enviado para publicación.

- M López-Pliego et al. Histological study of the docking site after bone transport in lambs. Manuscrito en preparación.

- J Martínez-Reina, J García, J Mora-Macías, E Reina-Romo y J Domínguez. Composition of the woven bone of distraction callus. Manuscrito en preparación.

Conferencias

- I Pardo-Pardo, I Valverde-Pérez, R Hoseimpour, J Mora-Macías, E Sánchez de Rojas - de Pedro, M Urbano-Luque, E Reina-Romo, J Domínguez y A Ordóñez. Nuevo dispositivo banding ajustable para el control del flujo de la arteria pulmonar. Congreso Nacional de la Sociedad Española de Cardiología Pediátrica y Cardiopatías Congénitas. Valladolid, España, Mayo de 2016.

- J Mora-Macías, A Alneami, J Hollmann, M Niedre, C DiMarzio y SJ Shefelbine. Tuning a device to monitor blood perfusion in bone with near-infrared spectroscopy. IV Reunión del Capítulo Español de la Sociedad Europea de Biomecánica. Valencia, España, Noviembre de 2014

Chapter 1

Motivation, objectives and outline

The motivation of this Thesis is founded on the clinical and economical impact of distraction osteogenesis as well as the lack of knowledge about some mechanical and biological factors that rule the process. Increasing the knowledge of these factors would improve the clinical applications. The main objectives of this Thesis, a brief description of the contents, and the publications of the results are also included in this Chapter.

1.1 Motivation

Distraction osteogenesis consists of generating new bone tissue by the gradual separation of two bone fragments from an osteotomy. Since distraction osteogenesis was introduced by Ilizarov [76, 78, 79], this technique has been used in long bones as well as in irregular or flat bones applications. Some of the most important applications are: limb lengthening [78, 79, 155] (Fig. 1.1), treatment of non unions [25, 82, 83, 131], foot reconstruction [37, 60, 130] mandibular lengthening and widening [156], maxillary and midface distraction [44], cranial distraction [14, 106, 156] and treatment of bone defects. In this last case, it is called bone transport. Bone transport is widely used for the treatment of long bone defects by means of the displacement of a bone transportable segment relative to the end segments of an original bone. This displacement generates a distraction callus with respect to the former segment of the original bone at the same time that closes a gap with respect to the second segment [20, 31, 72, 76, 131].

Nowadays, distraction osteogenesis is used frequently in hospitals worldwide. For example, over 2000 patients are seen annually by the team of Limb Reconstruction of the Oxford University Hospital (UK) and 4-5 Ilizarov cases are performed weekly [70]. Up to 100000 people are diagnosed with limb-length disorders in US each year and about 500 limb-lengthening surgeries are performed each year at Sinai Hospital in Baltimore (US) [48]. In addition, currently, distraction osteogenesis is not being used only for health problems of the limbs. More than 30 hospitals around the world are offering cosmetic leg lengthening [71]. It is becoming an important economic activity which involves costs between 10000 and 150000 USD per surgery for patients [71].

The growth of the new bone tissue in a distraction callus depends on the mechanical en-

vironment [95, 150]. It has been suggested that one of the factors of influence in the differentiation of the tissues from granular tissue to mature bone in fracture healing is the strain status of the callus [22, 23, 135, 136]. Therefore, during the last decades, distraction osteogenesis has been studied by multidisciplinary teams: doctors and engineers. They have carried out both experimental and computational works to understand the mechanobiology of the distraction callus and improve the distraction osteogenesis techniques. Experimental works using instrumented fixators have tried to provide the evolution of some mechanical parameters (force, callus stiffness, interfragmentary movements...) of the distraction osteogenesis process *in vivo* [4, 8, 20, 31, 43, 46, 55, 177]. *Ex vivo* experiments have also been performed to assess the material properties of the callus [47, 123]. Other experimental works have obtained histologies, radiographies and other medical outcomes [7, 9, 11, 38, 49, 78, 79, 92, 124]. Later, the development of computational technologies allowed engineers to set up numerical models of distraction osteogenesis which have included different tissue differentiation theories where tissue evolution depends on the mechanical environment within the callus [15–17, 85, 140–145].

However, although distraction osteogenesis is an increasing demanding field and some studies have been published, currently, there are limited instructions available. Most of the surgeons are self-taught and complications are still considerable when this technique is applied [67, 170, 171] due to different reasons. Firstly, mechanobiologic mechanisms which regulates the bone tissue production and ossification during the process are not totally known. For example, there is no concordance in the literature about tissue differentiation during distraction osteogenesis. Some authors reported intramembranous ossification in the distraction callus [9, 39, 50, 51, 78, 79, 158, 160] whilst others demonstrated the prevalence of endochondral ossification [92, 173, 178] or both [49] and therefore the presence of cartilage. Secondly, the wide variety of experimental works make difficult the comparison among them and obtaining conclusions. The distraction osteogenesis process has different applications and may be applied at different bones. Moreover outcomes depend on the animals used. For example, ossification is faster in little animals such as rats or rabbits [11, 148] than in pigs or sheep [20, 31], for which ossification time and load conditions in the distraction callus are closer to humans. Finally, as far as the author knows, no study relates *in vivo*, *ex vivo* and computational results of the same specimens. *Ex vivo* results and computational studies are limited since it is difficult to reproduce the real loading conditions. In addition, frequently computational studies are based on mechanical parameters or provide results that have not been validated with experimental studies that reproduce the same conditions. Nevertheless, *ex vivo* and computational techniques may provide outcomes that are not possible to obtain *in vivo* and are complementary among them for similar conditions.

Therefore, the main motivation of this thesis is to carry out a multiple study which allows obtaining *in vivo* general mechanical parameters (force through the callus and fixator, callus stiffness...), *ex vivo* local mechanical properties of the callus (elastic modulus and hardness) and biological quantifiable aspects (callus volume, bone tissue production rate...) during the complete process of distraction osteogenesis from the same animal experiment. Outcomes are also analyzed by means of computational techniques to obtain *in silico* measurements of different parameters of the model. It would allow increasing the knowledge of the mechanobiology of the distraction osteogenesis process and improving the applications techniques.

Figure 1.1: Patient before treatment (left) and after lengthening and remodeling the shape of her leg (right) [155]

1.2 Objectives

The general objective of this Thesis is to quantify and relate during the complete distraction osteogenesis process quantifiable biological parameters (the bone tissue volume and its distribution in the distraction callus, proportions of different tissue types...) with mechanical parameters (the force through the fixator and through the callus, the mechanical properties of the callus tissue during the process...). *In vivo* and *ex vivo* experiments were carried out in the same specimens and conditions with the aim of providing results in multiple directions of analysis to be connected and related among them, directly or indirectly by means of the use of numerical analysis techniques which were also developed. Next, some of the partial objectives are itemized:

- To provide a new and calibrated distractor tested in preliminary *in vivo* experiments. It allows measuring force through the callus and callus stiffness *in vivo* at any time under real load conditions during the distraction and consolidation phases of the bone transport process. The device is designed to be applied during sheep bone transport experiments to

study mechanical properties of the callus distraction, and to be used in other cases with some adaptations.

- To improve the experimental database of force monitoring during distraction phase in long-bone, specially continuous measurements of force relaxation curves after bone transportable segment displacement. Obtaining these curves from bone transport experiments instead of from bone lengthening experiments minimizes effects of surroundings tissue and muscle resistance in force through callus measurements.

- To provide an experimental model of the mechanical behavior of the callus tissue after each step of distraction by fitting experimental results above.

- To quantify and relate the following parameters during the complete phase of the bone transport process: the bone tissue volume and its distribution in the distraction callus, the bone tissue production rate, the force through the fixator and through the callus during gait, and the callus stiffness during the consolidation phase of the process.

- To evaluate the spatial and temporal variations of the distraction callus mechanical properties by means of nanoindentation experiments that provide local elastic modulus of the woven bone tissue.

- To analyze quantitatively the relationship between the ossification states of the distraction callus during bone transport with variations in gait conditions and to assess the possibility of using gait analysis as a method to evaluate distraction osteogenesis process status.

- To carry out a computational analysis to obtain an estimation of the callus stiffness and the distribution of the tissues within the callus. The computational analysis uses as feedback the experiments mentioned above, which provide spatial and temporal mechanical properties of the complete geometry of the callus tissue from experimental measurements of different mechanical parameters.

1.3 Organization of the Thesis

Animal experiments of the bone transport process were performed by an interdisciplinary team of mechanical engineers of the department of Mechanical Engineering and Manufacturing of the University of Seville, orthopaedics surgeons of the department of Orthopaedic of the Universitary Hospital Virgen del Rocío of Seville and veterinarians of the department of Animal Medicine and Surgery of the Veterinary Hospital of the University of Córdoba. This Thesis integrates the engineering works carried out during these experiments (design and calibration of devices, monitoring of forces, etc.) as well as the analysis of the results based on mechanical aspects of the process (force relaxation of the callus tissue, evolution of the callus stiffness and volume, spatial and temporal variations of the mechanical properties of the woven bone, gait analysis, etc). Most of these outcomes have been published or submitted for publication in different journals (see section 1.4) and most of the Chapters of this thesis are based on these

papers as is detailed below. The remaining of this Thesis is composed of nine Chapters and one appendix, which are organized as follows:

Chapter 2 introduces the distraction osteogenesis process: a brief description of the process, its different phases, mechanisms that rule the callus growth... It also deals with the different applications of the distraction osteogenesis, specially the bone transport since it was the technique applied in the experiments performed in this Thesis. In addition, the state of the art of the research in distraction osteogenesis is treated in Chapter 2. The main findings about the biological and mechanical aspects of the distraction osteogenesis process since the process was released by Ilizarov [77–79] are presented.

The bone transport experiments carried out are described in Chapter 3. The animals selection, the surgery and the bone transport protocol used are explained. Furthermore, Chapter 3 includes how the different mechanical measurements were performed both *in vivo* and *ex vivo*. The proceeding of sample harvest for *ex vivo* experiments as well as the time points analyzed for each test were also detailed.

Chapter 4 includes the design of the distractor. It describes the instrumentation of the fixator and the acquisition system used for monitoring of the force through the callus and the callus stiffness. On the other hand, the calibration of the system and the preliminary force and callus stiffness measurements were reported. This Chapter is based on a paper published in literature [113]: **J Mora-Macías, E Reina-Romo and J Domínguez. Distraction osteogenesis device to estimate the axial stiffness of the callus *in vivo*. *Medical Engineering & Physics*, 37(10):969-78, 2015**.

Chapter 5 analyzes the *in vivo* measurements of force relaxation of the callus tissue during the distraction phase. It provides the contribution of the callus traction and the docking-site compression to the distraction force. Two different models of the mechanical behavior of the callus are proposed which give an experimental band for the residual force value after each step of distraction. These results are included in a paper published in the literature [114]: **J Mora-Macías, E Reina-Romo and J Domínguez. Model of the distraction callus tissue behavior during bone transport based in experiments *in vivo*. *Journal of the Mechanical Behavior of Biomedical Materials*, 15(61):419-430, 2016**.

Chapter 6 deals with the evolution of the force through the callus during the consolidation phase, the callus stiffness and the woven bone volume within the callus. These data were reported from *in vivo* measurements and computerized tomographies. These outcomes relate biological aspects (callus volume and tissue production rate) with mechanical parameters (callus force and stiffness) of the distraction osteogenesis process. These results, the methods used to obtain them and the discussion of them were also published [115]: **J Mora-Macías, E Reina-Romo, M López-Pliego, MA Giráldez-Sánchez and J Domínguez. *In vivo* mechanical characterization of the distraction callus during bone consolidation. *Annals of Biomedical Engineering*, 43(11):2663-74, 2015**.

Chapter 7 comprises *ex vivo* experiments of nanoindentation carried out in callus samples to characterize the material properties of the woven bone within the callus. Woven bone samples from the bone transport experiment harvested at different time points and location within the distraction and the docking site calluses were nanoindented. Spatial and temporal variations are reported and compared with the temporal evolution of other mechanical parameters obtained in Chapters above such as the callus stiffness or the volume of the callus. This Chapter is based

on a paper submitted for publication: **J Mora-Macías, A Pajares, P Miranda, J Domínguez and E Reina-Romo. Spatial and temporal variations of the mechanical properties of the woven bone during bone transport**.

Chapter 8 presents a method to evaluate the stiffness of the distraction callus after removal of the instrumented fixator used previously in bone healing [161]. It consists of finite element analyses based on computed tomographies. Results of two different approaches to assign the mechanical properties to the tissues developed within the distracted callus are compared: manual segmentation or based on the level of Hounsfield Units. The contents of this Chapter are also included in a paper submitted for publication: **J Mora-Macías, M López, J Domínguez and E Reina-Romo. Finite element versus experimental mechanical characterization of the distraction callus**.

The evolution of the gait conditions during the bone transport process are analyzed in Chapter 9 by means of measuring the ground reaction force from the surgery to more than one year later. Results show, as a preliminary approach to be confirmed with more experiments, that gait analysis could be used as an alternative method to control distraction osteogenesis or bone healing. These outcomes are published [116]: **J Mora-Macías, E Reina-Romo, J Morgaz and J Domínguez. *In vivo* gait analysis during bone transport. *Annals of Biomedical Engineering*, 43(9):2090-100, 2015**.

The main conclusions of this Thesis, together with a brief summary, the main original contributions here presented and the future work lines are collected in Chapter 10.

Finally, an appendix is included at the end of the Thesis that adds information about the methods used in Chapter 7. Appendix A deals with the temporal variation of the elastic modulus measurements via nanoindentation in the same cortical and woven bone samples. Outcomes included in this appendix were submitted for publication: **J Mora-Macías, A Pajares, P Miranda, J Domínguez and E Reina-Romo. Time-dependence of nanoscale mechanical properties of cortical and woven bone**.

1.4 Publications

1.4.1 Publication of the results of this Thesis

The main results of this work have been partially published in the following journals and conferences or are in preparation:

Journals

- J Mora-Macías, E Reina-Romo, J Morgaz and J Domínguez. *In vivo* gait analysis during bone transport. *Annals of Biomedical Engineering*, 43(9):2090-100, 2015.
- J Mora-Macías, E Reina-Romo and J Domínguez. Distraction osteogenesis device to estimate the axial stiffness of the callus *in vivo*. *Medical Engineering & Physics*, 37(10):969-78, 2015.
- J Mora-Macías, E Reina-Romo, M López-Pliego, MA Giráldez-Sánchez and J Domínguez. *In vivo* mechanical characterization of the distraction callus during bone consolidation.

Annals of Biomedical Engineering, 43(11):2663-74, 2015.

- J Mora-Macías, E Reina-Romo and J Domínguez. Model of the distraction callus tissue behavior during bone transport based in experiments *in vivo*. *Journal of the Mechanical Behavior of Biomedical Materials*, 15(61):419-430, 2016.
- J Mora-Macías, A Pajares, P Miranda, J Domínguez and E Reina-Romo. Time-dependence of nanoscale mechanical properties of cortical and woven bone. Manuscript submitted for publication.
- J Mora-Macías, A Pajares, P Miranda, J Domínguez and E Reina-Romo. Spatial and temporal variations of the mechanical properties of the woven bone during bone transport. Manuscript submitted for publication.
- J Mora-Macías, M López, J Domínguez and E Reina-Romo. Finite element versus experimental mechanical characterization of the distraction callus. Manuscript submitted for publication.
- J Mora-Macías, M López, J Domínguez and E Reina-Romo. Mechanical characterization of the woven bone of docking-site callus by means of finite element analysis. Manuscript in preparation.

Conferences

- J Mora-Macías, E Reina-Romo and J Domínguez. Diseño de dispositivos para el análisis del proceso de transporte óseo en ovejas. XXIX Encuentro del Grupo Español de Fractura. Bilbao, Spain, March 2012
- J Mora-Macías, E Reina-Romo and J Domínguez. Monitorización de fuerzas durante el proceso de transporte óseo en ovejas. II Reunión del Capítulo Español de la Sociedad Europea de Biomecánica. Sevilla, Spain, October, 2012
- J Mora-Macías, M López-Pliego, MA Giráldez-Sánchez, J Morgaz, E Reina-Romo and J Domínguez. Bone stiffness during bone transport: device design. 19^{th} Congress of the European Society of Biomechanics. Patras, Greece, August, 2013
- J Mora-Macías, M López-Pliego, MA Giráldez-Sánchez, J Morgaz, E Reina-Romo and J Domínguez. Análisis experimental del proceso de transporte óseo en ovejas: mecanobiología del callo de distracción. III Reunión del Capítulo Español de la Sociedad Europea de Biomecánica. Barcelona, Spain, October 2013
- J Mora-Macías, E Reina-Romo, J Morgaz, M López-Pliego, MA Giráldez-Sánchez and J Domínguez. *In vivo* gait analysis during bone transport. 7^{th} World Congress of Biomechanics. Boston, United States of America, July 2014
- J Mora-Macías, E Reina-Romo, MA Giráldez-Sánchez, J Morgaz, M López-Pliego and J Domínguez. Monitorización 3D del callo en distracción osteogénica. IV Reunión del Capítulo Español de la Sociedad Europea de Biomecánica. Valencia, Spain, November 2014

- J Mora-Macías, E Reina-Romo, M López-Pliego, MA Giráldez-Sánchez, J Morgaz and J Domínguez. Force relaxation in distraction callus during bone transport. 21^{th} Congress of the European Society of Biomechanics. Prague, Czech Republic, July, 2015

- J Mora-Macías, M López, J Domínguez and E Reina-Romo. Predicción numérica de la rigidez del callo de distracción en base a tomografías computarizadas. V Reunión del Capítulo Español de la Sociedad Europea de Biomecánica. Madrid, Spain, November 2015

- J Mora-Macías, E Reina-Romo, A Pajares, P Miranda and J Domínguez. Variación espacio-temporal de las propiedades mecánicas del hueso inmaduro durante el transporte óseo. V Reunión del Capítulo Español de la Sociedad Europea de Biomecánica. Madrid, Spain, November 2015

1.4.2 Other contributions of this Thesis

Apart from the publications about the results obtained, the work carried out during this Thesis has contributed to the generation of works published in other lines of research. Some of these works have been focused on other biological aspects of the results of the experiments carried out that were not analyzed in this Thesis (histologies of the callus, composition of the woven bone, measures of angiogenesis...). Other works have used the experience in medical devices design generated during the realization of this Thesis:

Patents

- C Pardo-Pardo, A Ordóñez, I Valverde-Pérez, SL Pardo-Prieto, J Mora-Macías, E Reina-Romo and J Domínguez. Dispositivo de control de flujo de sangre en un vaso sanguíneo. OEPM Madrid (Spain) P201630066, January 20, 2016

Journals

- E Reina-Romo, M Giráldez-Sánchez, J Mora-Macías, P Cano-Luis and J Domínguez. Biomechanical design of less invasive stabilization system femoral plates: computational evaluation of the fracture environment. *Proceedings of the Institution of Mechanical Engineers, Part H: Journal of Engineering in Medicine*, 228(10):1043-52, 2014.

- M López-Pliego, MA Giráldez-Sánchez, J Mora-Macías, E Reina-Romo and J Domínguez. Histological evolution of the regenerate during bone transport. Experimental study in sheep. Manuscript submitted for publication.

- M López-Pliego et al. Histological study of the docking site after bone transport in lambs. Manuscript in preparation.

- J Martínez-Reina, J García, J Mora-Macías, E Reina-Romo and J Domínguez. Composition of the woven bone of distraction callus. Manuscript in preparation.

Conferences

- I Pardo-Pardo, I Valverde-Pérez, R Hoseimpour, J Mora Macías, E Sánchez de Rojas - de Pedro, M Urbano-Luque, E Reina Romo, J Domínguez, A Ordóñez. Nuevo dispositivo banding ajustable para el control del flujo de la arteria pulmonar. Congreso Nacional de la Sociedad Española de Cardiología Pediátrica y Cardiopatías Congénitas. Valladolid, Spain May 2016.
- J Mora-Macías, A Alneami, J Hollmann, M Niedre, C DiMarzio, SJ Shefelbine. Tuning a device to monitor blood perfusion in bone with near-infrared spectroscopy. IV Reunión del Capítulo Español de la Sociedad Europea de Biomecánica. Valencia, Spain, November 2014

Chapter 2

Introduction

The following sections introduces the concept of distraction osteogenesis and the main applications of this process. Among the main applications, bone transport is treated with special interest because it was applied in the experiments of this Thesis. The main biological principles and aspects of the distraction osteogenesis process are explained: the phases of the process, the tissue types that are generated within the distraction callus and how the callus grows according to experimental works. Besides, a state of the art in the evaluation of the mechanical aspects of the distraction osteogenesis process is included. In addition, it contains information about the different fixation technologies for distraction in limbs, computational models that have analyzed the influence of the mechanics of the process, experimental outcomes in literature about the mechanical behavior of the callus tissue during the distraction phase and the evolution of different mechanical parameters (forces, callus stiffness and mechanical properties) during the complete process. Finally, a summary of the main biomechanical factors that influence the growth of the callus is also included.

2.1 Distraction osteogenesis and its applications

Distraction osteogenesis is a technique for generating new bone tissue from the gradual separation of two bone fragments. Under the influence of the tensional stress, the tissues within the gap between bone segments differentiate and ossify. The callus is developed since bone is a strain-sensitive tissue that reacts to the mechanical environment [95, 150]. Many tissues besides bone have been observed to form under tension stress, including mucosa, skin, muscle, tendon, cartilage, blood vessels, and peripheral nerves [78, 79]. Therefore, distraction osteogenesis involves a process of continuum tissue formation. Although distraction osteogenesis has numerous applications (limb lengthening [78, 79, 155] (Fig. 1.1), treatment of non unions [25, 82, 83, 131], foot reconstruction [37, 60, 130] mandibular lengthening and widening [156], maxillary and midface distraction [44], cranial distraction [14, 106, 156], bone transport [20, 31, 72, 76, 131] . . .) that may be used in long bones as well as in irregular or flat bones, this thesis is focused on the application of bone transport in long bones. Bone transport refers to the distraction osteogenesis process where the regenerated bone is used to fill a defect [20, 31, 72, 76, 131]. Details of the main applications of the distraction osteogenesis process

which are used today follows:

- *Bone transport*. It consists of distracting a bone transportable segment osteotomized from an original bone where there is a previous defect due to trauma, oncologic resection, non-union or congenital anomalies. The aim is to create two focuses of bone regeneration on both sides of the bone transportable segment. First, a distraction callus is generated with respect to the former segment of the original bone. Second, in the docking site, on the other side of the bone transportable segment, the defect between it and the other end of the original bone is filled until both segments dock [20, 31, 72]. Several bone transport techniques have been developed. According to Ilizarov, the techniques are divided into three groups based on the numbers of distraction calluses and docking sites: monofocal, bifocal and trifocal. As example, it can be observed in Fig. 2.1 the monofocal bone transport procedure carried out by Claes et al. [31] in an animal experiment in the metatarsus of sheep.

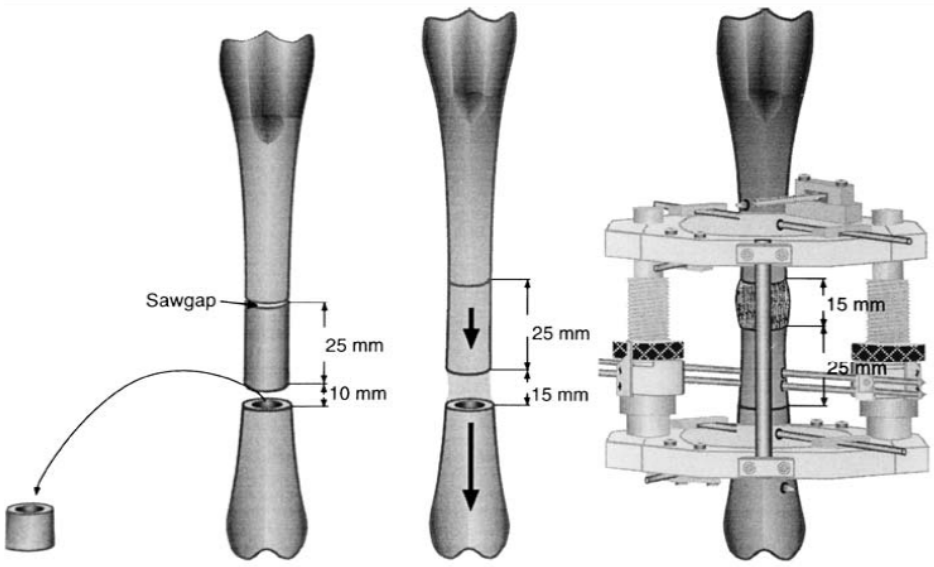

Figure 2.1: Diagram of the bone transport operative procedure: left, creation of the mid-diaphyseal defect; middle, adjustment of the length of the defect to 15 mm; and right, daily segmental bone transport of 1 mm in two steps [31].

- *Limb lengthening* (Figs. 1.1 and 2.2). Distraction osteogenesis may be used in limb lengthening in the case of patients that suffer limb reduction deficiencies. These limb reduction deficiencies may be due to different reasons: congenital anomalies, childhood fractures of the femur, osteomyelitis, dysplasia (malformation), destruction of the hip joint, achondroplastic dwarfism... An interesting application of limb lengthening is the ability to lengthen both lower limbs and increase the height. This has the most logical application in achondroplastic dwarfism (Fig. 2.2). However, currently, the application

of distraction osteogenesis to increase the height is not being used only for health problems of the limbs. More than 30 hospitals around the world are offering cosmetic leg lengthening [71].

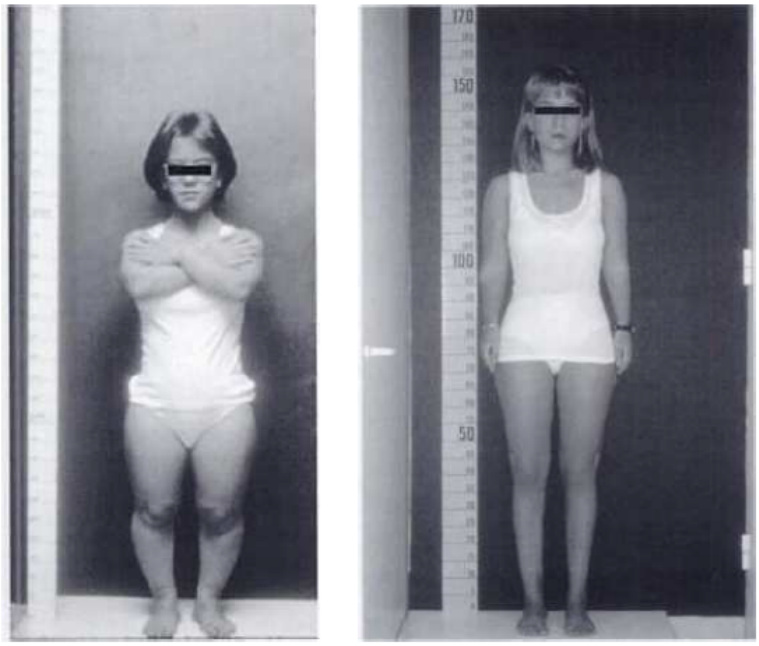

Figure 2.2: Achondroplastic dwarf who underwent limb lengthening and achieved 31 cm of height without complications [137].

- *Arthrodiastasis*. Arthrodiastasis are angular joint deformities that may cause stiffening of joints. Distraction osteogenesis can also be used for correcting these deformities [65, 99].
- *Foot reconstruction*. Deformities in foot may be due to different causes: untreated, residual, or recurrent clubfeet[1] in adults, post-traumatic deformity and degenerative joint disease, failed ankle fusion and a variety of deformities such as vertical talus. All these cases may be treated with distraction osteogenesis [37, 60, 130].
- *Mandibular lengthening, widening and bone transport*. Distraction osteogenesis is usually used for patients with hemifacial microsomia. Hemifacial microsomia is a congenital asymmetrical malformation of both the bony and soft tissue structures of the cranium and face. It is the second most common facial birth defect after clefts, with an incidence in the range of 1 in 5000 [34]. In addition, bone transport in the craniofacial region is frequently used for correction of large mandibular defects, reconstruction of neocondyles, cleft lip and alveolar defects for dental implants.

[1] congenital deformity of the foot

- *Periodontal ligament distraction*. It consists of the distraction of the periodontal ligament by means of orthodontic progressive tooth movement [156].
- *Cranial distraction*. As in long bones, distraction osteogenesis may also be applied to cranial bones [156]. Distraction osteogenesis is applied clinically for reconstruction of cranial deformities and cranial vault defects.

2.1.1 Particularities of bone transport

Bone transport in long bones of limbs was applied in the experiments carried out in this Thesis. This section deals with some aspects that differentiate this application of the distraction osteogenesis process from the others applications described above, specially bone lengthening:

- *The role of the surrounding soft tissues*. Bone transport aims to correct a bone defect. Therefore, the length of the original bone does not vary. It means that soft tissues surrounding the distraction callus are not elongated [20]. This fact may be taken into account in the mechanical analysis of the process since traction force during distraction osteogenesis is distributed between the callus tissue and the surrounding soft tissue and muscle. There is not consensus about the amount of contribution of the surrounding tissues and the callus tissues. Some studies reported that the distraction forces are primarily due to the elongation of the callus tissues [8, 18, 177, 185]. In this case, the relaxation after distraction would be caused by the viscoelastic nature of the callus tissues [2, 148] and/or the callus tissue growth/differentiation. However, in the case of bone lengthening, other studies have reported that the surrounding muscles and soft tissues are the primarily responsible for the distraction forces [2, 54, 55, 122]. In any case, although no data were reported in literature, during bone transport the contribution of the surrounding soft tissue to distraction force is expected to be lower compared to bone lengthening.
- *Two focuses of ossification: the docking-site and the distraction callus*. On the one hand, the existence of two ossification focuses could also affect the distraction force distribution. In the case of bone transport, although minor contribution of the surrounding tissue is expected with respect to bone lengthening, there is another factor that contributes to the distraction force apart from distraction callus traction and elongation of surrounding tissues: the compression of the docking site. The contribution of the callus traction and the docking-site compression to the total distraction force necessary to move the bone transportable segment was not assessed. Hyodo el al. [72] suggested that probably the contribution of the docking-site compression dominates the distraction force; nevertheless, they did not report any experimental results. On the other hand, the existence of a second focus of ossification complicates the process because of the difficulty of the docking-site consolidation [51, 73, 111]. However, as far as the author knows, most of the studies about mechanical parameters assessment have been focused on the distraction callus and not on the docking-site callus [20, 31, 72].
- *Possibility of force monitoring during gait*. Some studies in fracture healing [108, 159] proposed gait analysis as a valuable tool for monitoring the course of the callus ossification. However, as far as the author knows, the evolution of the gait conditions during

distraction has not been studied and has not been practiced in clinical cases to assess load bearing capacity. Applications such as limb lengthening could difficult assessment by means of gait analysis since the elongation of the limb also produces changes in gait. However, gait analysis could be used in bone transport applications of limbs, since it does not imply limb lengthening.

2.2 Biology of distraction osteogenesis

This section deals with the main biological aspects and particularities that define the bone distraction process: the phases of the process and the tissue types which may appear within the callus. In addition, results of studies which have evaluated the biological callus development are reported: histological evolution, tissue types assessment, callus volume quantification etc

2.2.1 Phases of distraction osteogenesis

The evolution with time of the mechanical environment and the biological activity within the distraction callus makes possible establishing five fundamental sequential phases in the distraction process (Fig. 2.3):

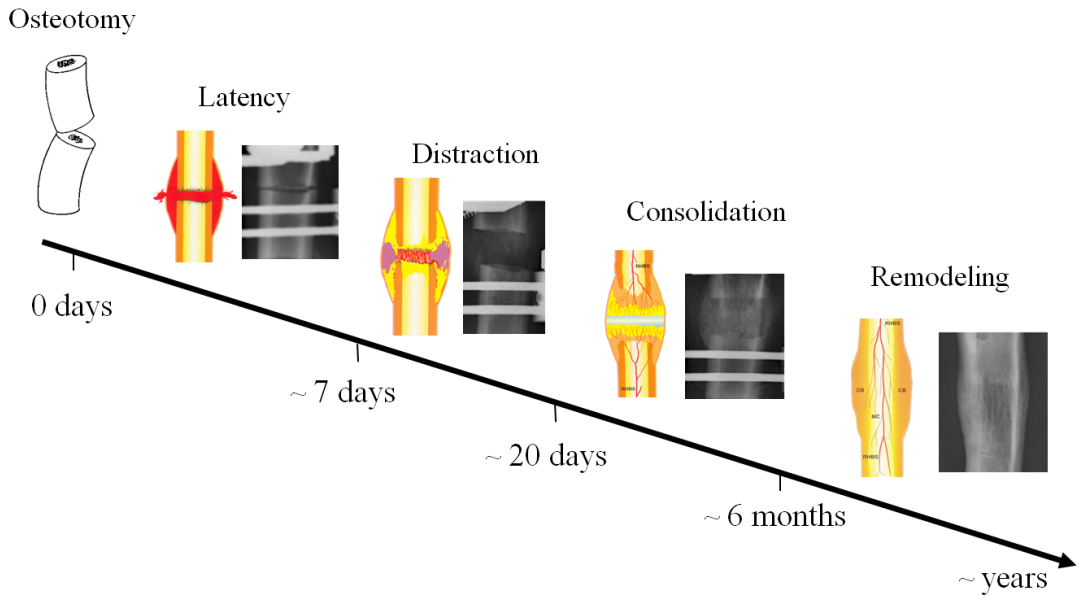

Figure 2.3: Phases of distraction osteogenesis.

- *Osteotomy*. This phase is carried out during the surgery and consists of dividing the intervened bone into two segments, resulting in a loss of continuity and mechanical integrity. The bone fragments need to be fixed before by means of a distractor/external fixator to allow the limb to keep its structure. Some works in literature have shown the importance

of preserving or causing the minimum damage to the periosteum [84, 105] since it is a focus of cellular activity [58] and blood supply for ossification.

- *Latency phase*. It is the period between performance of the osteotomy and the distraction phase. During this phase that usually takes some days a soft callus is formed from the initial clotting appeared after surgery.

- *Distraction.* This phase allows the extension of the callus from the osteotomy gap to the final desired length separating the two bone segments progressively. The application of tensional stress caused by the separation of the bone fragments creates a dynamic microenvironment [39] that stimulates changes at the cellular and subcellular level [90]. These changes result in the evolution of the tissue types within the callus and the generation of the woven bone.

- *Consolidation*. The consolidation period begins after the callus has achieved the desired length and the distractor is removed. Therefore no traction forces are applied through the callus during this period. During the consolidation phase callus completes its ossification and the woven bone tissue begins to organize as mature bone tissue. Although the production of bone tissue begins during the distraction phase, the bony bridging of the callus is completed during this phase [148].

- *Remodeling*. It consists of the complete remodeling of the newly formed bone under the application of full functional loading. During this period, the cellular bony activity is focused on the reorganization of the callus woven bone structure with the aim of recovering the shape and mechanical properties of the initial bone. For example, both the cortical bone and marrow cavity are restored during this phase that usually takes more than a year. Although the main activity of remodeling is observed after the consolidation phase, the remodeling of the newly formed bone begins at the completion of distraction and continues throughout the consolidation period [120].

2.2.2 Tissue types during distraction osteogenesis

From the initial clotting in the osteotomy gap after the surgery, different tissue types grow within the callus. These tissue types are mainly connective tissues which are generated from undifferentiated mesenchymal cells in the marrow and the periosteum [58]. Connective tissues are comprised in the major structural parts of the body (bone, tendons, ligaments...) providing and maintaining form in the body. For example, they allow organs to resist stretching and tearing forces. Besides, connective tissue has an important role in providing a medium for oxygen and nutrients to diffuse from capillaries to cells, and carbon dioxide and waste substances to diffuse from cells back into circulation.

The structure of the connective tissues is composed of ground substance, cells and fibers. The extracellular matrix of the connective tissues consists of different combinations of protein fibers (collagen, reticular and elastic), most of which are collagen fibers and ground substance [89]. The morphophysiological characteristics of the tissues depend on the extracellular matrix that is the main component of the connective tissues. It explains the capacity of providing and

maintaining form in the body of connective tissues over other tissue types. Of the more than 20 types of collagen thus far identified, types I to III are found mainly in connective tissues [69].

Among the different types of connective tissues (cartilage, tendons, ligaments, bone and the adipose tissues as well as skin, blood and lymph [35]) the following sections deal with those that are involved in the distraction osteogenesis process. On the one hand, those tissues that appear within the distraction callus during the distraction osteogenesis process: woven bone and soft tissues (mainly cartilage, fibrous and granulation tissues). On the other hand, the bone, since the woven bone tissue within the callus develops to reach the properties of mature bone at the end of the process. In addition, the original bone segments form the boundary of the distraction callus.

Bone.

In the case of bone, components of the extracellular matrix are calcified (bone matrix). This fact makes bone tissue to be characterized by its rigidity and high resistance to both tension and compression. Moreover, Julius Wolf stated in the 19^{th} century that bone may adapt to the load stimulus. If loading on a particular bone increases/decreases, the bone will remodel itself over time to form/miss new bone. Therefore, the bone tissue is capable of repairing structural damage through the process of remodeling [151]. For example, in fracture healing, distraction osteogenesis or loss of bone due to diseases. Mechanosensitive cells within the bone (osteoblasts, osteoclasts and osteocytes) allow these processes of remodeling and repairing. Another significant characteristic of bone is that it is a vascular tissue. It determines some of its functions in the human organism. Major functions of the bone follows: support, protection, mineral storage, blood cell production (hematopoiesis) and locomotion through the attachment of muscles.

The bone tissue can be classified into compact / cortical bone and cancellous / trabecular / spongy bone (Fig. 2.4) attending to its structure. The cortical bone is found in the diaphysis of the long bones or shaft of the bone and outer layer of the trabecular bone. At the macroscopic level, it seems a compact and continuous solid. However, at the microscopical level, it may be observed that it consists of lots of osteons with a lamellar organization around the Haversian channels (Fig. 2.4). On the other hand, the trabecular bone is found in the epiphysis of the long bones. The trabecular bone structure consists of large, open spaces surrounded by thin, anastomosing plates of bone. These plates of bone are called trabeculae. Therefore, this type of bone is not as dense as cortical bone. Trabecular bone is highly vascular and frequently contains red bone marrow which fills the spaces among trabeculae. With the exception of the articulating surfaces, both types of bone are completely enclosed by the periosteum, a tough, highly vascularized and innervated fibrous tissue really important in the healing of bone during distraction osteogenesis (Fig. 2.4) [39, 183].

According to the tissue level, bone may be classified in three categories: primary bone, secondary bone and woven bone. Primary bone can exist in cortical and trabecular bone. Unlike woven bone, primary bone must replace a preexisting structure, either a cartilaginous model or previously deposited woven bone. Secondary bone is only deposited during remodeling and replaces primary cortical or trabecular bone. Therefore the woven bone is the bone tissue that is generated during biological processes in which new bone tissue has to extend to areas without

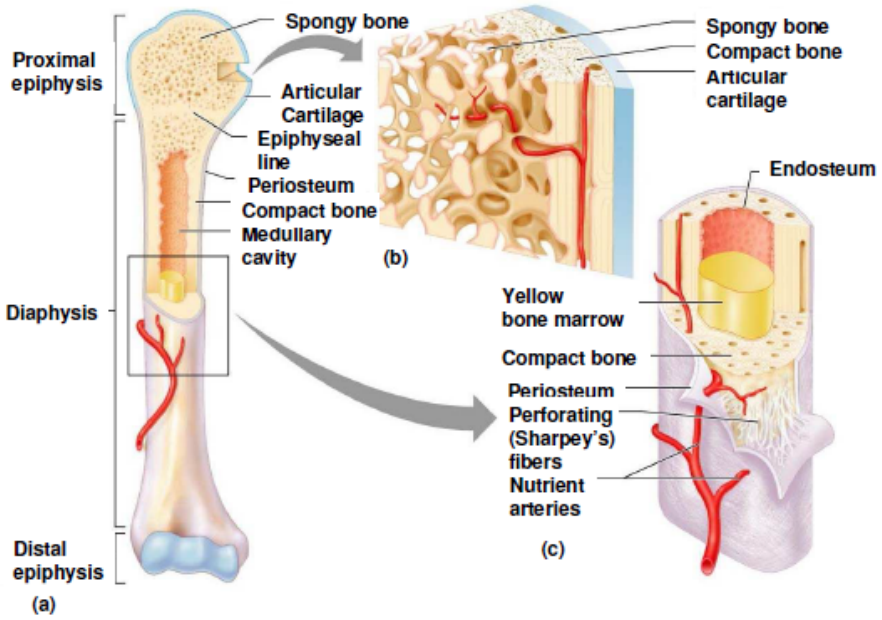

Figure 2.4: Long bone structure, a) human tibia, b) epiphysis, c) diaphysis [146]

bone because it can be deposited without a preexisting membrane, bone or cartilaginous model [112].

Woven bone.

The woven bone can be found in a fracture callus and in areas undergoing active endochondral ossification. In addition, it is the bone tissue that appears during the ossification of the distraction callus. Therefore it is the bone tissue of most interest for this Thesis. The woven bone follows a cancellous bone structure, i.e., trabeculae that surrounds spaces of soft tissue. Trabeculae of woven bone are generated rapidly as a disorganized arrangement of collagen fibers and osteocytes. The disorganized pattern decreases the mechanical properties of woven bone compared with the primary or secondary bone. Furthermore, the cell to bone volume ratio is high because the main purpose of the woven bone is to provide a temporary and rapid mechanical support, such as following traumatic injury.

Chemical analysis of this bone type has revealed lower content of mineral and water, and higher of collagen compared with normal bone [53] (see Fig. 2.5). These lower portions of mineral also decrease the mechanical properties of woven bone compared with the cortical bone as the disorganized pattern cited above. Manjubala et al. [109] showed that the level of the structural density, the mechanical properties and the mineral content of the woven bone generated during bone healing increase with time and similar trends may be expected in distraction osteogenesis. Therefore, the evolution of these parameters among others are related with the recovery of the stiffness and the load bearing capacity in limbs intervened where these pro-

cesses are carried out. In addition, they are direct results of the mechanobiological mechanism that rules the production of bone tissue during these processes.

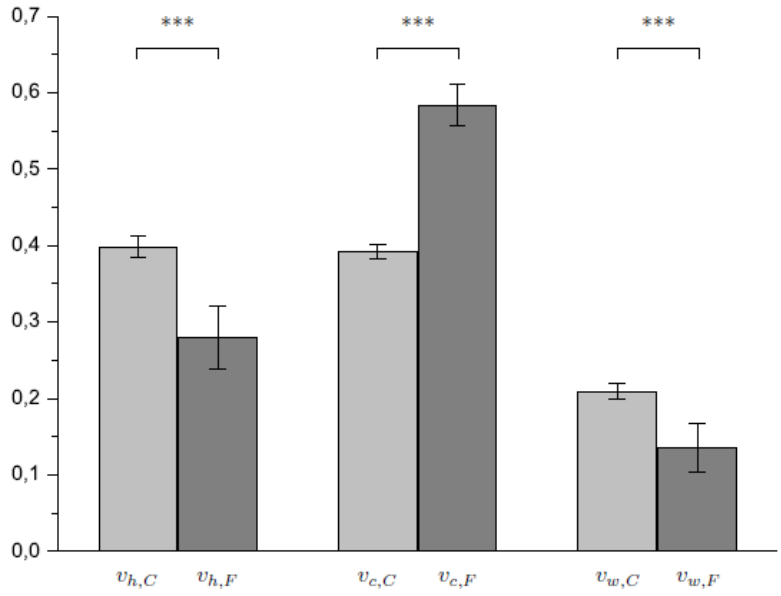

Figure 2.5: Volumetric composition of the woven bone (F) within a distraction callus compared with mature compact bone (C) of the same animal: mineral, v_h, collagen, v_c, and water v_w [53].

The development of the woven bone tissue is carried out by means of intramembranous or endochondral ossification. The main difference between both types of ossification is the presence or not of cartilage. During the intramembranous ossification, the mesenchymal cells differentiate directly into osteoblasts that later secrete bone tissue. The new bone tissue is generated from an ossification center which appears in a richly vascularized mesenchymal membrane within the fibrous connective tissue. The endochondral ossification consists of the synthesis of bone on a mineralized cartilage scaffold. Currently, there is not consensus about the type of ossification that is carried out in the distraction callus: endochondral [92, 173], intramembranous [9, 9, 32, 39] or both [11, 45, 49, 51, 79].

Soft tissue

Since there is not consensus about the type of ossification that is carried out in the distraction callus, the soft tissue types and the order in which they appear within the callus during the distraction osteogenesis process is controversial. In this section the main soft connective tissues that may appear within the distraction callus are introduced assuming that the woven bone within the distraction callus could be generated by intramembranous, endochondral ossification or both: cartilage, fibrous and granulation tissue.

Cartilage has intermediate mechanical properties between dense connective tissue and bone. It is suitable for both tension and compression loads. It is composed of specialized

cells called chondrocytes and chondroblasts that produce a large amount of extracellular matrix composed of collagen fibers, abundant ground substance rich in proteoglycan and elastin fibers. This structure makes the cartilage tissue tough and flexible at the same time. In general, these properties are necessary in the locations of this tissue type e.g., joints. Here the cartilage absorbs shock during walking and avoids the wear of the bones. Cartilage does not contain blood vessels (avascular) or nerves (aneural). It receives by diffusion from the blood vessels located in the connective tissue membrane surrounding it [110]. Therefore, compared to other connective tissues, cartilage grows and repairs slower.

Fibrous connective tissue consists of a high concentration of elastic fibers and small spaces with liquid. This tissue type has relatively high tensile strength and great elasticity. The cells of fibrous connective tissue are mostly fibroblasts, irregular, branching cells that secrete strong fibrous proteins as an extracellular matrix. Within the distracted gap during the distraction osteogenesis process, the two different types of fibrous tissue usually appear: loose and dense connective tissue [81]. The loose connective tissue appears at early stages of the process such as the latency phase. The main difference between both types of tissue is the greater consistency of the dense connective tissue due to the amount and the order of the collagen fibers.

Granulation tissue is a loosely organized connective tissue that forms on the surface of a wound during the healing process. This tissue replaces the clot that appears after the osteotomy at the beginning of the latency phase in distraction osteogenesis. Granulation tissue consists of tissue matrix supporting a variety of cell types, most of which can be associated with different functions: formation of extracellular matrix, operation of the immune system, vascularization...

2.2.3 Monitoring and assessment of the callus growth

Most of the studies about distraction osteogenesis assessed the maturation of the callus tissue by means of radiographies and histologies [7, 9, 11, 38, 45, 45, 49, 51, 78, 79, 90, 92, 105, 123, 124, 148, 182]. The study of Ilizarov [78, 79], which is considered the basis of the distraction osteogenesis, used both methods to report his main conclusions: maximum preservation of the periosseous and intraosseous soft tissues enhanced bone formation; the new bone formed parallel to the tension vector even when the distraction is performed perpendicular to the bone's mechanical axis; 1 mm per day was found to be the optimum distraction rate in canine tibia (0.5 mm and 2 mm per day were also analyzed); and the bone grows mainly by means of intramembranous ossification although some endochondral ossification focuses may also be found. These results reported by Ilizarov were corroborated after by studies that measured forces [8, 167], displacements [31] or used computational models [3, 16, 142] which will be treated in the section below.

The type of ossification was also analyzed in other histological studies but no consensus was established. This way, some authors found only endochondral ossification within the callus [92, 173], whilst intramembranous ossification [9, 9, 32, 39] or a combination of both [11, 45, 49, 51, 79] was reported by others. The difference in the mode of ossification found could be due to the differences in loading conditions as well as the variety of fixations used. López-Pliego [105] pointed out that the fixator employed is different according to the animals type.

Monolateral mini-fixators used in most small animals favor the increase of mobility in the regenerate, increasing the appearance of endochondral ossification foci. Aronson et al.

[9] found differences in the alignment of collagen bundles, subsequent ossification and axial rigidity of the callus for groups of animals that used different fixators. However, all groups fully bridged the experimental gap by intramembranous ossification with similar volume of bone tissue.

The conditions of the experiments in literature vary and different contributions of intramembranous and endochondral ossification to the development of the distraction callus have been reported. Thus, different types of soft tissues and orders of appearance have also been found. Few histological studies provided quantifiable distribution of tissue types over the distraction osteogenesis process [11, 45, 51, 105]. Fig. 2.6 shows results of these studies for comparison. It may be observed approximately linear increase of woven bone percentage and decrease of soft tissue (sum of cartilage and fibrous tissue) percentages. Little or no amounts of cartilage were found. It implies prevalence of intramembranous ossification. Aronson et al. [11] used rats and reported high percentages of woven bone during the first days compared to the rest of studies in dogs (Fink et al. [45]) and sheep (García et al. [51, 105] and López-Pliego [105]). It could be explained because in small animals, ossification takes place earlier than in bigger animals. These differences could make small animal models inappropriate to approach human model studies. In addition some of the studies have been carried out with only 2 or 3 time points of evaluation [45, 51] making their outcomes not useful for validating computational models which try to understand the mechanobiology of the process and predict the amounts of callus tissue with time [16, 85, 140–145]. More outcomes of quantifiable callus tissue distribution along the entire process would contribute to improve computational models and compare with mechanical aspects from other experimental estudies in distraction osteogenesis.

Tissue segmentation from computerized tomographies (CT) is an alternative method to histology which allows quantifying the proportion of bone tissue volume within the callus. Claes et al. [28] demonstrated the feasibility of fracture healing stimulation by the temporary application of distraction and compression using this method to quantify the bone tissue volume. Other studies measured the bone volume from CT to analyze the effect in callus ossification of applying different substances during fracture healing [74, 103] and during bone lengthening [87]. Kontogiorgos et al. [93] evaluated the structure and material properties of native mandibular bone and those of early regenerate bone, produced by bone transport. Regarding distraction osteogenesis in long bones, Richards et al. [148] used rabbits for measuring the increase of bone within the callus at four time points from the end of the distraction phase to 3 weeks after. They reported that the highest increase of bone volume takes place after the distraction phase. The first week after distraction the bone volume of the callus increased more than 150% whilst after the first week of consolidation the increase of bone volume was under 20%. Morgan et al. [117] reported, at the same time, the evolution of bone volume within the callus and the vascular development until the end of the consolidation phase using CT images. They found that the increase with time of the volume of the mineralized tissue in the regenerate was correlated with the vessel volume, and occurred primarily during consolidation. The potential of callus volume quantification from CT could provide more findings for the research of the distraction osteogenesis process. For example, none of the works above measured the bone callus volume after the end of the consolidation period. It could be interesting to know how the callus volume decreases during bone remodeling. In addition, the evolution of bone

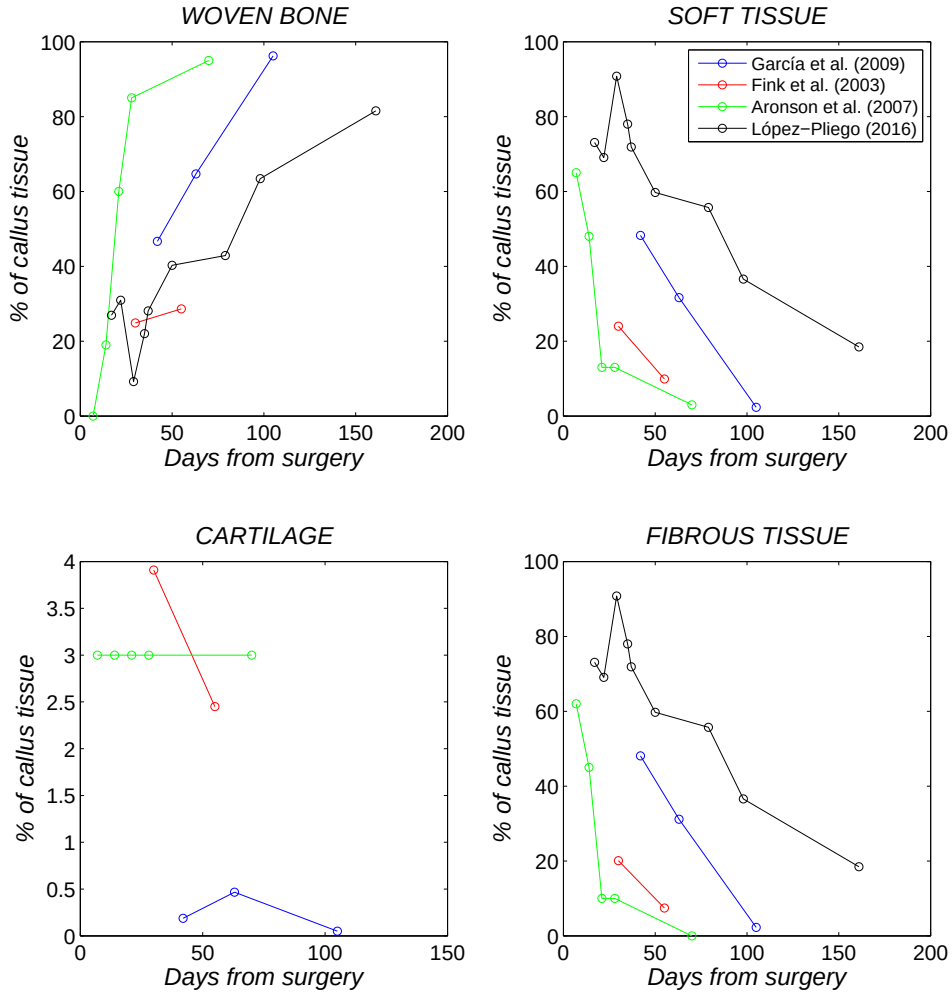

Figure 2.6: Tissue type distribution within callus during the distraction osteogenesis process reported in literature in sheep (García et al. [51] and López-Pliego [105]), dogs (Fink et al. [45]) and rats (Aronson et al. [11]).

tissue volume with time was not correlated with mechanical parameters of the same experiments (callus stiffness, force through the callus, callus mechanical properties etc). It would provide information to validate and improve computational models [16, 85, 140–145] which allow perfecting clinical applications.

2.3 Mechanics of distraction osteogenesis

Since clinical and experimental observations demonstrated that bone is a strain-sensitive tissue that reacts to the mechanical environment [95, 150], many studies about the processes which involve bone regeneration, such as fracture healing or distraction osteogenesis, have focused on analyzing and characterizing the mechanical parameters involved. This section deals with the mechanical aspects of the distraction osteogenesis process. On the one hand, existing fixation technologies are described. The properties of the fixator have high influence in the mechanical environment within the distraction callus. In addition, instrumentation of the fixator allows monitoring *in vivo* some mechanical parameters involved in distraction osteogenesis. On the other hand, findings of works which have studied the mechanical aspects are reported. Experimental works measured these mechanical parameters and assessed the material properties of the callus using different methods (mechanical testing of *ex vivo* samples, *in vivo* monitoring, numerical analysis ...). Moreover, computational models proposed different mechanobiology theories about the effects of mechanical loading on tissue differentiation, growth, adaptation and maintenance.

Despite all these experiments performed, consensus about the optimal mechanical environment for distraction osteogenesis, as well as the quantitative rules that govern the mechanobiology of the process have yet to be established.

2.3.1 Fixation technologies for distraction in limbs

The evolution of the distractors (fixation technologies for distraction) has been linked to the history of the distraction osteogenesis process. The application of traction forces in broken bones has been used since ancient times [134]. Rudimentary external distractors have been used. First distractors applied traction force in limbs without fixing any piece to the bone segments. For example, the Malgaigne's external skeletal clamp, 1847 [156]. In 1905, Codivilla used osteotomy and fixation to calcaneus to perform distraction of legs in one step (up to 8 cm) (Fig. 2.7 [33]). This single phase lengthening was complicated by serious nerve lesions and persistent and uncontrollable convulsions [33].

Later, various methods of limb lengthening were used but resulted in high complication rates until the 1950s, when the Russian Ilizarov developed the distraction osteogenesis technique. He designed a new distractor which consisted of two metal rings fixed to the proximal and distal bone segments of the osteotomy by means of pins (Fig. 2.8). This type of distractor is still used today. Ilizarov established the first protocol of distraction osteogenesis (5- to 7-day latency period, followed by a distraction rate of 1 mm per day performed in four increments of 0.25 mm) and the principles of the process (see section 2.2.3) [78, 79].

After the Ilizarov design, other distractors appeared with the aim of simplifying the technical application and implantation. For example, that was the case of the Wagner's design (1971) [174]. He proposed a monolateral distractor technically simpler but offered no major advantages regarding early mobilization of the patient and distribution of forces through the distraction callus. Other possible configurations are distractor with half-pins frames [128] or intramedullary rods [20]. All these different designs of distractor, including Ilizarov, are used today and exhibit advantages or disadvantages according to the concrete application. The latest

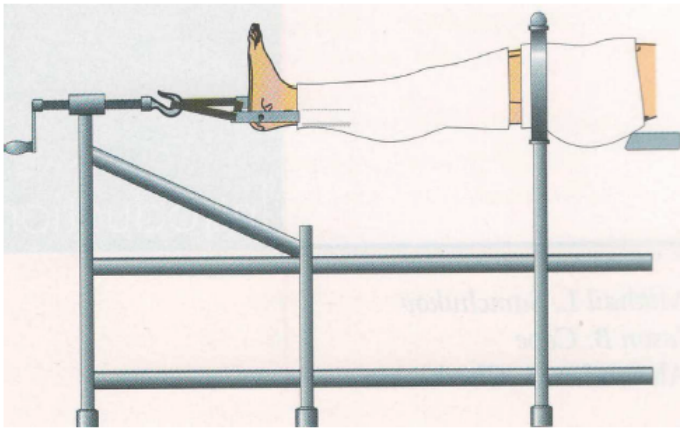

Figure 2.7: Codivilla's calcaneal pin traction plaster [33]

.

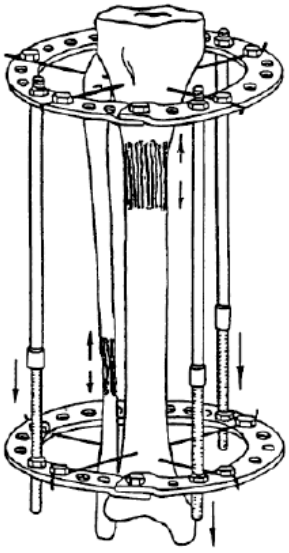

Figure 2.8: Ilizarov apparatus design [78, 79].

designs allow applying gradual mechanical forces and movements of bone in any plane (frontal, sagittal or transverse) or direction (axial, angular, translational, rotational or any combination). Furthermore, there are distractors able to cross active joints [37] and generate motion in two or three planes at the same time (Taylor Spatial Frame).

Apart from the possible configurations for distractors, some improvements were aimed to the instrumentation of these apparatus. Instrumentation of distractor allows monitoring *in vivo* mechanical parameters involved in the distraction osteogenesis process such as the forces or displacements through the distraction callus or its stiffness. Some techniques have been applied to measure interfragmentary displacements [31, 55] and forces in fracture healing [62], bone

transport [20], and bone lengthening [7, 46, 55, 177] processes. In other cases, both force and displacement measurements were combined to estimate the callus stiffness. Torsional [180], bending [43, 68, 149], and compressive [4, 29, 36, 41] loads were experimentally applied in bone healing [36, 68, 149] or limb lengthening [4, 43, 180] but not in bone transport experiments.

Methods of estimation the callus stiffness are currently in study since the cited methods above present different drawbacks. For example, some of them do not allow measuring the callus stiffness during real load conditions e.g., during gait [4, 36, 43, 68, 149, 180], present risk of bone misalignment during measurements [43, 68, 149] or were not calibrated before using in patients. Although instrumented fixators have shown to be useful in monitoring the status of the callus, none of the designs existing are used today in clinical application for different reasons. First, they are expensive and unconformable for patients. Second, their use is complicate for clinicians. Finally, since the instrumentation increases the volume of the fixator, it complicates the use of other method of evaluation of the callus such as radiographies or computerized tomographies.

2.3.2 Mechanical behavior of the callus tissue during the distraction phase

During the distraction phase, traction force is applied through the callus at each step of distraction to separate the bone segments. At the time when the bone segment is displaced, a peak of traction force is achieved and after, force relaxation takes place (Fig. 2.9). Some works in the literature measured both the distraction peak force required to move the segment and the posterior relaxation [2–4, 8, 18, 18–20, 54, 55, 72, 96, 172, 177]. However, it has not been established if the force decreases totally or until a residual value that is the pre-distraction force of the next step of distraction. The maximum peak force value achieved at the end of the distraction phase and the main data about some of the works in literature are shown in Table 2.1 for comparison.

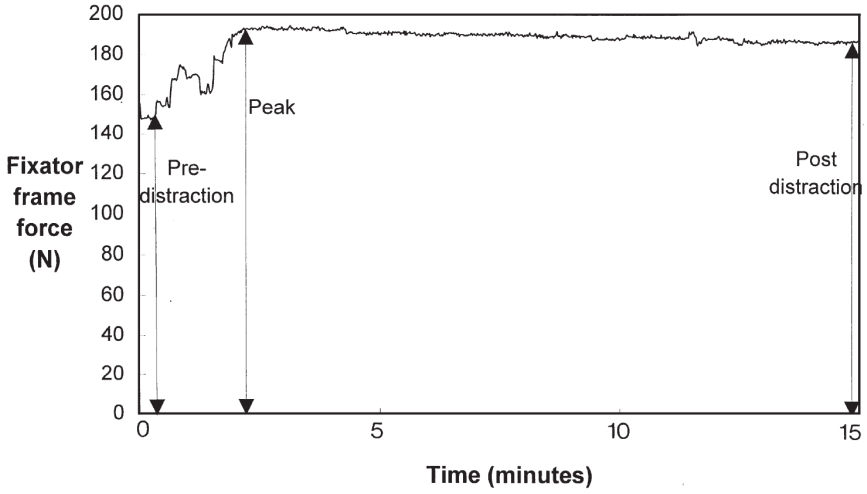

Figure 2.9: Typical temporal variation of force during incremental distraction in human tibia [55].

Table 2.1: Comparison of the values of peak distraction force at the end of the distraction period (MPF) reported by different studies in bone lengthening (BL) or bone transport (BT). The specie of the study, the distraction rate (R) and the total length distracted (L) are indicated. (MPF) values were normalized by the total length distracted (MPF_L).

Author	Application	Species	L (mm)	R (mm / day)	MPF (N)	MPF_L (N/mm)
Gardner et al. [55]	BL	Humans	58.5	0.75	370	6.3
Aarnes et al. [2]	BL	Humans	45	1	300 / 400	8.9
Aronson et al. [8]	BL	Dogs	28	1	140	5
Hyodo et al. [72]	BT	Dogs	36	1 / 2	200 / 250	5.5 / 6.9
Brunner et al. [20]	BT	Sheep	20 / 45	1	300 / 400	7.8 / 17.5
Wee et al. [177]	BL	Sheep	38	1	550	14.4
Waanders et al. [172]	BL	Rabbits	9	0.75	45	5

Distraction forces in humans were measured in a few studies [3, 55]. Gardner et al. [55] measured forces in two male subjects who underwent single tibial diaphyseal lengthening. Forces peaked at 370 N approximately after 6.2 and 5.5 cm of total distraction using three 0.25 mm increments each day. Pre-distraction force and force after 15 minutes relaxation were also measured obtaining values of 200-250 N and around 350 N at the end of the distraction period. Aarnes et al. [3] compared high and low distraction frequencies in two patients (0.25 mm x 4 in the first leg and 1/1440 mm once every minute in the other). They found that the peak distraction force decreased for high distraction frequencies. At the last day of distraction, the peak distraction force was 400 N for the low frequency case versus 300 N approximately for the high frequency case.

Distraction forces measured in tibias of sheep provided similar values to those obtained in

human experiments. For example, Brunner et al. [20] measured forces of 300-400 N in sheep tibias at the end of bone transport and Younger [184] recorded peak forces of 285 N in average. Higher values were reported by Wee et al. [177] in bone lengthening experiments exceeding 500 N after the end of the distraction phase.

Lower forces are required to distract rabbit and dogs tibias. Waanders et al. [172] measured an averaged distraction force ranging from 8 to 45 N for peak values, from 4 to 30 N for post-distraction values and from 3 to 20 N for pre-distraction values. In the case of dogs, maximum residual peak force values around 140 N were reported by Aronson and Harp [8]. Hyodo et al. [72] reported values closer for bone transport experiments, achieving around 200 N for a distraction rate of 1 mm per day and around 250 N for a distraction rate of 2 mm per day.

Although these experiments provided useful outcomes, different animal characteristics, surgical techniques, fixator types, latency periods and distraction rates make difficult the comparison among different studies. Currently, many questions about the forces involved in the distraction phase have not been answered. For example, it has not been determined the origin of the reaction force after each step of distraction. Some studies reported that the distraction forces are primarily due to the elongation of the callus tissues [8, 18, 177, 185]; however, other studies have reported that the surrounding muscles and soft tissues are the primarily responsible of the distraction forces [2, 54, 55, 122]. As is explained in section 2.1.1, the applied load to move the bone transportable segment in bone transport should be lower than in bone lengthening because in the second case, the elongation of the distraction callus implies the elongation of the soft tissues of the limb. Therefore, those works that measure the traction forces during the distraction phase in bone lengthening applications [2, 3, 8, 18, 18, 19, 54, 55, 96, 172, 177] should be differentiate from those that measure distraction forces in bone transport application [20, 72]. In the case of bone transport, only two studies were found by the author [20, 72]. These studies did not provide the contribution to the distraction forces of the callus traction and the compression of the tissues in the gap. Therefore, force through the callus tissue during each step of distraction cannot be determined although distraction force was measured and forces of the surrounding tissues to the callus were considered negligible in the case of bone transport. Knowing the contribution of the callus traction to the distraction force measurements would be very useful to characterize the mechanical behavior of the callus tissue from distraction force measurements *in vivo*. Another controversial point about the distraction force during the distraction phase is whether there is a residual force before each step of distraction or there is a total relaxation of traction force before the next step of distraction. As far as the author knows, although Reina-Romo et al. [144] estimated numerically the effect of these hypothetical residual forces after each distraction step, the experimental works carried out did not provide enough continuous measurements between two distraction steps to assess the residual forces [20, 172].

2.3.3 Evolution of the distraction callus mechanical properties

The evolution of some mechanical parameters involved in the distraction osteogenesis process such as the force through the callus or the callus stiffness have been determined experimentally. Both *ex vivo* and *in vivo* studies have been carried out. The former provided mechanical properties of callus samples tested mechanically. The second monitored the force involved in

the process and the callus stiffness using instrumented fixators.

Ex vivo assessment of the callus mechanical properties during the process

Ex vivo studies which were carried out with the aim of measuring mechanical properties of the distraction callus consist of testing the whole intervened bone using conventional material testing techniques such as compression tests, three point bending tests or torsion test [10, 11, 47, 123, 167, 175]. Ohyama et al. [123] obtained the load-deflection and relaxation curves of the callus at different time points. They detected the increase of stiffness with time as well as the time-dependent behavior of the callus tissue. Aronson et al. [10] assessed the tensile stiffness, the three point bending to failure and the energy to failure evolution with time in a rat model of distraction osteogenesis. They detected that the callus reached a maximum level of stiffness during the consolidation and later, the stiffness decreased at the same time that the volume of the callus decreased due to bone remodeling. However, the failure parameters always increased during the process. More recently, Floerkemeier et al. [47] compared different types of the callus stiffness evaluation methods (compression, bending and torsion tests) and they observed differences within the increase of stiffnesses during consolidation depending on the type of stiffness assessed. This fact should be considered in the assessment of the callus load-bearing capacity from stiffness measurements.

Although these studies provided interesting findings in the evaluation of the callus mechanical properties, they are limited. For example, it is not posible to reproduce in the lab the same loading conditions and physiological environment of the callus tissue *in vivo*. Moreover, for early stages of the ossification process the distraction callus does not have enough stiffness to place and fix it in a material testing machine for macroscopic experiments. The influence of the loading conditions and the physiological environment of the sample are negligible if the measurements are focused on the local mechanical properties of a point of the sample. Nanoindentation technique allows determining elastic modulus and contact hardness of materials point by point with a high spatial resolution [125]. Moreover this technique could provide results from little samples unlike conventional tests with material testing machines which required larger and stiffer samples. Nanoindentation studies reported new data about the nanoscale mechanical properties of the callus during fracture healing [5, 97, 98, 109]. Although they found high scattering, Leong and Morgan [97] obtained the elastic modulus of the different tissue types within the callus during fracture healing in rats 35 days after fracture (Table 2.2). Manjubala et al. [109] reported, for the woven bone tissue of the callus during bone healing in sheep, the mean values of the elastic modulus evolution with time, the spatial variation with the distance from the cortex periosteum and the heterogeneity by means of elastic modulus maps among others. They found that the mean elastic modulus of the woven bone increases with time from 5-6 to 11-12 GPa (Fig. 2.10). Fig. 2.10 also shows that the increments of elastic modulus were slower with time. It may be observed in Fig. 2.10 and Table 2.2 that for the same time point (35 days after surgery), there is not coincidence in the experimental values of elastic modulus reported by Manjubala et al. [109] and Leong and Morgan [97]. This may be due to the different animal models and fixations used; nevertheless, more studies should be carried out. Furthermore, as far as the author knows, nanoindentation was not applied in the evaluation of the mechanical properties of the callus tissues during the distraction osteogenesis process. It is

expected that the evolution of the mechanical properties of the tissue within the callus varies between fracture healing and distraction osteogenesis since these processes present different mechanical environment and stimuli.

Table 2.2: Elastic modulus (E) ranges of the different tissue types within the callus during fracture healing 35 days after fracture reported by Leong and Morgan [97]

Tissue	E (MPa)
Granulation tissue	0.61 - 1.27
Chondroid tissue	1.39 - 4.42
Woven bone	26.92 - 1010.00

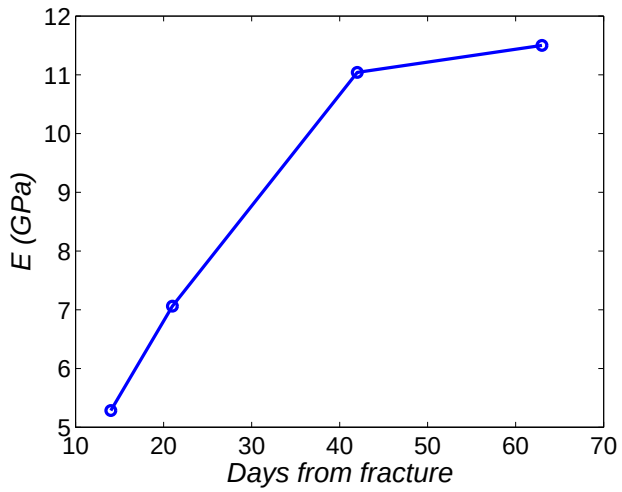

Figure 2.10: Evolution of the mean elastic modulus of the woven bone within a fracture callus [109].

In vivo assessment of mechanical parameters during distraction osteogenesis

Besides the difficulties for simulating the real loading conditions and the physiological environment of the callus tissue *in vivo*, the *ex vivo* studies in general have a main limitation: they require the sacrifice of animals to obtain samples. Therefore, *ex vivo* experiments are non-viable for assessing the evolution of the callus stiffness or other mechanical parameter in clinical applications. In addition, using *ex vivo* techniques increases the costs of the experiment since a group of animals at each time point of evaluation is required. As a solution for the drawbacks of the *ex vivo* experiments, instrumented fixators were used for *in vivo* monitoring of different mechanical parameters involved in the processes of fracture healing [29, 36, 62, 68, 68, 149, 159] and distraction osteogenesis [1–4, 8, 18–20, 31, 41, 43, 46, 54, 55, 72, 96, 113, 115, 116, 166, 172, 177, 180].

Knowing the distribution of force between the callus and the fixator during consolidation in distraction osteogenesis or fracturing healing allows evaluating the progress of ossification. *In vivo* models of fracture healing have measured forces through the fixator during healing [4, 46, 62]. Grasa et al. [62] reported in sheep that force through the fixator is about the ground reaction force in the intervened limb after surgery and decreases under 10 % of the initial value approximately 40 days after surgery. It means that 90 % of the initial force is loading the callus at this moment. Similar evolution of force is expected during the consolidation phase of distraction osteogenesis. Nevertheless, as far as the author knows, the forces through the callus during the consolidation phase for distraction osteogenesis have not been previously evaluated. The inter-fragmentary movements during the consolidation phase of distraction were evaluated by Claes et al. [31] to examine the effect of the stiffness of the fixator on reducing the time for maturation of the callus. They found that flexible fixations which permit interfragmentary movements below 2mm may favor the ossification.

Among the parameters to be measured to obtain the mechanical properties of the callus, the stiffness has been the most frequently studied. The callus stiffness is defined as the force or torque applied to the callus divided by the displacement or angle induced, respectively. *In vivo* studies have assessed the stiffness of the callus and of the total affected limb both in bone lengthening [4, 43, 181] and fracture healing [29, 36, 68, 149]. They used different devices that allow measuring torsional, [181] bending [36, 43, 68, 149] or axial [4, 29, 36] stiffness of the callus. The study of Cunningham et al. [36] was among the first works that evaluate the callus stiffness during fracture healing. This work reported an increase of the axial stiffness from 150-350 N/mm to 1000-1400 N/mm between 2 and 11 weeks post fracture in the intervened human tibia. The increase of axial stiffness corresponded with an increase of bending stiffness from 3-6 Nm/deg to 16-21 Nm/deg in the same time period. Hente et al. [68] found values of bending stiffness of the same order in human tibial fractures (10-40 Nm/deg at 11 weeks post fracture). Richardson et al. [149] determined a bending stiffness of 15 Nm/deg in the sagittal plane as indicator of union in human tibial fractures. This work also reported a comparison among previous stiffness measurements in literature in fracture healing and suggested the temporal evolution of bending stiffness (Fig. 2.11). According to this figure, during the consolidation, the stiffness increases and overcomes the stiffness of the intact tibia which is achieved after. In the case of bone lenthening, Dwyer et al. [43] found unions when bone bending stiffness reached 15 Nm/deg in human tibias and 20Nm/deg in human femurs. The study reported exponential increased of bending stiffness after the end of leg lengthening. Different rates of stiffness increase could be observed since the lengthening varied from 30 to 85 mm. For example, for the tibia lengthening cases, 15 Nm/deg was achieved between 9 and 29 weeks after the end of distraction (Fig. 2.12). Aarnes et al. [4] compared the load-share ratio between the bone and the fixator in human tibia lengthening. None of the patients experienced fracture after removal of the fixator when the load-share ratio dropped below 10 %, that corresponded with an axial stiffness of 1000 N/mm approximately.

The works described have reported that the assessment of the callus stiffness is a method capable of providing information about the process. However, more studies are necessary in the case of distraction osteogenesis. For example, the particularities of the bone transport process during consolidation have not been analyzed since all the studies carried out in long bone were about leg lengthening. Furthermore, the evolution of the callus stiffness with time is unknown

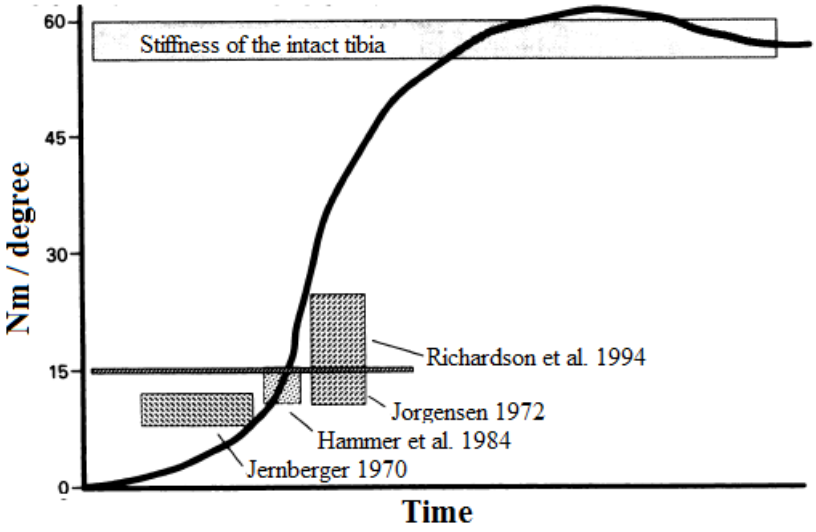

Figure 2.11: [149] Changes in fracture stiffness during the healing of tibial fractures.

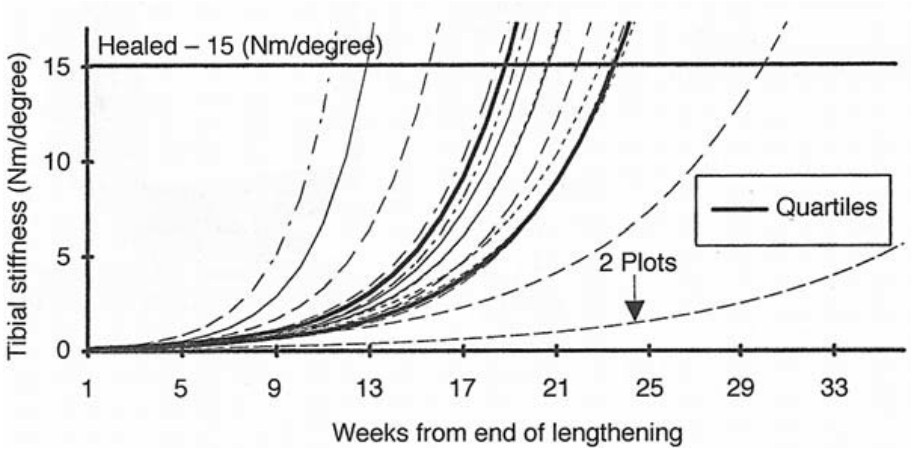

Figure 2.12: [43] Best-fit plots of the increase in tibial stiffness (Nm/deg) with time in 13 patients during bone lengthening.

at the end of the distraction osteogenesis process and the curve proposed by Richardson et al. [149] (Fig. 2.11) was not validated. Moreover the devices that were used have some drawbacks. For instance, they do not measure the callus stiffness under real load conditions in patients, e.g., during gait. Knowing the callus stiffness under real load motion conditions is useful for estimating the real load sustained by the callus because the callus presents a non-linear viscoelastic behavior [20, 55]. Additionally, the risk of bone misalignment exists in bending cases [36, 43, 68, 149]. Finally, most of these studies did not provide any calibration data for their respective devices.

The methods viewed to assess callus stiffness and load-share between the callus and the

fixator, implied the use of an instrumented fixator. Using a unique instrumented external fixator for each patient is not always viable in clinical routine since it is too expensive, complicates the surgery and may be uncomfortable for the patient. Therefore, some works in the literature have tried to evaluate mechanical parameters during the callus ossification without using instrumented fixators. Macri et al. [108] studied changes in the gait during the bone healing process but did not measure forces, thereby preventing a quantitative assessment. Seebeck et al. [159], in a study of bone healing in sheep, used a force platform to measure the ground reaction forces of the limbs during the bone healing process. The study reported that all animals unloaded the operated and overloaded the contralateral hind limb. Therefore, gait analysis was proposed as a valuable tool for monitoring the course of the callus ossification. However, as far as the author knows, the evolution of gait conditions during distraction has not been studied and has not been practiced in clinical cases to assess load bearing capacity.

2.3.4 Computational methods in distraction osteogenesis

Computational methods have been used for studying the maturation of the callus tissue both in fracture healing and distraction osteogenesis. Interpretation and analysis of experimental outcomes have been performed by means of numerical methods. In addition, mechanobiological models have been developed to predict the evolution of the callus and to analyze the effect of different biomechanical factors on the outcome of the process.

Computational models of distraction osteogenesis

Computational models have been developed to predict results of the distraction osteogenesis process and analyze different biomechanical factors that may influence the maturation of the callus: vascular supply [6, 30, 161, 162], latency period [17], rate of distraction [85, 142], frequency of distraction [16, 75] or stiffness of the fixator [140].

Fracture healing and distraction osteogenesis proceses share the same cellular healing process [88, 94]. Therefore, most existing models of distraction osteogenesis are based on existing models of fracture healing. First computational models analyzed how the geometry, material properties and loading conditions at a specific time point affect the mechanical environment around the osteotomy [15, 23, 26, 91, 102, 118, 157]. Later evolutive models were capable of predicting the spatial and temporal tissue differentiation patterns based on the existing differentiation theories such as the model presented by Prendergast et al. [138]. Idelsohn et al. [75] analyzed the influence of different distraction frequencies. Other studies predicted the tissue distribution during the entire period of distraction under different rates and frequencies of distraction [85]. In addition, Boccaccio et al. [16, 17] studied the influence of the rate of distraction and the latency period duration in human mandible distraction osteogenesis. They determined a maximum latency period of 1 week to avoid premature bony union and an optimal distraction rate of around 1.2 mm/day. Furthermore, although only in bone healing, it has been analyzed the effect of vascularization [6, 30, 161, 162], the effect of growth factors [13], angiogenesis and directed cell migration [56, 57]. Some of these models were compared with experimental results and demonstrated their potential therapeutical value [57].

Other recently models based on the mehanoregulation theory of Gómez-Benito, Doblaré

and García-Aznar [40, 52, 59] have been applied to distraction osteogenesis [140–145]. These models predicted forces in the interfragmentary gap, analyzed the influence of the distraction rate [142] and the fixator stiffness [140]. The stress accumulation during limb lengthening was also studied [144].

Predictions of computational models of distraction osteogenesis are useful and necessary to understand the process and improve the clinical applications. However, the existing computational models assumed too many inputs and they can not be used as a guaranteed tool. For example, constant values for the mechanical properties of the tissues within the callus are assumed. However, it is known that the callus tissue is heterogeneous and each tissue type varies its properties with time during the process of distraction osteogenesis or bone healing [97, 109]. Therefore, experimental studies should be performed to provide new inputs to the computational models. For instance, no works about spatial and temporal variations of the callus mechanical properties during distraction osteogenesis may be found in the literature. On the other hand, the computational models need to be validated with experiments. Many computational models have not been validated because experimental techniques do not allow measuring some of the mechanical parameters that these models use as input or output. Therefore, to facilitate validation it is important to plan computational works thinking in experimental ones and vice versa.

Analysis of experimental outcomes by means of numerical methods

Numerical methods increase the possibilities of the experimental studies and allow obtaining inputs for computational models. For example, using finite element analysis, stress and strain fields could be provided from *in vivo* experiments that measure forces (e.g. [20, 72]) if the geometry of the distraction callus is also evaluated be means of computerized tomographies [148].

Prediction of the bone tissue mechanical properties by means of CT images based finite element analysis has been assessed for reliability in the literature. Harp et al. [66] demonstrated that the stiffness of tubular bones, cortical and cancellous, can be accurately predicted by quantitative CT images. The bone mineral content in a fracture callus from CT images was correlated with experimental measurements of callus stiffness in a previous work [12]. The CT images finite element analysis method consists of obtaining the estimation of the stiffness of a bone tissue specimen using a finite element model which imports both three dimensional geometry mesh and material properties of each element (depending on the grey scale) from CT images. This method has been used in previous studies in mature bone tissue [27, 63], reconstructed bones [163], trabecular bone [119, 169], osteoporotic bone [121] and fracture callus [161]. In the last case, the method to assess fracture stiffness using computed tomography and finite element analysis was developed and validated with plastic phantoms tested experimentally in four point bending and torsion. Finite element model predictions of callus rigidity correlated significantly better with experimental torsional rigidity than other common measures of healing progress such as callus area, bone mineral density, or area moment of inertia. However, as far as the author knows, CT images based finite element analysis has not been used to estimate de stiffness of the callus during the distraction osteogenesis process.

2.4 Biomechanical factors of distraction osteogenesis

Sections above show that the distraction osteogenesis process must be studied from a biological or mechanical point of view since both aspects have influence on the process. Therefore, during the application of distraction osteogenesis there are multiple mechanical and biological factors that affect to the quality and quantity of the regenerated bone that have to be taken into account by the clinicians. The main biomechanical factors are summarize below:

- *Vascular supply*. The angiogenesis has an important role in the growth of the callus [7, 79]. It has been shown that the blood supply to the tissues within the gap after an osteotomy comes from the periosteum and the bone marrow [76, 79]. Some authors have indicated that the periosteum is the major contributor to osteogenesis during distraction [39, 183].

- *Duration of the latency period*. Experimental outcomes showed that a latency period ranged from three to ten days after the osteotomy improve the formation of bone [7, 179]. Variations in the duration of this phase affect the later ossification of the callus.

- *Rate of distraction*. It is the total displacement carried out per day of distraction. In general there is consensus about a distraction rate of 1 mm/day is suitable for bone formation[7, 79, 79, 80], although the appropriate rate of distraction may vary according to the particularities of the process.

- *Frequency of distraction*. It is the number of increments per day into which the rate of distraction is divided. Distractors that allow high frequency of distraction favor the formation of bone within the distraction callus.

- *Age of the patient*. The youth of patients promotes the ossification in the regenerate. During a distraction osteogenesis experiment in rats, Aronson et al. found higher amounts of mineralized bone in the younger rats than in the elder ones [10].

- *Length of the distraction callus*. The greater the length of the callus, the longer the time that the callus is loaded with traction stimuli and the stiffer the tissues within the callus at the end of the distraction phase. In addition, the time needed for treatment will be greater. If certain limits value for the length of the distraction callus are exceeded, depending on the particularities of the process, non-union may take place.

- *Tissue-related factors*. The properties of the tissues involved in the distraction process (bone and soft tissues) vary depending on the bone intervened, the distraction site or the animal specie where the distraction is applied. These parameters associated to the tissues involved in the process are also important factors that affect the quality of the forming distraction regenerate.

- *Stiffness of the distractor*. The mechanical environment within the distraction callus depends on the stiffness of the fixations among other factors. Therefore, the stiffness of the distractor affects the development of the distraction callus [31]. It depends on the number, length, and diameter of the fixation pins, the rigidity of the distraction device, the material properties of the device, etc.

- *Orientation of the distraction*. The regenerate within the distraction callus is always formed along the axis of the applied traction [78]. It should be taken into account specially if the distraction device or the distraction site does not allow that the distraction follows the anatomical axis of the bone segments.

Chapter 3

Design of the animal experiments

This Chapter explains the general terms of the animal experiment carried out during this thesis: the animals selection, the distraction osteogenesis application, the surgery process, the main magnitudes measured during the experiments and how the *ex vivo* samples were collected.

These experiments require the participation of an interdisciplinary team of mechanical engineers of the department of Mechanical Engineer and Manufacturing of the University of Seville, orthopaedics surgeons of the department of Orthopaedic of the Academic Hospital Virgen del Rocío of Seville and veterinarians of the department of Animal Medicine and Surgery of the Veterinary Hospital of the University of Córdoba. In this hospital, the animals were cared and the surgeries and the measurements *in vivo* were carried out. *Ex vivo* mechanical experiments, design, manufacturing and calibration of the distractor were carried out in the laboratory of the department of Mechanical Engineering and Manufacturing of the University of Seville. Last but not least, nanoindentation experiments were carried out at the department of Mechanical, Energy and Materials Engineering of the University of Extremadura.

3.1 Animals selection

This Thesis used big animals to work with conditions as close as possible to human models. According to López-Pliego [105], the differences between the distraction systems used and their anatomical characteristics (with different load distribution to human) make small animal (rats, mouses, rabbits...) models inappropriate to approach to human model studies. Sheep was chosen among big animals because they are docile and inexpensive. In addition, the sheep metatarsus, which was the bone selected to carry out the distraction osteogenesis process, has a very thin layer of surrounding soft tissue. A thin layer of soft tissue contributes to obtain accurate measurements of force through the callus (see Chapters 5 and 6).

Animals selected for this study (Fig. 3.1 A) met the following requirements: female Merino sheep, skeletally-mature, 3-5 years old, 35-70 kg body weight (BW), metatarsal length of at least 14 cm (Fig. 3.1 B) and a minimal diameter of 10 mm in the thinner area. A total of 11 animals were used. Animals without those requirements, with wounds or scars of previous injuries, bone deformities affecting the gait, local or systemic infections that could complicate the postoperative period and previous surgeries on the limbs were excluded.

Figure 3.1: Animals selection. (A) Group of selected sheep for experiments. (B) Checking the approximate length of the metatarsus.

The welfare of the animals was guaranteed by the experimentation ethics committee of the University of Seville and the supervision of the veterinarian team of the University of Córdoba. Veterinarians also trained animals to ensure welfare conditions and that animals had a controlled behavior during the *in vivo* force and stiffness measurements (see Chapters 5, 6 and 9). During a week before surgery, a similar weight to the distractor was placed in the future intervened limb and the procedures of monitoring during the distraction phase (sheep lying on the floor) and during the consolidation phase (gait tests) were simulated (see section 3.4.2).

3.2 Bone transport protocol

Among the different applications of the distraction osteogenesis process (see section 2.1), bone transport was chosen in these experiments. Bone transport was selected over the rest of applications due to its particularities (see section 2.1.1). It does not involve limb lengthening, therefore gait analysis may be carried out. In addition, it allows the study of distraction force since the force due to elongation of the surrounding tissues may be negligible with respect to the force through the distraction callus [20]. Furthermore, some aspects that affect the bone transport application are unknown or not enough studied as far as the author knows, such as the contribution to the distraction force of callus traction and docking-site compression or the influence of ossification in the recovering of gait conditions.

The complete bone transport process (see Fig. 3.2) began with a latency period of a week after surgery. From the seventh day after surgery, the distraction phase (Fig. 3.2 A) was carried out, moving the bone transportable segment (2) 1 mm each day for 15 days to fill the defect (3), of 15 mm length. After distraction, the consolidation phase (Fig. 3.2 B) was performed, until the distraction callus (1) was completely ossified. During this phase another callus was generated in the docking-site (3), i.e., the compressive union between the bone transportable segment and the distal segment of the original bone. After consolidation of the distraction and the docking-site calluses, the distractor was removed, and bone remodeling continued. The

time of the distractor removal was decided according to the force and stiffness measurements, to the X-ray controls and to the experience of the orthopedics surgeons and veterinarians that have collaborated in this experiment. The time of the distractor removal varied for each animal, being 153 ± 44 days from surgery. This variation was due to individual geometries of the bone and peculiarities of the callus maturation process for each sheep.

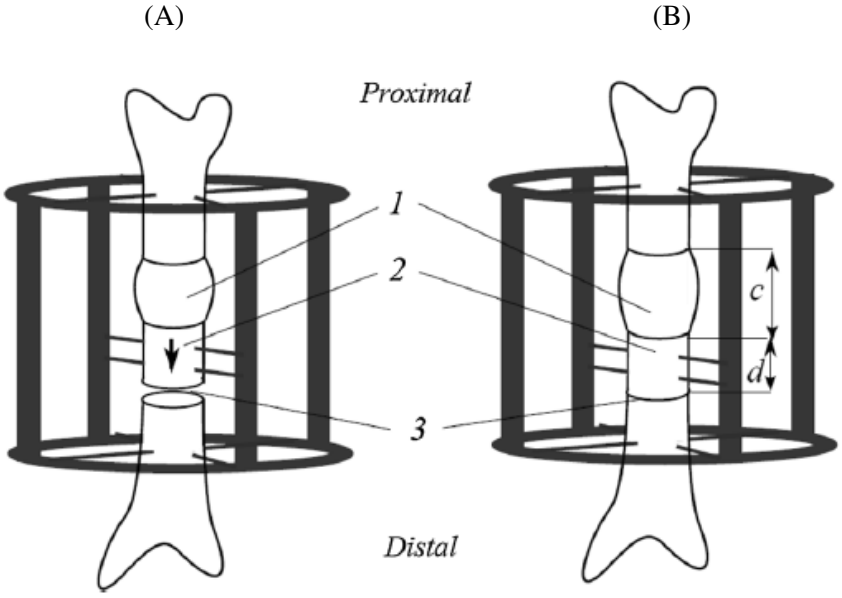

Figure 3.2: Scheme of the bone with the distractor: (A) during the distraction phase and (B) during the consolidation phase. (1) Distraction callus ($c = 15$ mm); (2) bone transportable segment ($d = 25$ mm); (3) docking site [116]

3.3 Surgery

A standard bone transport surgery was performed for each animal using general anesthesia to implant an Ilizarov type distractor instrumented with load cells in the right hind metatarsus. The fixator consisted of two circular aluminum frames (Fig. 3.2). The two frames were fixed to the bone by Schanz screws (two bicortical and one unicortical 4 mm in diameter for the distal and proximal frames) and to each other by two pairs of bars. One pair of bars (guide bars) joined the two frames, and the other pair (mobile bars) had a threaded nut system to permit the movement of the bone fragment. The mobile bars were connected to the transportable bone fragment through two bicortical Steinmann pins 3 mm in diameter. On each bar, one or two load cells were added to measure the forces (see more details about the distractor in Chapter 4).

Before the first intervention, surgeons, veterinarians and engineers repeated the procedure *ex vivo* until mistakes and unforeseen were overcome. A total of 5 surgery simulations were performed. The aims of the *ex vivo* surgery training were: to know in detail the anatomy of

the intervened limb, to optimize the pin drill, to establish the best protocol for the assembly of the distractor, to practice different methods for the osteotomy procedure, to avoid future complications and to learn the use of the designed surgical devices.

These surgical devices were the distractor described in Chapter 4 and a device designed to drill and direct the Steinmann pins and the Schanz screws of the distractor (Fig. 3.3). This device for directing pins and screws consists of two edges where two bearings can be moved and positioned at each point where a pin has to be drilled. Each bearing has guiding tubes to get an exact drilling trajectory. Before pins are drilled, the limb is fixed to the auxiliary tool's frame on proximal and distal ends and also in the middle one so that limb cannot move.

To ensure the fast before surgery and minimize problems of regurgitation and postoperative bloat, solid food and water were avoided 36 hours and 6 hour prior of surgery respectively. The complete surgery process lasts 4 hours approximately and consists of the following steps:

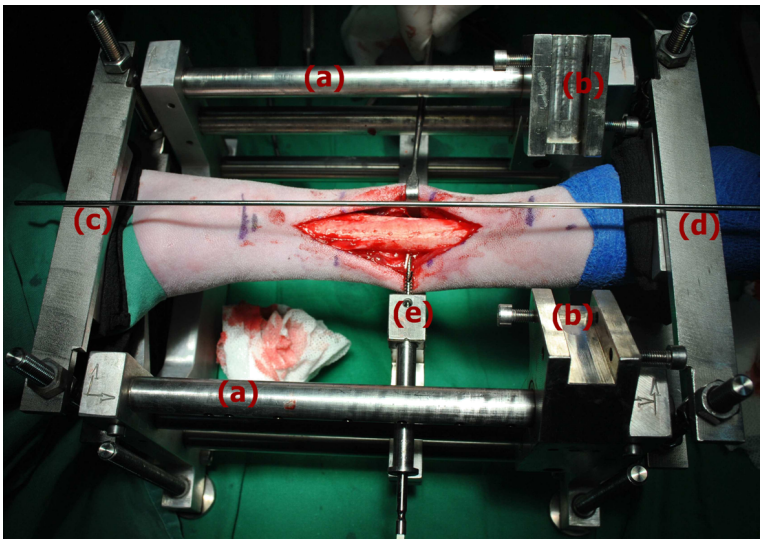

Figure 3.3: Auxiliary tool used during surgery: (a) edges; (b) bearings; (c-e) proximal, distal and middle limb fixation respectively.

- *Anesthesia induction and monitoring* (see Fig. 3.4 A). First, the animal was immobilized and its external jugular venous was catheterized. After, it was premedicated using dexmedetomidine (*Dexdomitor*® 0.5 mg/ml; Orion Pharma, Espoo, Finland), butorphanol (*Torbugesic*® 1%, Fort Dodge, Girona, Spain) and cefazolin (*Kurgan*® 1 g; Normon, Madrid, Spain). 15 minutes later, endotracheal intubation and anesthesia induction using propofol ($Propofol - Lipuro$® 1%; BBraun VetCare, Barcelona, Spain) were carried out. Anesthesia was maintained using isoflurane to an inspired concentration of 1.4% - 1.5% ($Isoflo$®; Esteve, Barcelona, Spain). The monitoring during the surgery included electrocardiography, pulse oximetry, capnography / capnometry, invasive blood pressure (using the femoral artery of the left leg), body temperature, and anesthetic gases analysis.

- *Surgical approach*. The animal was placed in right lateral decubitus, holding the left leg with a bandage, leaving the right leg placed on a side table, with the medial face exposed to surgeons. Once the animal was disposed, surgeons marked in the limb the location where the distractor had to be implanted according to the animal anatomy particularities (tendons and vessels location, size of the bone etc), the location of the osteotomies and the initial wound. After dissection by planes was performed with cold scalpel, using electrocautery in case of bleeding, the metatarsus is separated from all the soft tissues around it (see Fig. 3.4 B).

  Before, the limb was shaved and cleaned up with soap and water, isolating the hoof with a self-cohesive bandage. The surgical field was isolated from the rest with the help of sterile drapes. The whole procedure was carried out under strict aseptic measures.

(A) (B)

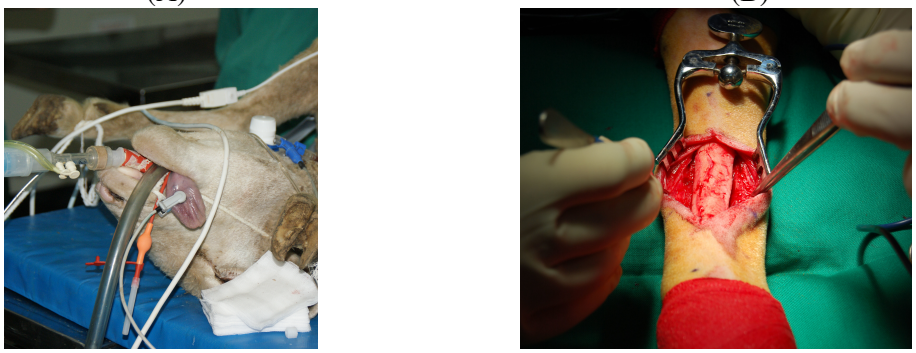

Figure 3.4: Images during the anesthesia induction (A) and after the surgical approach (B)

- *Fixation of the limb*. The limb was fixed to the device designed to drill and direct the pins and the screws of the distractor. This device holds the limb applying a controlled pressure in the ends of the limb by means of two adjustable plates. The limb was protected with foams. In addition, the fixation of the limb to the device was ensured by a screw drilled in the segment that was removed after creating the 15 mm defect (see Fig. 3.5 A).

- *Drilling of screws and pins*. Once the limb was fixed to the device for drilling and directing the pins and the screws, those were drilled from distal to proximal since the metatarsus has a smaller diameter in the distal region. The use of the auxiliary tool allows drilling the fixator's Schanz screws and the Steinmann pins in the correct direction. Therefore, the bone overloading due to correction of trajectory was avoided. Fig. 3.5 shows the limb after the first Schanz screw was drilled (B) and after all, 6 Schanz screws and 2 Steinmann pins were drilled (C). To facilitate the operation, the Schanz screws, 4 mm in diameter, were drilled after predrilling with a 3.5 mm pin and the Steinmann pins, 3 mm in diameter were also pre-drilled with 2.5 mm.

- *Assembly of the fixator*. The pieces of the distractor were assembled to the pins and screws fixed before (Fig. 3.6). Firstly, the proximal and distal circular frames of the fixator were fixed to the proximal and distal sets of Schanz screws. Secondly, the bars

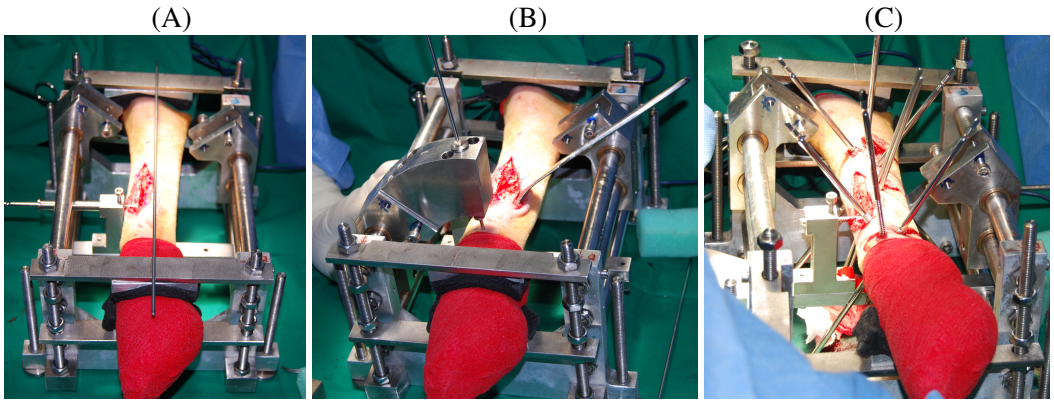

Figure 3.5: Image after the fixation of the limb to the device director of pins and screws (A), after the drilling of the first Schanz screw (B) and after the complete process of drilling (C).

of the fixator were assembled to the proximal and the distal frames. Thirdly, the mobile bars were fixed to the Steinmann pins. Finally, all the screws that join the different pieces were inspected and fixed. During the surgery, bars without load cells were mounted since load cells do not support the sterilization process for pieces which are used during the surgery. One week later, at the end of the latency period, the surgery bars were replaced by other with load cells which may be connected to the acquisition system. During the change of each bar the stiffness of the fixation is guaranteed by the connection of the other three bars.

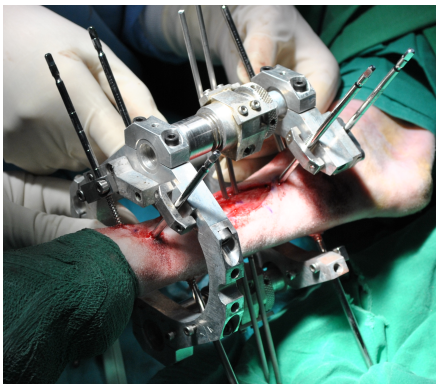

Figure 3.6: Assembly of the fixator.

- *Osteotomies*. Once the bone was fixed to the distractor, osteotomies are carried out using an oscillating saw guided by a tool also designed for this case (Fig. 3.7 A). Three osteotomies were made resulting in two small bone fragments in the mid diaphysis. The distal bone fragment was retired, creating the defect, and the proximal, the bone transportable segment, fixed to the distractor before cutting. Thus, there were two focus areas during the bone transport process: the distraction callus and the docking site (Fig.

3.2). The former, the distraction callus, represents the distance created by distracting the proximal osteotomy whilst the latter, the docking-site, is the gap or the callus of union (depending on the phase, distraction or consolidation respectively) between the bone transportable segment and the most distal segment of the metatarsus (Fig. 3.2). Fig. 3.7 B shows the bone after osteotomies were carried out and the defect was created.

Before each osteotomy, the periosteum located at osteotomy area was cut using a periosteotome and rolled up with the aim of separating 2 - 3 mm. This method was followed to avoid damage in the periosteum tissue because of the high temperature in the cutting area of the oscillating saw. It was also used in other works [31] to preserve the periosteum. Some authors have indicated that the periosteum is the major contributor to osteogenesis during distraction [39, 183].

(A) (B)

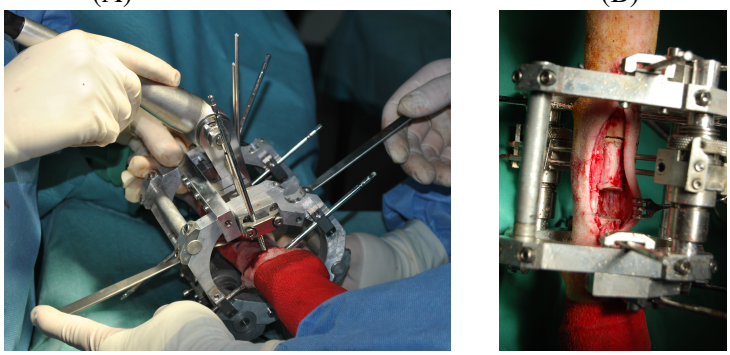

Figure 3.7: Image during the first osteotomy (A) and after the three osteotomies were carried out (B)

- *Stitching of the wound.* (3.8 A) After osteotomies were carried out, the area intervened was cleaned with saline solution and the skin was stitched. The area of the wound was covered with an insulating elastic bandage and another bandage was used to cover the distractor.

- *Reanimation*. (3.8 B) Finally, the animals were moved to a reanimation area where they were under control of the veterinarian team until they were free from some effect of anesthesia.

3.4 Experiments planning

This section aims to summarize the planning of the experiments carried out during this thesis. Both *in vivo* and *ex vivo* tests were carried out; therefore the design of the experiment during the animal life and after sacrifice is explained. The different tests and measurements that were performed during the experiments may be classified as mechanical monitoring, clinical monitoring and numerical analysis. The mechanical monitoring includes the following measurements: *in vivo* distraction force, *in vivo* force through the callus and the fixator during

Figure 3.8: Sewing of the wound (A) and one of the animals just after the reanimation process (B)

gait, *in vivo* gait analysis, *in vivo* stiffness estimation and elastic modulus via nanoindentation *ex vivo*. In the case of the clinical monitoring, it includes: radiographies, angiographies, histologies, composition analysis, CT images and 3D reconstruction. The numerical analysis was used for the estimation of the callus stiffness based on CT images and 3D reconstruction. These tests and measurements were used in the following Chapters according to their particular aim: calibration of *in vivo* force and stiffness measurements (Chapter 4); *in vivo* force monitoring during the distraction phase and x-rays (Chapter 5); 3D callus reconstruction from CT images, *in vivo* force and stiffness monitoring (Chapter 6); elastic modulus measurements via nanoindentation and micrographies of *ex vivo* samples (Chapter 7); numerical analysis using 3D callus reconstruction from CT images (Chapter 8); and gait analysis (Chapter 9). Moreover, other measurements were performed which were not used in this Thesis but were part of other studies, e.g., histologies [105], angiographies or analysis of composition [53]. Tables 3.1 and 3.2 include the complete planning of the experiments. The different tests and measurements carried out for each animal and each time point are explained briefly in the next sections and more details may be found in their corresponding Chapters. For each week or day of the process, the tests and measurements that were performed are detailed. The week or day in which each animal was sacrificed is also indicated.

3.4.1 Harvest of samples for *ex vivo* studies

10 of the 11 animals were sacrificed (using T-61® intravenously) interrupting the bone transport process at different stages: 17, 22, 29, 36, 37, 51, 79, 98, 161 and 525 days after surgery (see Tables 3.1 and 3.2). In these cases, to avoid misalignment of the bone segments, the distractor was removed only after the limb with the fixator from each sacrificed animal was frozen. Once, free of fixations, computerized tomography images of the limb were obtained. Later, the distraction and the docking-site calluses were harvested from each limb and divided for using in histology, Ca composition and nanoindentation studies. The limbs were cut in the longitudinal direction as it is indicated in Fig. 3.9 dividing it in three pieces: a half for the histology study, a quarter for nanoindentation studies and the remaining quarter for composition studies.

Table 3.1: Planning of the experiments for animals sacrificed until 51 days after surgery. S, animal sacrifice. Clinical monitoring: X, x-rays; A, angiographies; H, histologies; C, composition analysis; T, CT images. Mechanical monitoring: F_d, *in vivo* distraction force measurement; F_g, *in vivo* force through the callus and the fixator measured during gait; K_g, *in vivo* stiffness estimation from force measurements; F_{g2}, *in vivo* gait analysis; E, *ex vivo* nanoindentation measurement of the callus elastic modulus. Numerical analysis: K_n, estimation of the callus stiffness based on CT images

	Time after surgery	Sheep code					
		9	7	8	6	3	11
Latency	week 1	X	X	X	X	X	X
Distraction	day 8		F_d	X, F_d	X, F_d, A	X, A	X
	day 9		X, F_d	F_d	F_d, F_g		
	day 10		F_g				
	day 11		F_d				
	day 12		F_d, F_g	F_d			
	day 13		F_d				
	day 14		F_d				
	day 15		F_d		F_d		
	day 16		F_d	F_d	F_d, F_g		
	day 17	X, S, H T, K_n	F_d		F_d		
	day 18		F_d	F_d	F_d, F_g		
	day 19			F_d	F_d		
	day 20			F_d			
	day 21		X	F_d	X	X	
	day 22		S, H, T, K_n	X, F_d			X
	day 23				F_d, F_g, K_g		
Consolidation	week 4				F_g, K_g	X, A	
	week 5			X, S, H T, K_n	X, S, H, C T, E, K_n	X, A	X
	week 6					S, H, C, T, K_n	X
	week 7						X
	week 8						X, S, H, C T, E, K_n

The pieces of the limb were stored frozen at -80°C until each test was carried out.

3.4.2 Mechanical monitoring

In vivo stiffness and force measurements

The force through the distraction callus and the fixator were monitored during the distraction and the consolidation phases. In addition, the distraction callus stiffness was estimated from the force measurements at the time points indicated in Tables 3.1 and 3.2:

- *In vivo distraction force measurements.* Daily force measurements were performed during each step of distraction. These tests consisted of monitoring continuously (100 pps) the force through the load cells of the fixator. Different forces were calculated from these measurements: the force through the callus and the force through the docking-site during the movement of the bone transportable segment, and the posterior force relaxation (see more details about how forces were measured, the acquisition system and results in Chapters 4 and 5). A minimum of 8 force relaxation measurements were performed per animal in 7 of the animals during the 15 days of distraction (see Tables 3.1 and 3.2). The duration of each test varied between 10 and 50 minutes depending on animal conditions. During data acquisition, the animals were in a lying sideway position with their limbs immobilized. These measurements allowed obtaining a model of the distraction callus tissue behavior (Chapter 5).

- *Force through the callus and the fixator during gait.* For 9 of the 11 animals, gait tests

Table 3.2: Planning of the experiments for animals sacrificed from 51 days after surgery, (A) latency and distraction phases, (B, next page) consolidation and remodeling phases. *S*, animal sacrifice. Clinical monitoring: *X*, x-rays; *A*, angiographies; *H*, histologies; *C*, composition analysis; *T*, CT images. Mechanical monitoring: F_d, *in vivo* distraction force measurement; F_g, *in vivo* force through the callus and the fixator measured during gait; K_g, *in vivo* stiffness estimation from force measurements; F_{g2}, *in vivo* gait analysis; *E*, *ex vivo* nanoindentation measurement of the callus elastic modulus. Numerical analysis: K_n, estimation of the callus stiffness based on CT images.

(A)

	Time after surgery	Sheep code				
		2	1	4	5	10
Latency	week 1	X	X	X, A	X, A	X
Distraction	day 8	X, A, F_d		X, F_d, F_{g2}	X	F_{g2}
	day 9			F_d,F_g, F_{g2}		F_d,F_g, F_{g2}
	day 10		X	F_d,F_g, F_{g2}		X, F_{g2}
	day 11			F_d,F_g	F_d, F_g, F_{g2}	F_d, F_{g2}
	day 12					
	day 13					
	day 14				F_d, F_g, F_{g2}	F_{g2}
	day 15	F_d, F_g			F_d, F_g, F_{g2}	F_d
	day 16	F_d, F_g	X		F_d, F_{g2}	F_d, F_{g2}
	day 17	F_d, F_g		F_d,F_g, F_{g2}	F_d	F_d
	day 18	F_d		F_d,F_g, F_{g2}	F_d	F_d, F_{g2}
	day 19	F_d, F_g		F_d,F_g, F_{g2}	F_d	F_d
	day 20	F_d, F_g		F_d, F_{g2}	F_d	
	day 21	F_d		X, F_d, F_{g2}	F_d, F_{g2}	X, F_d, F_{g2}
	day 22			F_d, A, F_{g2}	X, F_d, F_g	F_d
	day 23	X, F_d, F_g	X	F_g, K_g, F_{g2}		F_g, K_g, F_{g2}

(B)

	Time after surgery	Sheep code				
		2	1	4	5	10
Consolidation and remodeling	week 4	X		X, F_g, K_g, F_{g2}	F_g, F_{g2}	X, F_g, K_g, F_{g2}
	week 5	X, A		X, F_g, K_g, F_{g2}	X	X, F_g, K_g, F_{g2}
	week 6	X, A, F_g, K_g	X	X, F_g, K_g, F_{g2}	X, F_g, K_g, F_{g2}	X, F_g, K_g, F_{g2}
	week 7	X, F_g, K_g		X, F_g, K_g, F_{g2}	X, F_g, K_g, F_{g2}	X, F_g, K_g, F_{g2}
	week 8	X, F_g, K_g	X	A, F_g, K_g, F_{g2}	X, F_g, K_g, F_{g2}	F_g, K_g, F_{g2}
	week 9	F_g, K_g	X		F_g, K_g, F_{g2}	X, F_g, K_g, F_{g2}
	week 10	X, A, F_g, K_g	X	X, A, F_g, K_g, F_{g2}	X, F_g, K_g, F_{g2}	F_g, K_g, F_{g2}
	week 11		X	F_g, K_g, F_{g2}	F_{g2}	X, F_{g2}
	week 12	X, A, S, H C, T, E, K_n	X	X, F_g, K_g, F_{g2}	F_g, K_g, F_{g2}	X, F_{g2}
	week 13			F_{g2}		
	week 14		X, A, S, H T, E, K_n	X, F_{g2}		
	week 15			A	X	X, F_{g2}
	week 16					X
	week 17					F_{g2}
	week 19			X, A	X	
	week 20					X, T, K_n
	week 21				X	F_{g2}
	week 22			X	X	
	week 23			S, H, T, E, K_n		
	week 25					X
	week 26				X	
	week 28				X	F_{g2}
	week 29					X
	week 30				X	T, K_n
	week 32				X	
	week 34					X
	week 35				F_{g2}	
	week 36				X	
	week 37				F_{g2}	
	week 40				X, T, K_n	F_{g2}
	week 41				F_{g2}	
	week 45				X	T, K_n
	week 48				F_{g2}	
	week 49				X	
	week 54				X	
	week 55				T, K_n	
	week 60				F_{g2}	
	week 68				T, K_n	
	week 75				S, H, E	

were carried out three times per week a maximum of three times a week since distraction began (see Tables 3.1 and 3.2). As it may be observed in Tables 3.1 and 3.2, it

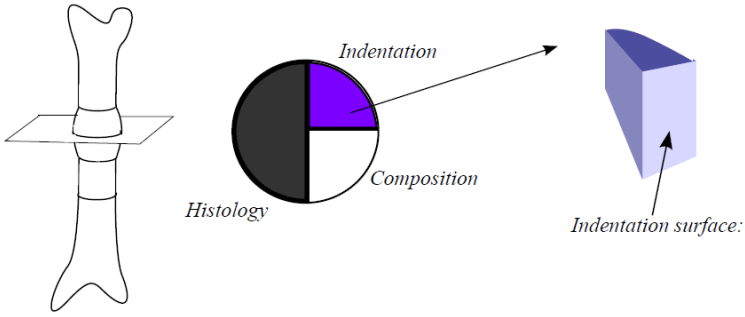

Figure 3.9: Distribution of the limb pieces to obtain the different samples for the *ex vivo* studies carried out (histology, composition and indentation).

was not possible to repeat the tests every week for all animals because of animals limitation and equipment availability (see more details in Chapter 6). Each gait test (Fig. 3.10) consisted of measuring the ground reaction force (GRF) and the force through the fixator in the test before the fixator removal. Afterwards, the rest of forces involved in the bone-fixator system while the sheep was walking (force through the callus, force through the docking-site) were estimated as described in Chapter 4. For a complete set of measurements, the animal had to tread at least 10 times with the intervened limb on the force platform. Mean forces of 5 valid treads were obtained. A tread was considered valid if the force data was measured when the sheep walked at 2-4 km/h [42, 115, 116]. More details about the methods for *in vivo* force measurements during gait are included in Chapters 6. In Chapter 6 *in vivo* force measurements during gait were used in the assessment of the force through the callus and through the fixator during the consolidation phase, before the distractor removal.

- *In vivo callus stiffness assessment during the consolidation phase.* The stiffness of the callus has been assessed during the consolidation phase from the *in vivo* force measurements (see results in section 6). In Chapter 4 the methods to calculate stiffness from force measurements are explained.

- *Gait analysis.* In Chapter 9, GRF measurements were used in gait analysis during the complete process of bone transport. In this case, gait tests were performed even after the distractor was removed to collect the GRF measurements. See more details in Chapter 9

Ex vivo measurement of the callus mechanical properties

Nanoindentation tests were performed to obtain the elastic modulus of the woven bone. It was carried out in distraction and docking-site calluses samples harvested from sacrificed animals in which most of the callus tissue was ossified (35, 50, 79, 98, 161 and 525 days after surgery; see Tables 3.1 and 3.2). See methods and results of the nanoindentation experiments in Chapter 7.

Figure 3.10: Sheep during a gait test [115]: (1) force platform; (2) wooden platform; (3) instrumented fixator; (4) A/D converter for the load cells signals.

3.4.3 Clinical monitoring

X-ray study

Radiographies were performed to control the maturation of the callus and validate other results such as force distribution, callus stiffness, callus volume etc. The frequency of the x-rays was once per week since the surgery to 8-9 weeks after, once per two weeks from 8-9 to 14-15 weeks after surgery and once per month from 14-15 weeks after surgery (see Tables 3.1 and 3.2). To ensure that the callus growing was being balanced, x-rays were performed in two different views: from anterior to posterior and from lateral to medial.

Vascularization study

Evolution of the vascularization in the intervened limb was assessed by means of angiographies. Angiographies consisted of performing radiographies while a contrast substance is injected to the vessels of the intervened limb. Angiographies were done at different time points in some of the animals (see Table 3.1 and 3.2). The quantification of the level of vascularization of the distraction callus and the docking-site was not an objective of this Thesis.

Histological and composition study

Although they were not aims of this thesis, it is worth mentioning that samples from all animals of the experiments carried out for this thesis were used for a histological study [105] and some of them for a composition study (sheep 3, 6, 11 and 2: 35, 37, 50 and 79 days after surgery) [53] (see Table 3.1 and 3.2).

CT and 3D reconstruction

CT images of the intervened limb were taken at different moments of the process to assess the state of maturation of the callus with time. The resolution of the CT images was 200-300 μm/voxel. The callus 3D reconstruction was obtained from CT images by segmentation, using the software MIMICS® (Materialise, Leuven, Belgium). The total volume was quantified as well as the external and the internal callus volumes for the distraction callus (see Chapter 6). Furthermore, the percentage of bone and soft tissue volumes within the callus were assessed (see Chapter 8). CT images were performed both *in vivo* and *ex vivo* (see Tables 3.1 and 3.2). CT images could not be performed *in vivo* in limbs which had the fixator installed due to the reflections of the metallic parts. To carry out CT images before callus was ossified completely, nine animals were sacrificed interrupting the process at different stages (17, 22, 29, 35, 37, 51, 79, 98, and 161 days after surgery). The other two animals were studied after the callus had been totally ossified and the distractor had been removed. Hence, it was not necessary to sacrifice these animals and various CT images *in vivo* could be taken at different time points (137, 205, 277, 311, 379 and 471 days after surgery).

3.4.4 Numerical analysis

The 3D reconstruction of the distraction callus was also used to create finite element models (see Chapter 8). Material properties were assigned to the elements of these models using different methods and the callus stiffness was estimated for each time point of CTs (see Tables 3.1 and 3.2).

Chapter 4

Distraction osteogenesis devices to monitor force and callus stiffness *in vivo*

This Chapter is based on a paper published: J Mora-Macías, E Reina-Romo and J Domínguez. Distraction osteogenesis device to estimate the axial stiffness of the callus *in Vivo*. *Medical Engineering & Physics*, 37(10):969-78, 2015. It includes the design and the calibration of the distractor used in the experiments carried out and in the measurements of force and stiffness of the distraction callus reported in the Chapters below.

Chapter 5

In vivo study of force relaxation during distraction

In this Chapter a model of the callus tissue behavior during the distraction phase is proposed based in the experiments *in vivo*. These results are included in a paper published in literature: J Mora-Macías, E Reina-Romo and J Domínguez. Model of the distraction callus tissue behavior during bone transport based in experiments *in vivo*. *Journal of the Mechanical Behavior of Biomedical Materials*, 15(61):419-430, 2016.

Chapter 6

In vivo mechanical characterization of the distraction callus during bone consolidation

This Chapter reports the measurements of forces through the fixator and the callus stiffness *in vivo* during the consolidation phase of the bone transport process. The evolution of the bone volume of the callus at different stages is also presented. These outcomes allow relating quantifiable biological aspects (callus volume and tissue production rate) with mechanical parameters (callus force and stiffness) using data from the same bone transport experiment (Chapter 3). All these results, included in this chapter, were published: [115]: *In vivo* mechanical characterization of the distraction callus during bone consolidation. J Mora-Macías, E Reina-Romo, M López-Pliego, MA Giráldez-Sánchez and J Domínguez. *Annals of Biomedical Engineering*, 43(11):2663-74, 2015.

Chapter 7

Spatial and temporal variations of the callus mechanical properties via nanoindentation

In previous Chapters the evolution of the distraction callus stiffness, the force through the callus *in vivo* and the volume of the woven bone during the bone transport process have been provided. To understand the mechanobiology mechanisms that rule these macroscopic parameters it is necessary to know the mechanical properties of the callus tissue at a smaller scale. The aim of the work presented in this Chapter is to characterize the spatial and temporal variations of the woven bone within the docking-site and distraction calluses by means of nanoindentation experiments. The results presented here are based on a paper submitted for publication: J Mora-Macías, A Pajares, P Miranda, J Domínguez and E Reina-Romo. Spatial and temporal variations of the mechanical properties of the woven bone during bone transport.

7.1 Introduction

From its introduction by Ilizarov [78, 79], distraction osteogenesis has been studied by means of histology and radiography studies [7, 9, 11, 38, 49, 78, 79, 92, 124]. These works evaluated the callus tissue types, the ossification modes and other parameters such as angiogenesis within the callus. It was demonstrated that the differentiation and the stiffening of the tissues within the distraction callus depend on the mechanical environment [95, 150]. Therefore, knowing the evolution of the callus mechanical properties and tissue types over time contributes to understand the mechanobiology of the new bone regeneration and optimizes the application of distraction osteogenesis in clinical practice by means of numerical models [85, 140–145]. Macroscopic mechanical properties of the distraction callus have been studied in the literature both *ex vivo* [47, 123] and *in vivo* [4, 20, 31, 43, 72, 113, 115, 116]. *Ex vivo* studies [47, 123] have provided values of the stiffness of the distraction callus at different time points during the process. *In vivo* studies also provided the evolution of the callus stiffness with time [4, 43, 113, 115, 116] although measurements were limited to the time of the distractor removal. In addition, these studies reported the increase of the force through the callus and

the woven bone tissue volume with time during the consolidation phase. Some of the *in vivo* studies carried out focused on other mechanical aspects such as the force relaxation within the callus tissue during the distraction phase [20, 72, 113, 115, 116] or the influence of the interfragmentary displacement [31]. Still all methods used in these works do not provide information on the material properties of the distraction callus through the stages of the bone tissue regeneration at a microstructural level. In addition, they do not allow obtaining local variations of the mechanical properties within the callus tissue.

Nanoindentation technique allows determining the elastic modulus and contact hardness of materials point by point with a high spatial resolution [125]. It has been applied successfully to assess the mechanical properties of biological tissues [127], both soft tissues [61, 126, 168, 186] and hard tissues [5, 21, 97, 98, 107, 109, 129, 147, 152–154, 164, 165]. These studies carried out in bone have provided some findings about the influence of nanoscale heterogeneity in bone strength [164, 165], the bone permeability changes [154] or the values of elastic modulus of the callus in bone healing [5, 97, 98, 109]. In the last case, Leong and Morgan [97] measured the elastic modulus of the tissues within the callus during fracture healing. Although they obtained the elastic modulus for different tissue types, the results presented high scatter and the study only used one time point during the bone healing process. Manjubala et al. [109] reported, for the bone tissue of the callus during bone healing, the mean values of the elastic modulus evolution with time, the spatial variation with the distance from the cortex periosteum and the heterogeneity by means of elastic modulus maps among others.

As far as the author knows, no mechanical properties of callus tissue were assessed via nanoindentation during distraction osteogenesis. Information about spatial and temporal variation of the local elastic modulus and hardness of the callus during distraction osteogenesis could contribute to clarify controversial or unknown aspects in literature about distraction osteogenesis. For example, it is unknown the contribution of the increase of the bone tissue volume within the callus and the mechanical properties of the callus tissues to the increase of the macroscale callus stiffness during the process. On the other hand, in the particular case of bone transport, as far as the author knows, most of the studies about mechanical parameters assessment have been focused on the distraction callus and not in the docking site callus [20, 31, 72]. However, docking site is known to be a frequent source of problems because of the difficulty of its consolidation [51, 73, 111]. Therefore, the aim of this work is to assess the spatial and temporal variations of the elastic modulus of the woven bone tissue within the distraction callus during the bone transport process carried out in the experiments described in Chapter 3. Bone transport was applied in sheep and callus samples were evaluated via nanoindentation at different time points of the process and different regions of interest within each specimen.

7.2 Materials and methods

7.2.1 Sample preparation

The samples used in this study came from the above mentioned bone transport experiments carried out (see Chapter 3, [113, 115, 116]). During these experiments, animals were sacrificed at different time points and a quarter of the intervened bone (right metatarsus) cut in longitu-

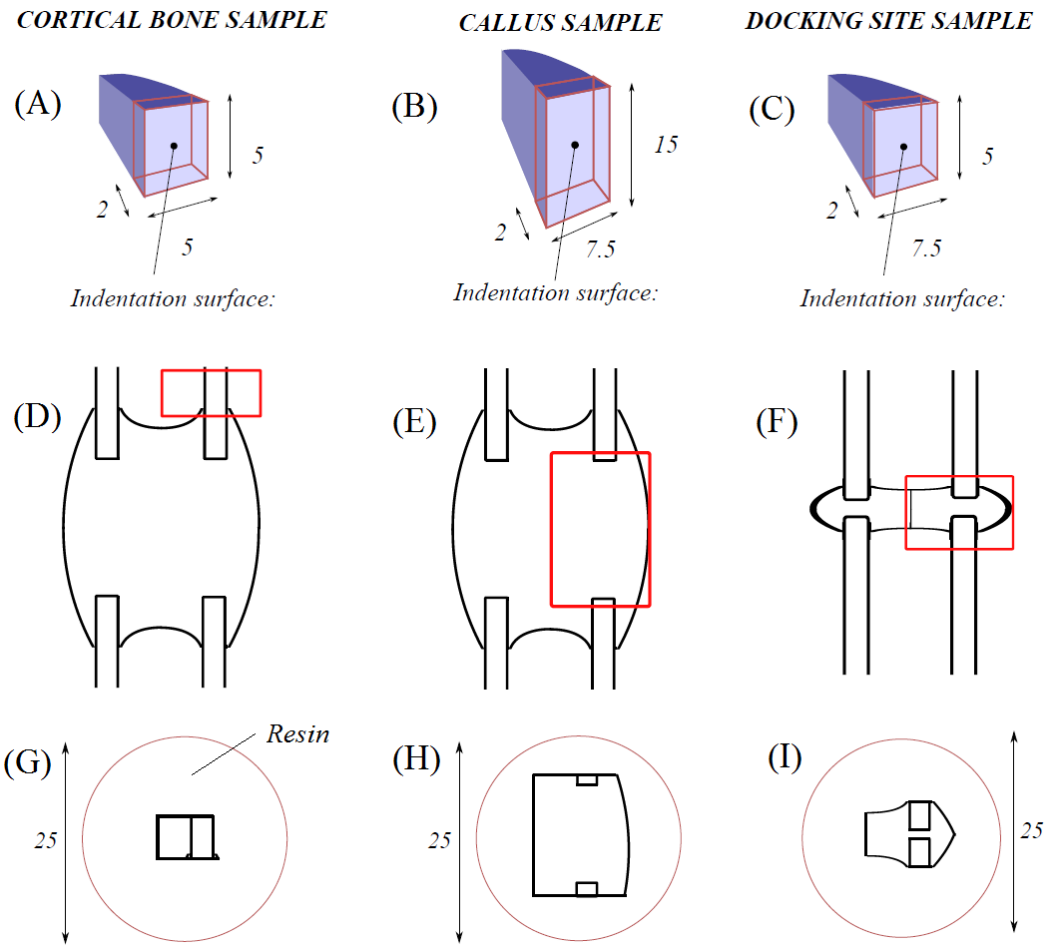

Figure 7.1: (A), (B) and (C), cortical bone, distraction callus and docking site samples from the quarter of the intervened limb designed for nanoindentation experiments. (D), (E) and (F), surface for nanoindentation within the cross section (parallel to frontal plane) of the area of cortical bone, distraction callus and the docking site. (G), (H) and (I), indentation surface of samples embedded en the resin cylinder of 25 mm in length and diameter.

dinal direction was preserved for indentation experiments by freezing at -80 ^{o}C. Since the aim of this study was the characterization of the woven bone, only specimens in which the most of the tissue within the callus had been ossified were used (35, 50, 79, 98, 161 and 525 days after surgery). For each animal, two woven bone samples were needed from the two focuses of woven bone generated during bone transport: the distraction and the docking site calluses. In addition, a cortical bone sample from the proximal bone segment was also obtained for control measurements. Therefore, three segments of bone were extracted from the quarter of the limb selected for nanoindentation tests: one from the distraction callus, another one from the docking-site and the cortical bone samples (see Figs. 7.1 A, B and C). Fig. 7.1 shows in the frontal plane the piece (plane of indentation) of the limb corresponding to the cortical bone

sample (5 mm in length, Fig. 7.1 D), the piece of the callus sample (15 mm in length, Fig. 7.1 E) and the docking-site sample (5 mm in length, Fig. 7.1 F).

For each piece, a 2 mm width sheet in the surface of the piece parallel to the frontal plane was extracted and embedded in an Epofix® (Struers, California, US) resin cylinder. Figs. 7.1 G, H and I show a scheme of the indentation surface of each sample after embedding in the resin cylinders 25 mm in diameter and 25 mm in height. These surfaces were polished with carbide papers (P600 to P4000) and diamond slurry (from 3 to 0.25 μm). Colloidal silica slurry (0.04 μm) was used for the final polishing step. The samples were cleaned ultrasonically with distilled water between each polishing step. The total process of sample preparation took 3 days from thawing. Fig. 7.2 shows pictures of the three type of samples for one of the animals (161 days after surgery) after the polishing process was completed.

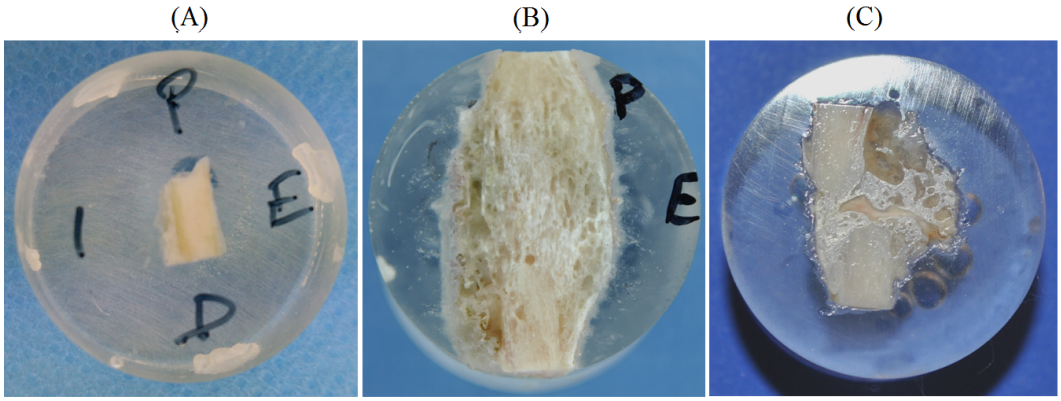

Figure 7.2: (A) cortical bone, (B) distraction callus and (C) docking-site samples of the sheep sacrificed 161 days after surgery.

7.2.2 Nanoindentation measurements

Instrumented indentation (Nanotest, Micro Materials Ltd. Wrexham, UK) was performed to determine the reduced elastic modulus (E_r) and hardness (H) of the cortical and woven bones using the Olive Pharr method [125] (see more details in Appendix A). The indentation tests were performed at ambient laboratory conditions using a Berkovich diamond indenter. The load was increased monotonically at a rate of 0.5 mNs^{-1} to a maximum load of 5 mN and held for 40 s before unloading at 0.5 mNs^{-1} rate. The load-depth data were processed using Oliver and Pharr method [125] to determine E_r. The accuracy of the nanoindentation equipment was evaluated by means of indentation in fused silica, whose mechanical properties are homogeneous and do not vary with time. Differences in these measurements were evaluated to be below $\pm$ 2 % for E_r.

Distribution of indentations in the cortical bone, distraction and docking-site calluses follows. For the tests carried out, distance between indentations was chosen according to the minimum trabecula thickness of the new bone tissue of the callus. It was evaluated by means of the histology images obtained from samples of the same experiments. For example, Fig. 7.3

A shows the histology images of different areas of the woven bone within the distraction callus 17 days after surgery [105]. Fig. 7.3 B shows quantitatively how the width of the trabeculae in the distraction callus increased with time after surgery [105]. The lowest values of trabecula thickness were measured for samples harvested before 50 days after surgery. The mean values of trabecula thickness were above 50 μm. Therefore, a distance between indentations of 50 μm was established to ensure that an aceptable number of indentations were carried out in woven bone and no in porous areas.

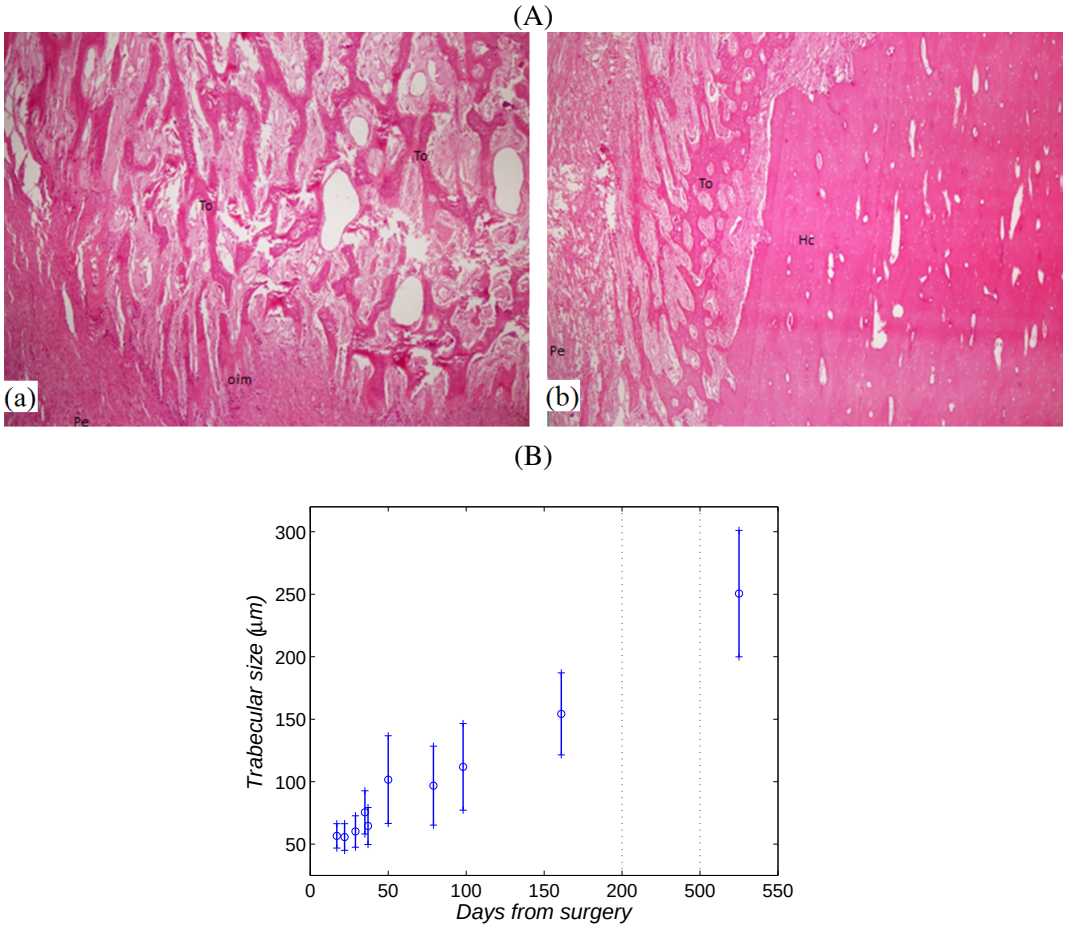

Figure 7.3: (A) Trabeculae thickness of regenerate 17 days after surgery. 40X magnification: (a) Proximal area, (b) Distal area, Pe: periosteum, To: woven bone trabeculae, Hc: compact bone, oim: intramembranous ossification focus [105]. (B) Quantification of the woven bone trabeculae thickness in the callus tissue of all the harvested samples [105].

Indentation experiments distribution and duration for the three types of samples of each sheep (cortical bone, distraction callus and docking site samples) are detailed in Fig. 7.4 and Table 7.1. A matrix of 16 x 16 indentations (750 x 750 μm) was performed in the cortical bone sample (A). In the callus sample two indentation lines were done in transverse and in longitudinal direction with distance between each indentation and between lines of 50 μm. Lines in

longitudinal direction were positioned following the cortical bone orientation, approximately among 3 and 7 mm from the central axis of the limb (B1). Lines in transverse direction were positioned approximately between 2 and 4 mm from the proximal end of the callus (B2), which is about a quarter of its total length. In addition, three matrices of 16 x 16 indentations (750 x 750 μm) were performed: in the middle of the section (B4), a quarter from proximal (B3) end and a quarter from distal end (B5). In the docking site sample two indentation lines were done in transverse direction just between two bone fragments, with distance between each indentation and between lines of 50 μm. (D1). Furthermore, a matrix of 16 x 16 indentations (750 x 750 μm) was performed just between the two cortical bone fragments in longitudinal direction (D2), in the exterior of the callus (some millimeters from cortical bone external diameter).

The time necessary to carry out the experiments is included in Table 7.1. Cortical bone sample (A) could be carried out in approximately 1 day, distraction callus samples (B1-B5) would need approximately 6 days and docking site samples 2 days. Results reported in Appendix A showed that the time-dependence of the nanoindentation measurements of E_r and H in bone and woven bone specimens prepared following the described procedure is not significant in the time needed for experiments (A maximum of 10 days taking into account the sample preparation and the duration of the indentation tests) compared to other factors of variation such as the heterogeneity of the tissue.

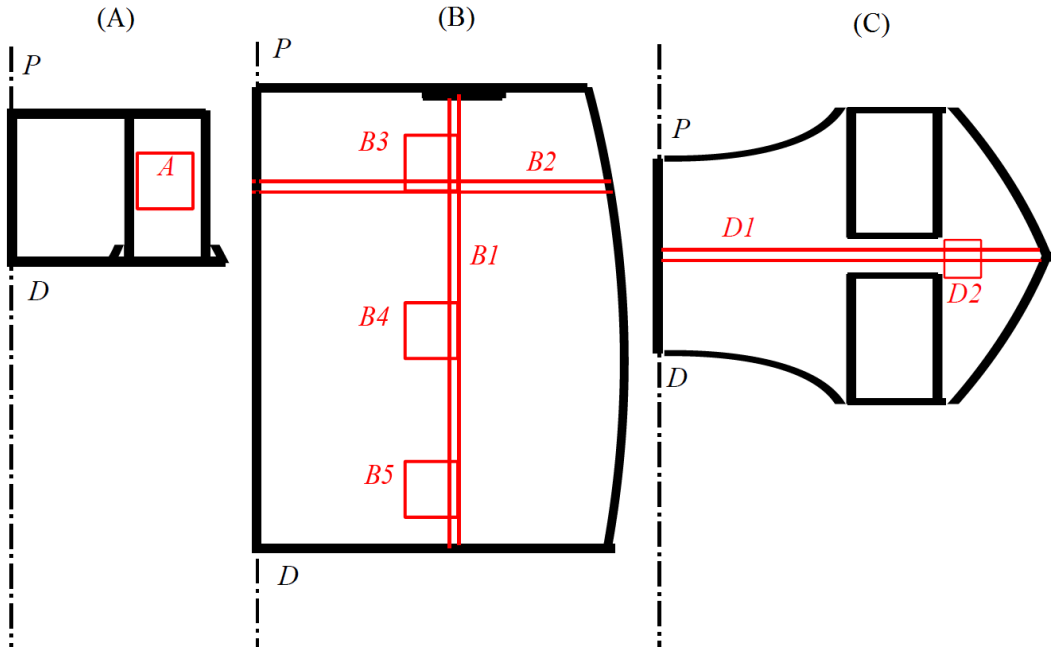

Figure 7.4: Distribution of indentations in (A) cortical bone samples, (B) distraction callus samples and (C) docking site samples. *P*: proximal; *D*: distal; the dash-dot line represents the axial edge of the limb.

Table 7.1: Size, number of indentations and duration for each area of indentation.

Area	Size (μm x μm)	Matrix	Indentations	Hours
A	750 x 750	16 x 16	256	21.33
B1	15000 x 50	301 x 2	602	50.17
B2	7500 x 50	151 x 2	302	25.17
B3	750 x 750	14 x 14	196	16.33
B4	750 x 750	14 x 16	224	18.67
B5	750 x 750	14 x 16	224	18.67
D1	7500 x 50	151 x 2	302	25.17
D2	750 x 750	16 x 14	224	18.67

7.2.3 Data processing

E_r of indentation lines with position were represented to analyze spatial variations. Besides, maps of E_r in matrix indentations were used to see and characterize the mean value of heterogeneity of the tissues. The heterogeneity in each matrix was also evaluated by means of the mean value and the coefficient of variation of indentations in each matrix. Moreover, the mean and the standard deviation of E_r of all indentations at each time point in distraction and docking site calluses specimens were evaluated and correlated with time to see temporal variations. All the measurements carried out in woven bone were compared with the mean of all indentations in cortical bone for all time points and specimens, which was used as control or reference value.

It is known that the woven bone has lower mechanical properties than cortical bone. Therefore, the evolution with time (t) of the mean values of E_r of the woven bone in distraction callus, docking-site callus and fracture callus [109] should be correlated with functions that allow an asymptotic increase from values of E_r of the woven bone initially generated to values close to cortical bone (E_{CB}). For example, the exponential expression

$$E_r = E_{CB} - a \cdot e^{-\frac{t-t_0}{b}} \tag{7.1}$$

is used in this analysis, where a and b are the fitting coefficients, t_0 is the number of days after surgery when the consolidation period started (21 days in the case of this experiments: 7 days of latency phase and 15 days of distraction phase). The goodness of each correlation was estimated by means of the coefficient of determination (R^2).

7.3 Results

For each animal sacrificed at a given time point, nanoindentation measurements of the E_r were obtained for samples of cortical bone, woven bone in the distraction callus and in the docking-site callus. For each type of sample, E_r values obtained in linear and matrix indentations are presented. Linear indentations are presented directly over the indented areas. Matrix indentations are presented as maps of E_r and as mean value $\pm$ the standard deviation to see spatial or temporal correlations.

7.3.1 Control measurements in cortical bone

Indentation matrices carried out in cortical bone (A) reported mean values of E_r between 16 GPa and 21 GPa (Fig. 7.5). The mean value for all the time points was 18.2 GPa, which was used as reference for comparison with woven bone E_r measurements. The coefficient of variation of the results of each indentation matrix was between 9% and 14% (Fig. 7.5).

Indentation maps of the 750x750 μm matrices in cortical bone also represent the scatter in measurements that is a result of the material heterogeneity. Fig. 7.6 shows the indentation maps in cortical bone for three of the samples analyzed. Similar results of scatter with respect to mean values were obtained in the rest of samples.

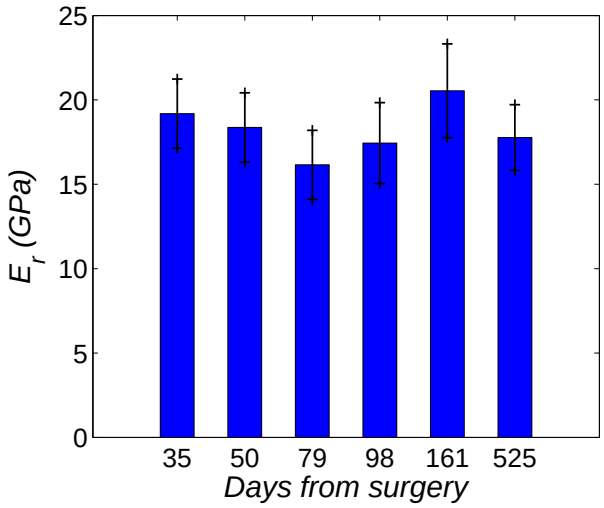

Figure 7.5: Mean values of $E_r \pm$ the standard deviation of indentation matrices in cortical bone in the different samples.

7.3.2 Spatial - temporal variations of the distraction callus mechanical properties

Fig. 7.7 shows the evolution with time of the mean values of E_r of all indentations carried out for each time point (lineal and matrix indentations). E_r values of the woven bone increased with time from 7 GPa 35 days after surgery to 14 GPa 525 days after surgery approximately, close to the mean E_r of cortical bone, 18.2 GPa. This graph shows that the rate of increment of the mean E_r of the woven bone per unit of time decreases with time. During the first weeks of the process the mean E_r increased quickly, from 7 GPa 35 days after surgery to 8 GPa 50 days after surgery, an increase of 1 GPa approximately in 2 weeks. After the sixth month from the surgery, E_r increased from 11 GPa 161 days after surgery to 14 GPa 525 days after surgery approximately. 17 weeks were needed for 1 GPa of increase of E_r approximately. According to the fit carried out using equation 7.1, values of 95% of the mean E_r measured in the cortical bone would be reached 1033 days after surgery.

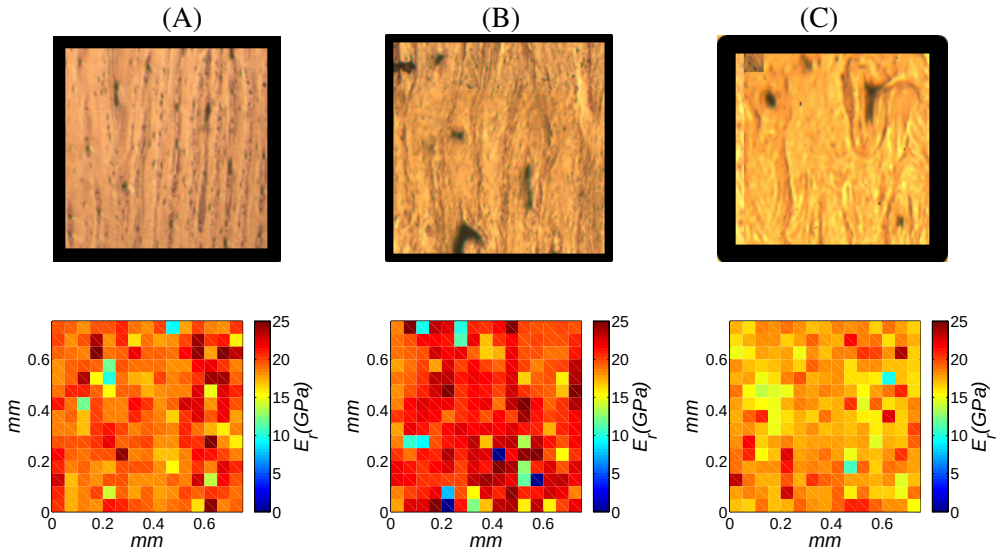

Figure 7.6: Detail of the micrographies in the matrix indented and the corresponding E_r map for the sheep sacrificed 35 (A), 161 (B) and 525 (C) days after surgery.

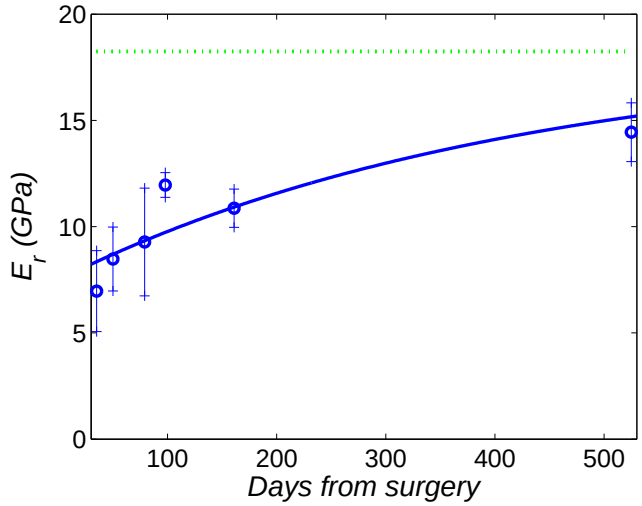

Figure 7.7: Experimental E_r mean values $\pm$ the corresponding standard deviation in the distraction callus versus time. E_r experimental values were fitted versus time using equation 7.1 (E_{CB} = 18.2 GPa; t_0 = 21 days; a = 10.2 GPa; b = 418.9 s). Mean value of the control measurements in cortical bone is also represented (dotted line).

Differences in the evolution of E_r with position, from proximal to distal, were reported by the mean values of E_r in the indentation matrices performed for each time point. Fig. 7.8 shows the mean values of E_r with their corresponding standard deviation for proximal (B3), central (B4) and distal (B5) matrices beside the same values for the matrix performed in

cortical bone. Increase of E_r from proximal to distal positions were found for measurements 161 days after surgery; nevertheless, a decrease trend was found for measurements 79 days after surgery. Other different trends were observed for the rest of animals, e.g. 50 days and 525 days after surgery samples reported higher values of E_r in the central matrix. Therefore no conclusions in the spatial variation of E_r could be obtained. Fig. 7.8 also shows that the standard deviation in matrices of the distraction callus were higher than in cortical bone. The value of the coefficient of variation of matrices in the distraction callus may vary depending on the measurement between 18% and 60% for most of the cases.

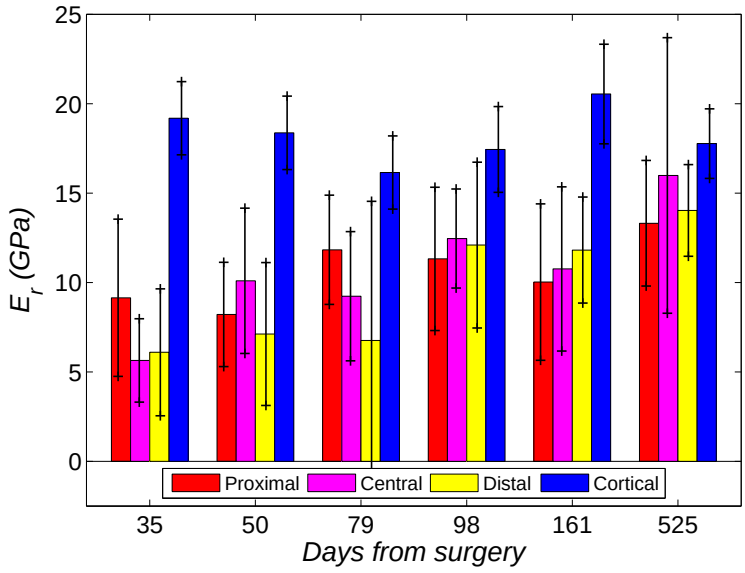

Figure 7.8: Mean values of $E_r \pm$ the standard deviation of indentation matrices in the distraction callus of the different samples (see Fig. 7.4). Values are presented beside values in cortical bone.

Indentation maps of the 750x750 μm matrices in cortical bone also represent the spatial scatter in measurements. Fig. 7.9 shows the indentation maps in cortical bone for three of the samples analyzed (35, 161 and 525 days after surgery). Maps show an increase of E_r with time, also observed in Fig. 7.8. Levels of scatter seem to be similar and independent of spatial and temporal variations. Similar results of coefficient of variation with respect to mean values were obtained in the rest of samples.

Micrographies of the callus sample show qualitatively the evolution of the ossification state of the callus (Fig. 7.10). 35 days after surgery (second week of consolidation) high porosity level may be observed between the trabeculae of woven bone, which presents a disorganized structure. 161 days after surgery some organization of the woven bone structure may be appreciated and the porosity level is lower in the longitudinal line that joins the cortical segments around the callus. 525 days after surgery, with the medular channel finished (see Chapter 6), some millimeters of tissue with similar appearance to cortical bone may be observed in the external perimeter of the callus which decreased in diameter considerably (see Chapter 6). The

rest of micrographs shows similar trends. Linear indentations in distraction callus (B1 and B2) show that the areas of high porosity correspond with lower levels of mechanical properties (Fig. 7.10). However, no spatial variation trends may be established because the reorganization and the production of the woven bone (and therefore the level of porosity and E_r) seem unrelated with the location within the callus.

For example, in Fig. 7.10 A, 35 days after surgery, it may be observed for B1 that E_r decreased from values around 10 GPa close to the proximal cortical bone segment to values around 5 GPa close to the porous in the center of the callus. However, different trends were observed in the evolution of E_r with respect to the position in the direction proximal to distal. Whilst in Fig. 7.10 A it may be observed a slight decrease of E_r from the proximal to the distal area of the callus, the opposite trend is observed in Fig. 7.10 B.

Fig. 7.10 B also shows the relationship between porosity and E_r, now attending to the longitudinal line between distal and proximal cortical bone segments, where it may be observed an area of reorganization of the woven bone structure. This area seems to provide higher values of E_r than indentations close to the axial edge of the limb or the exterior perimeter (see B2 in Fig. 7.10 B). Nevertheless, different trends were also observed in linear indentations from the axial edge of the limb to the exterior perimeter. For example, according to Fig. 7.10 C. E_r values from the interior to the exterior of the callus approximately do not vary.

7.3.3 Spatial - temporal variations of the docking-site callus mechanical properties

As in the case of the distraction callus, mean E_r of the docking-site callus increases with time. Fig. 7.11 shows mean values $\pm$ standard deviation versus time. The mean value of E_r increases from 8 GPa 35 days after surgery to 15 GPa 525 days after surgery, approximately. In general, it may be observed that the increment of the mean E_r decreases with time. According to the fit carried out using equation 7.1, values of 95% of the mean E_r measured in the cortical were reached 943 days after surgery.

Fig. 7.12 compares the values obtained in all indentation matrices for each time-point: proximal, central and distal distraction callus; docking-site callus and cortical bone. In general, the mean values of all indentations in the docking-site callus presented slight higher values of E_r than these values in the distraction callus.

Coefficients of variation of results were similar to results in woven bone of distraction callus: 20% - 40%. Maps of matrix indentations show with detail the spatial scatter of the indentation matrix measurements (Fig. 7.13).

E_r measurements in the docking-site did not provide significant trends with location within the callus either (Fig. 7.14). The same relation between porosity and E_r may be observed, e.g. Fig. 7.14 C. As it was seen in the distraction callus, the spatial proliferation and the porous density of the woven bone were different depending on each individual. However, attending to the more developed calluses (Fig. 7.14 B and C), higher values of E_r and more appearance of mature woven bone were found in the external area of the callus.

7.4 Discussion

The increase of the mechanical properties of the woven bone is one of the factors that contributes to the increase of stiffness of the distraction callus during distraction osteogenesis. This study has characterized the local elastic properties of the woven bone during bone transport. The results reported allow knowing spatial and temporal evolution of E_r in the distraction and the docking site calluses. Comparison with data of previous studies carried out in fracture healing callus [97, 109], where different mechanical conditions may appear, is also carried out.

The results of the temporal variation of mean value of E_r provided, show that it increased with time both in the distraction and the docking-site calluses (see Figs. 7.7 and 7.11) from 7 GPa to 15 GPa approximately. Properties of the woven bone generated during fracture healing were measured [97, 109] and may be compared with these values obtained in this Thesis. Leong and Morgan [97] carried out indentation experiments in samples from fracture healing in rats. They reported values of E_r of the woven bone of 27-1010 MPa 35 days after fracture, well under the values measured in this study, ranging between 4 and 18 GPa, approximately. The difference in the animal species could explain these variations since Manjubala et al. [109] reported similar range of values of E_r (2-18 GPa) of woven bone in fracture healing in sheep compared with results of this Thesis. Both the distraction and the docking-site calluses presented rates of increment of E_r with time slower along time. It means that the increase of mechanical properties of the woven bone has important contribution to the macroscopic increase of the callus stiffness measured in previous Chapters, apart from the increase of the callus volume also observed.

Normalization of the E_r measurements in woven bone at each time point with the mean value of measurements in cortical bone (18.2 GPa) provides information about the recovery of the mechanical properties within the callus. Mean values of the E_r of cortical bone measured (16-21 GPa with a coefficient of variation between 9% and 14%) were consistent with those reported in literature for cortical bone using similar sample preparation and measurement techniques [153]: 20.1 GPa with 19.4 % of coefficient of variation. Fig. 7.15 shows the evolution of E_r mean values normalized with the mean value of measurements in cortical bone (E_r^0) for the distraction and docking-site calluses versus time. For the distraction and docking-site calluses, mean value of E_r^0 with time shows the increase observed in Figs. 7.7 and 7.11 for absolute values of E_r. For the distraction callus, it was observed that E_r^0 values were close to 39% 14 days after the end of the distraction. E_r^0 values were increasing slower with time to 79% 500 days after the end of the distraction period. A similar increase was observed in the case of the docking site callus. However, E_r^0 values remained above values in distraction callus specially at the beginning of the process (about 48%, 14 days after the end of the distraction, and 81%, 500 days after the end of the distraction period). E_r^0 values using the same reference (18.2 GPa) obtained by Manjubala et al. [109] in fracture healing in sheep are also shown in Fig. 7.15. As for distraction and docking site calluses, it may be observed that the E_r^0 ratio of increment with time decreases along time. Nevertheless, some differences may be appreciated. First, the increase of mechanical properties was faster, specially at the beginning of the process (from 29%, 14 days after fracture, to 60%, 42 days after fracture). This fact caused that the values of E_r of the woven bone reached similar values to those measured in cortical bone faster in fracture healing cases. According to the fits carried out in Fig. 7.15, values of E_r in the

woven bone of 95% of the mean E_r measured in the cortical bone were reached after 185 days of consolidation in fracture healing versus 1012 and 922 days of consolidation (distraction and docking-site calluses respectively) needed in bone transport. Second, E_r^0 values 14 days after fracture are clearly lower than values after the same time from the end of the distraction period for the woven bone generated during bone transport. These facts may be explained attending to the differences in the mechanical conditions and in the evolution of the ossification in the distraction, docking-site and fracture calluses. On one hand, it may be suggested that the slower increase of E_r^0 in the distraction and docking site calluses may be related to the presence of traction stimuli that does not exist in the case of fracture healing. On the other hand, the high level of E_r^0 at the beginning of the process in the distraction and docking-site calluses could be caused by the presence of a distraction period (15 days in this experiment). During the distraction period the stiffness of the tissues within the distraction and the docking-site calluses increase (see Chapter 5) and, it has been shown that, although bony bridging is achieved during the consolidation phase, ossification starts before the end of the distraction period during the bone transport process (see Chapter 6).

Table 7.2: Parameters of the curve fit carried out in each case of Fig. 7.15

$E_r^0(\%) = E_{CB} - a \cdot e^{-\frac{t-t_0}{b}}$	E_{CB} (%)	t_0	a (%)	b (s)
Fracture	100	0	85.6	65.1
Distraction	100	0	56.2	418.9
Docking-site	100	0	46.4	414.6

.

Manjubala et al. [109] reported variations of E_r with the distance from the bone cortex (from the periosteum to the exterior perimeter of the callus) in a fracture healing callus. They found that E_r slightly increases near the periosteum. In this study, variations of E_r in two directions within the distraction callus were analyzed: from the axial edge of the callus to the exterior perimeter and, in longitudinal direction, from proximal to distal (see Figs. 7.10 and 7.8 for longitudinal direction). These results provided different trends in spatial variation of E_r which presented lower values in more porous areas. In one hand, interindividuals differences in the distribution of the local mechanical properties during the process would explain these different trends since samples at each time point were taken from different animals. On the other hand, it could also be assumed that spatial distribution of the mechanical properties vary with time for the same specimen. At the beginning of the process, it is expected that the woven bone close to the cortical bone segments has higher values of E_r because results in other studies [92, 148], and this experiment [115] (see Chapter 6) showed that the ossification begins close to the cortical bone segments. In fact, higher values of E_r are observed close to the cortical bone segments for the first time point analyzed (see Figs. 7.10 A and 7.8). However, from 50 days after surgery this trend was not kept. For example, 50 days after surgery and 525 days after surgery the central area of the callus had higher values of E_r than proximal and distal areas, closer to cortical bone segments (see Fig. 7.8). It would mean that from a period of time lower than 50 days, the value of E_r does not depend on the age of the tissue. If variation of local mechanical properties is associated to angiogenesis as is suggested in literature [57, 117],

according to both hypothesis above, it could be assumed that the growing of the blood vessels may vary particularly for each animal or that spatial distribution and growing of blood vessels vary with time for the same specimen. In fact, the growing and developing of the blood vessels with time have been demonstrated for one of the animals intervened in this study. Fig. 7.16 shows angiographies carried out at different time points for the sheep number 2 (see Tables 3.1 and 3.2). It may be observed in the different images the increment of size and number of the blood vessels with time. This increment has been quantified by means of the index of vascularization (Fig. 7.16). The index of vascularization at each time point is the area of blood vessels within the callus divided by the total area of the callus at each time point. The areas were measured in number of pixels in each radiography and the mean value between both radiographies was used at each time point.

Results of this work also show the level of heterogeneity of the woven bone. Figs. 7.9 and 7.13 show that E_r in the distraction and docking site calluses may vary from 1 to 20 GPa. The coefficient of variation for mean values was around 18-60% considerably higher than values in cortical bone (9-14%). The heterogeneity is important in order to understand the mechanical behavior of bony tissues. It has been demonstrated that heterogeneity may lead to higher energy dissipation before fracture and thus influence the toughness [164]. However, many computational studies in literature have considered homogeneous mechanical properties for the woven bone [85, 141–143]. The obtained data may be used to rule the building of heterogeneous meshes of elements in computational models.

Although the outcomes provided by this study are rewarding, there are some limitations associated to the methods employed. Firstly, the methods used for the evaluation of E_r from indentation measurements [125] assume linear elastic behavior. However, the tissue within the callus could present viscoelastic behavior specially during the distraction phase (see Chapter 5). The viscoelastic behavior depends on other mechanical parameters that were not assessed because this work is focused on the woven bone where the influence of the viscoelastic behavior is not significant compared to the soft tissues. Secondly, the need of using different animals for each time point introduces a source of variation in measurements. For example, it did not allow distinguishing if the E_r spatial variations found are due to the time or to the interindividuals differences. Finally, higher number of animals would allow more statistically significant conclusions of this study; however, no more than 6 samples could be included in the study due to funding limitations.

This work clearly shows that the mean E_r of the woven bone increases during the bone transport process. The rate of increment with time decreases along time both in distraction and docking-site calluses. The rate of increase of E_r is similar in the case of the distraction callus with respect to the docking-site callus. Both the distraction and the docking site calluses present lower increments of E_r with time than values observed in fracture healing calluses. Furthermore, no repeated relations between E_r and position within the callus were found. These results will be useful to characterize the mechanical behavior of the callus tissue during the distraction processes directly used for comparison with new experiments or by means of the incorporation of material properties data in computational models. Knowing the mechanical properties of the material and the mechanical response allows understanding the mechanisms of bone formation and their differences depending on the mechanical particularities of each process: bone transport, bone lengthening, fracture healing...

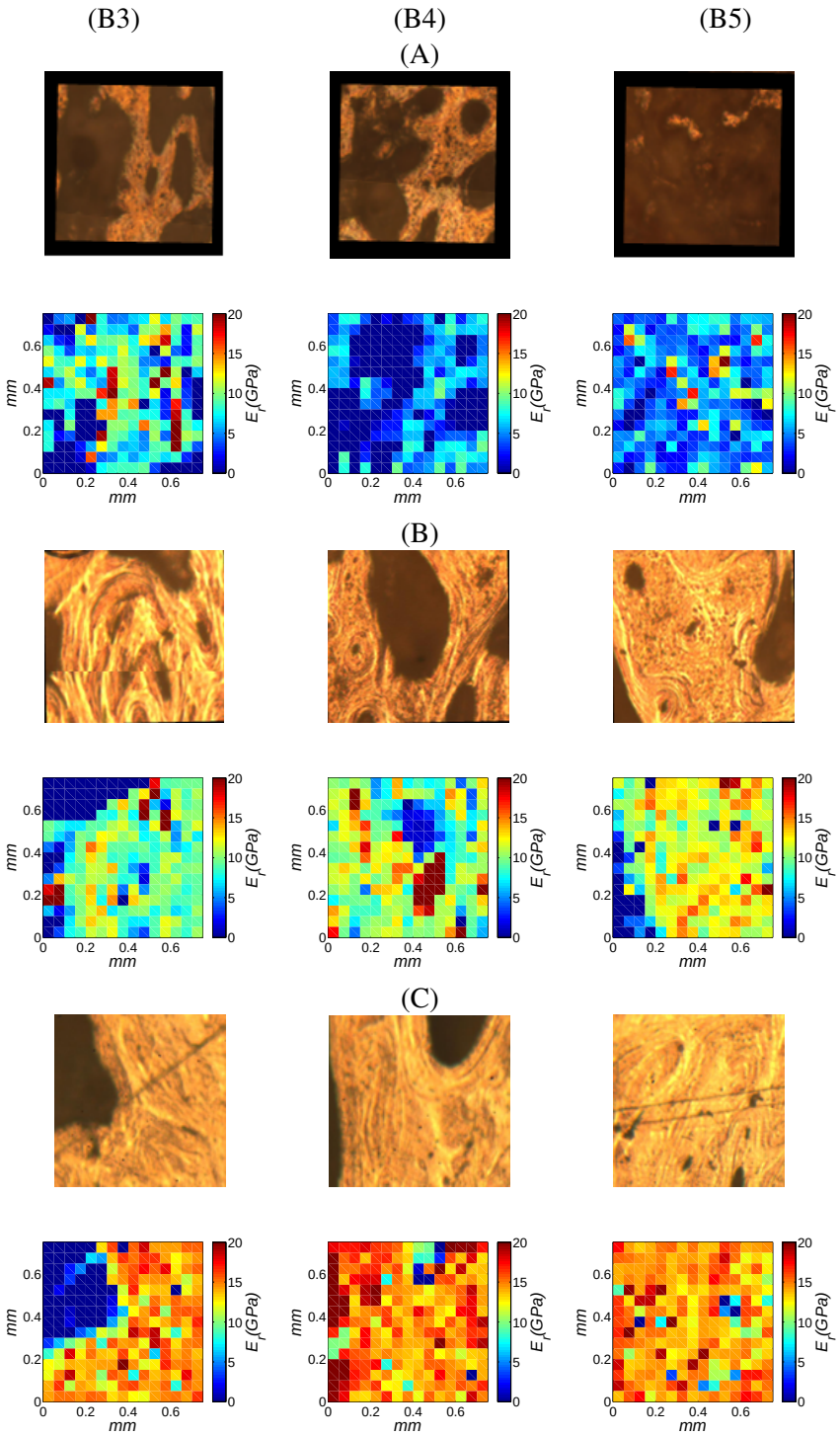

Figure 7.9: In cortical bone samples, detail of the micrographies in the matrix regions indented (B3, B4 and B5) and the E_r maps (below) in the distraction callus for the sheep sacrificed 35 (A), 161 (B), and 525 (C) days after surgery.

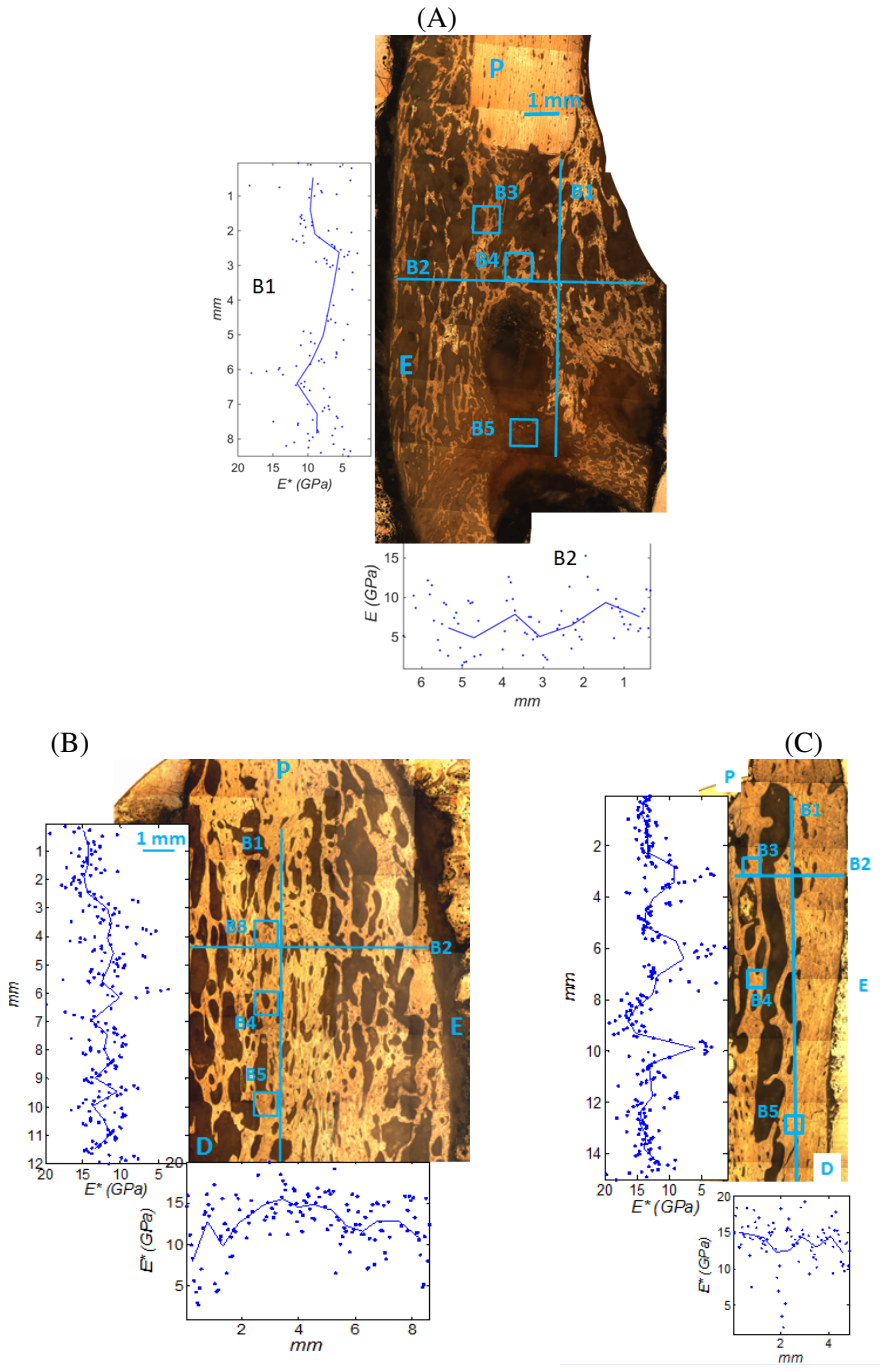

Figure 7.10: Micrographies of the callus samples with values of E_r in linear indentations for the sheep sacrificed 35 (A), 161 (B), and 525 (C) days after surgery. P, proximal side; E, external side with respect to the axial axis of the limb; B1 and B2, regions of the linear indentations; B3, B4 and B5, regions of the indentation matrices.

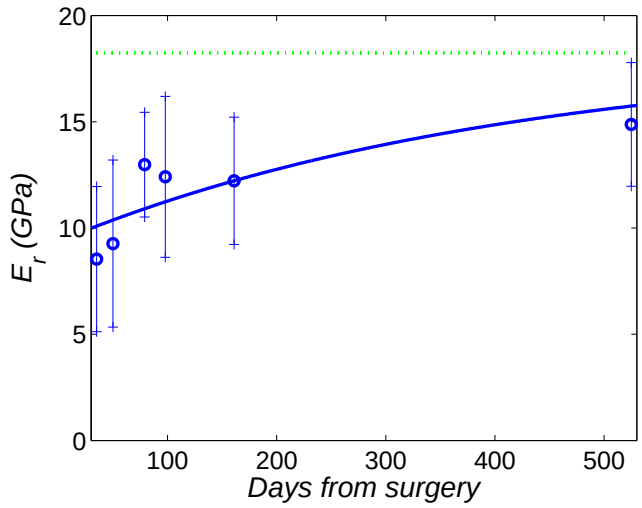

Figure 7.11: Experimental E_r mean values $\pm$ the corresponding standard deviation in the docking-site callus versus time. E_r experimental values were fitted versus time using equation 7.1 (E_{CB} = 18.2 GPa; t_0 = 21 days; a = 8.4 GPa; b = 414.6 s). Mean value of the control measurements in cortical bone is also represented (dotted line)

.

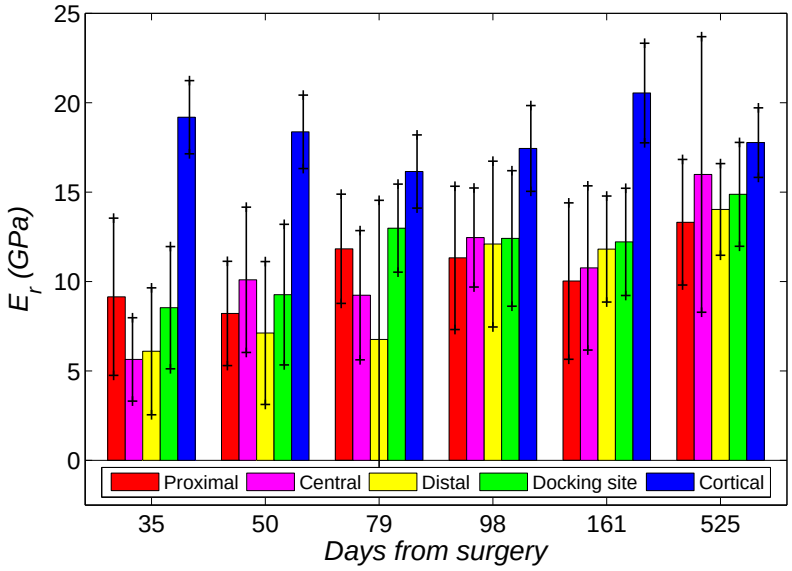

Figure 7.12: Mean values of E_r $\pm$ the standard deviation of the indentation matrices in the docking-site callus of the different samples. Values are presented beside values in cortical bone and distraction callus.

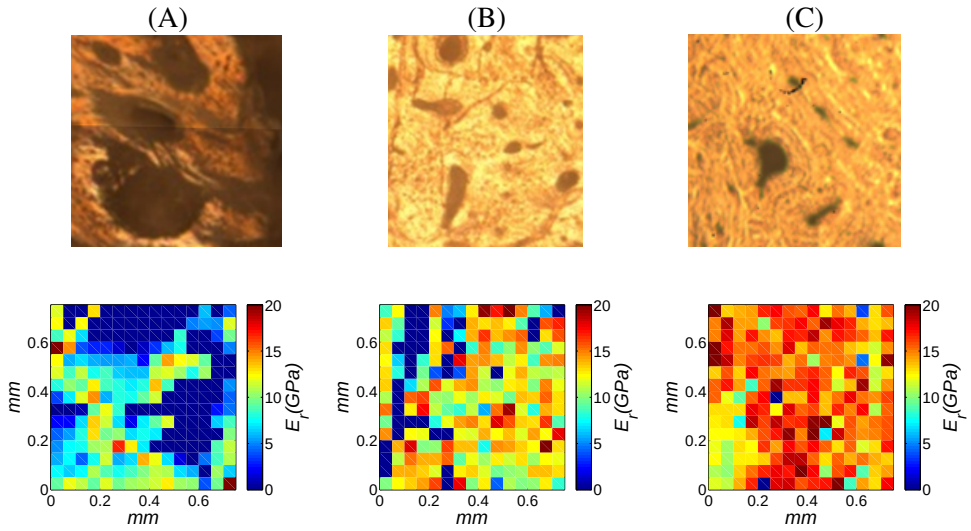

Figure 7.13: Detail of the micrographies in the matrix regions indented (D2) and its corresponding E_r maps (below) of the callus for the sheep sacrificed 35 (A), 161 (B), and 525 (C) days after surgery.

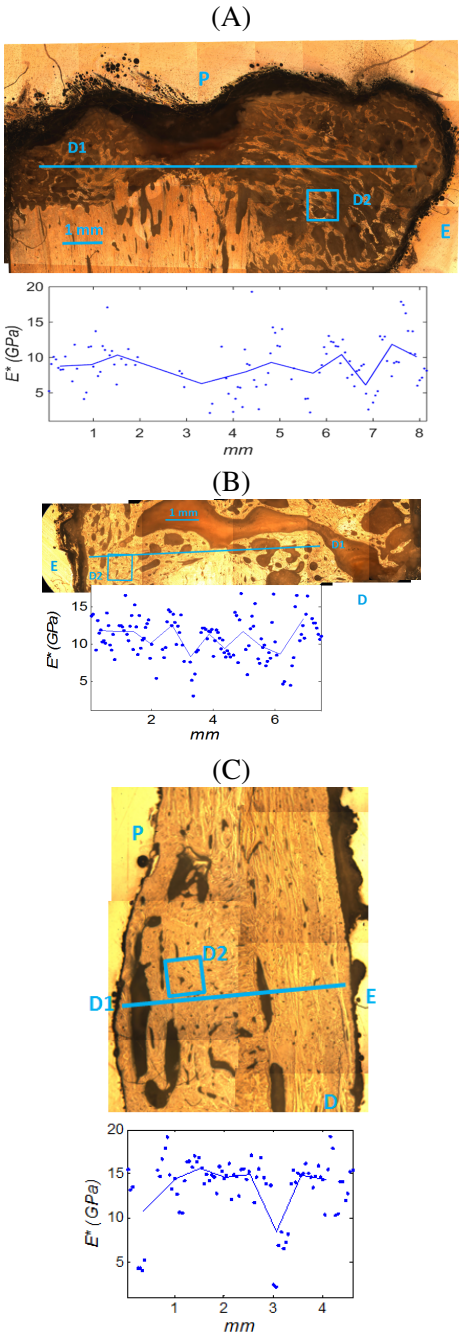

Figure 7.14: Micrographies of the docking-site callus samples with values of E_r in line indentations for the sheep sacrificed 35 (A), 161 (B), and 525 days after surgery. P, proximal side; E, external side with respect to the axial axis of the limb; D2, region of the linear indentation; D1, region of the indentation matrix.

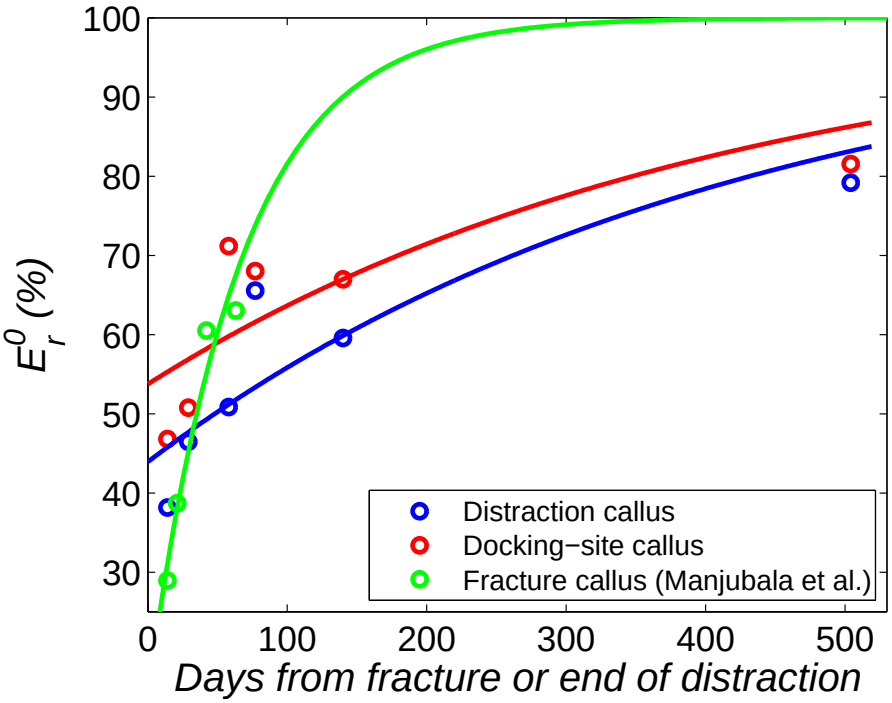

Figure 7.15: Normalized average values of E_r, represented as percentage of the mean value of the cortical bone (E_r^0), measured in the distraction and the docking-site calluses, versus time. Data for fracture callus obtained by Manjubala et al. [109] are also shown. Note that time scale was referred to the end of the distraction phase (for distraction and docking site calluses) or to the fracture to allow comparison among all the cases during the consolidation phases. The curves of fit carried out in each case according to equation 7.1 were also normalized (divided by the mean E_r value of cortical bone and using $t_0 = 0$, since time scale is referred to the beginning of the consolidation in both periods and no to the surgery) and represented in the figure. The values of the parameters in each case are reported in Table 7.2

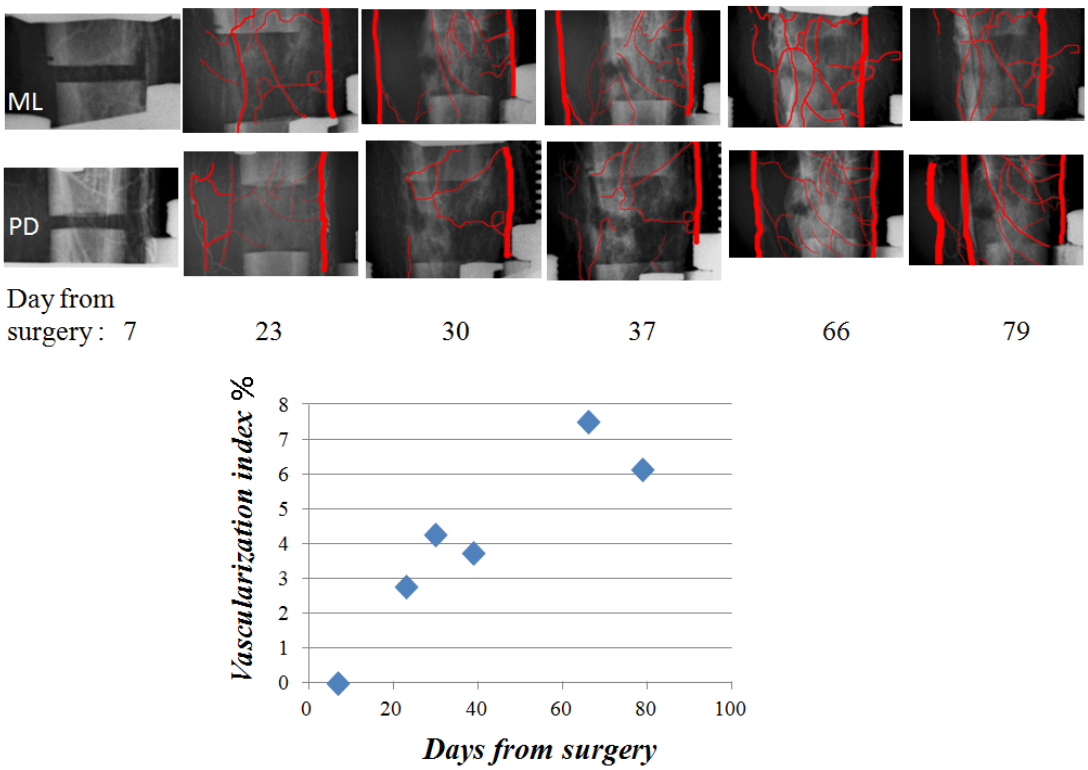

Figure 7.16: Angiographies carried out at different time points for the sheep number 2. Images in two projections were taken at each time point: medial - lateral (ML) and plantar dorsal (PD). To facilitate the visualization the vessels are indicated in red. The graph represents the area of blood vessels compared to the total area of the callus in each time point (index of vascularization).

Chapter 8

CT images based finite element analysis for the prediction of the callus stiffness

This chapter aims to provide estimations of the callus stiffness using computational methods based on experimental data: computerized tomography (CT) images. It demonstrates that *in silico* models combined with CT images can be very useful to improve current clinical protocols and for future finite element models. The contents of this Chapter are included in a paper submitted for publication: J Mora-Macías, M López, J Domínguez and E Reina-Romo. Finite element versus experimental mechanical characterization of the distraction callus.

8.1 Introduction

As in the fracture healing process, during distraction osteogenesis [78, 79], the woven bone grows within the distraction callus rapidly with a disorganized pattern, with the aim of providing temporary, rapid mechanical support. Assessment of the mechanical properties of the distraction callus is important for evaluating the clinical evolution of the distraction osteogenesis process. The increasing stiffness of the tissues within the callus through the process represents the mechanical stability of the distracted bone. Therefore, information about the mechanical properties increase rate of the callus will help to identify an endpoint of healing and may contribute to improve current treatment strategies. This is of great importance since in the field of distraction osteogenesis surgeons still lack of established instructions to correctly define the specific patient planning of the process.

Several techniques have been developed to quantify bone healing in mechanical terms. However, existing methods for assessing these callus mechanical properties are subjective and have some limitations. X-rays and manual clinical examinations, commonly used in daily clinical routines have proven to be inexact [132, 133, 176] and are not able to provide sufficient quantitative information. Assessment of the distraction callus stiffness *in vivo* using instrumented fixators provided suitable estimations of callus stiffness [4, 43, 46, 113, 115] (see Chapter 6). However, it is not always convenient or possible to use external and instrumented

fixators. In addition, with the last method, stiffness measurement cannot be provided after distractor removal. On the other hand, methods to evaluate the callus mechanical properties *ex vivo* in animal experiments such as nanoindentation [97, 109], or mechanical testing of the whole specimen [47, 123] involve that a group of animals has to be sacrificed for each time point of evaluation.

Non-invasive methods have been used to assess the stiffness of the callus *in vivo*, such as high resolution magnetic resonance [101], quantitative ultrasound [139] and computational tomography (CT) images based finite element analyses [161]. Unlike the other techniques, prediction of the bone tissue mechanical properties by means of CT images based finite element analysis has been assessed for reliability in the literature. Harp et al. [66] demonstrated that the stiffness of tubular bones, cortical and cancellous, can be accurately predicted by quantitative CT images. The bone mineral content in a fracture callus from CT images was correlated with experimental measurements of callus stiffness in a previous work [12]. The CT images finite element analysis method consists of obtaining the estimation of the stiffness of a bone tissue specimen using a finite element model which imports both three dimensional geometry and material properties of each element (depending on the grey scale values) from CT images. This method has been used in previous studies in mature bone tissue [27, 63], reconstructed bones [163], trabecular bone [119, 169], osteoporotic bone [121] and fracture callus [161]. However, as far as the author knows, CT images based finite element analyses have not been used to estimate the stiffness of the callus during the distraction osteogenesis process.

Segmentation of CT images may also provide information about the tissue types percentage within the callus (soft and hard tissues) since they could be differentiated by the level of grey scale. The bone tissue volume within the callus during distraction osteogenesis has been quantified from CT images in previous studies [115, 148]. However, as far as the author knows, these studies did not report the hard and soft tissue volume percentage. The percentages of callus tissue types were reported by histological studies in fracture healing [28] and bone transport [51]. Nevertheless, histological studies provide data from a determined area which may be not representative of the total callus volume since it is very irregular [115]. In addition, both studies did not report percentage of tissue types after 12 weeks of consolidation.

The aim of this work is to provide an estimation of the distraction callus stiffness during the process of bone transport by means of CT images based finite element analyses. It was possible to estimate the callus stiffness until 69 weeks after surgery, increasing the time range of *in vivo* measurements reported in the literature [115]. Finite element models were obtained from the CT images carried out during an experiment in merino sheep [115]. Two different approaches were used to assign the elements mechanical properties. In the first case, mechanical properties were assigned manually to a model divided in four zones: hard tissue, soft tissue, cortical bone and bone marrow. Mechanical properties of the hard tissue was taken from a previous nanoindentation study of woven bone (Chapter 8 of this Thesis). In the second case, the elastic properties of each element were assigned depending on the level of Hounsfield Units (HU), regardless its location [161]. The segmentation of the CT images allows obtaining the volume of different tissue types within the callus. These data of tissue volume have been compared with values obtained from histological studies until 69 weeks after surgery [105].

8.2 Material and methods

8.2.1 Three dimensional models of the metatarsus

Figure 8.1 shows the stages followed to predict numerically the stiffness of the distraction callus. Firstly, an experiment of bone transport has been carried out in the metatarsus of 11 female merino sheep [115, 116] (see Tables 3.1 and 3.2 in Chapter 3).

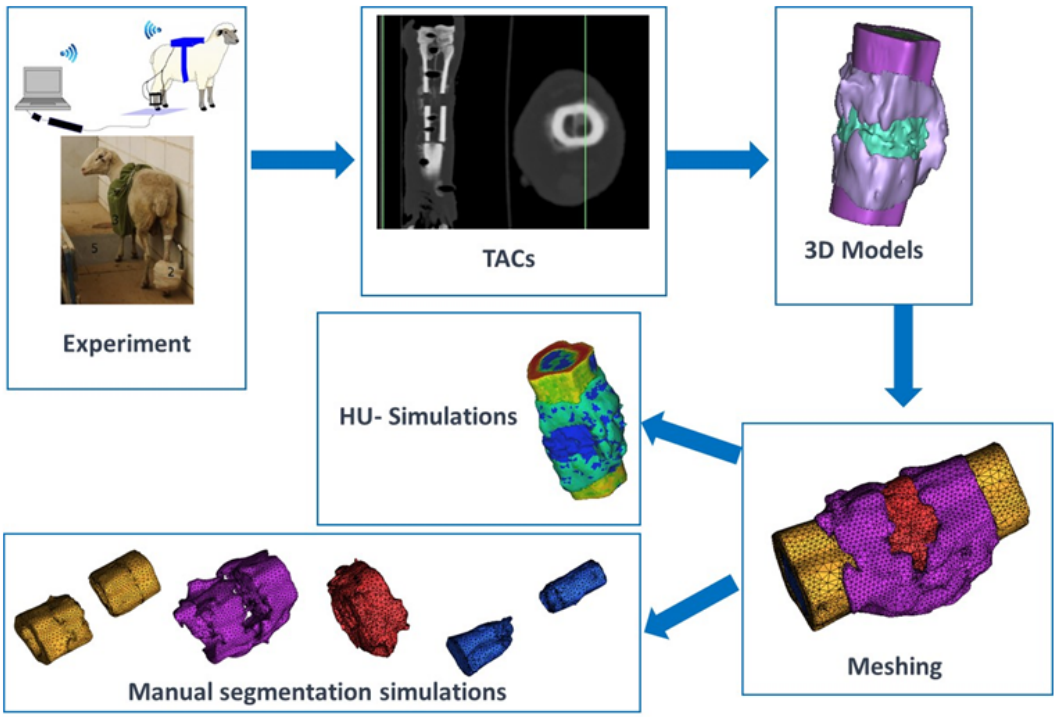

Figure 8.1: General scheme followed to predict the stiffness of the distraction callus

To be able to follow the whole process of bone consolidation, distraction calluses were imaged with a CT scanner at different time points of the healing process (see Tables 3.1 and 3.2 in Chapter 3). The resolution of the CT images was 200-300 μm/voxel. 9 sheep were sacrificed interrupting bone transport at different stages during the distraction and the consolidation phases: 17, 22, 29, 35, 37, 51, 79, 98 and 161 days after surgery (to avoid the artifacts caused by the metallic parts of the distractor). The remaining two sheep were studied during the remodeling phase, after the distractor was removed and the callus had completely ossified. Therefore, these animals were not sacrificed and several CT were performed *in vivo* on them (137, 205, 277, 311, 379 and 471 days after surgery).

3D models were generated in the commercial program Mimics® from the 15 *CTs* obtained. From them, meshes were created in Ansys ICEM® using tetrahedral element type c3d4 and simulations were carried out in ABAQUS®. Each model had a total number of elements between 100000 and 500000 depending on the volume of the models which vary due to the interindividual differences and the time point in which CT were taken (see Fig. **??** in Chapter

6). Meshes with different type and size of element were generated from the 3D model of the sheep number 2 (79 days after surgery). Displacement between the ends of the callus caused by the same axial load in these different meshes were obtained to analyze the sensitivity of the model to the type and size of element (Fig. 8.2). It may be observed that similar results were obtained increasing the number of elements (or decreasing the size) or using the element type c3d10, with more nodes. The mechanical behavior of the tissues was assumed linear elastic. The mechanical properties were assigned, as afore said, by two different ways: by manual segmentation or according to the Hounsfield Units (HU) [161] (Fig. 8.3). All materials were assumed to be linear, elastic and isotropic.

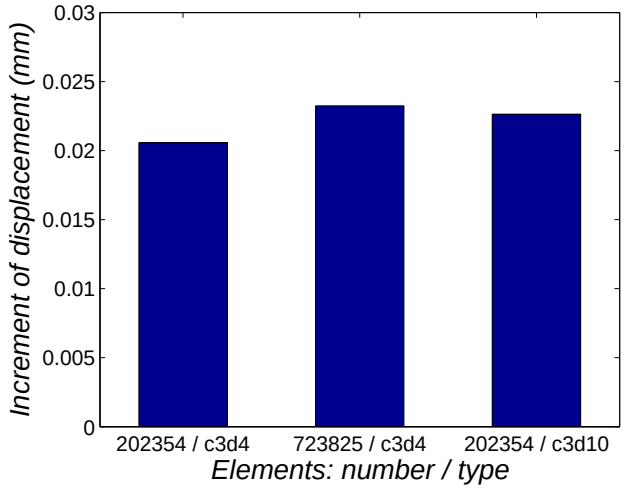

Figure 8.2: Displacement between the ends of the callus caused by the same axial load for meshes with different type and size of element, generated from the 3D model of the sheep number 2 (79 days after surgery).

8.2.2 Mechanical properties assignment: manual segmentation

Two different cases were analyzed in the manual segmentation (see Fig. 8.3): assuming constant mechanical properties taken from the literature, case 1, or variable mechanical properties for the hard tissues of the callus according to those obtained from nanoindentation studies performed in bone samples of woven bone in the same experiment (see Chapter 7), case 2.

Case 1. In the first case, constant mechanical properties taken from numerical studies of distraction osteogenesis were assigned to the different volumes manually segmented in the commercial program Mimics®: hard tissue, soft tissue, medullar tissue, and cortical bone. The soft tissue region was assumed to be mainly granular tissue [105] and was assigned an elastic modulus of 2 MPa and a Poisson coefficient of 0.13 [144]. The Young's modulus of the hard tissue of the callus was selected to be E=1000 MPa with a Poisson's ratio of ν=0.29 [144]. The mechanical properties of the cortical bone were considered homogeneously distributed (E=17000 MPa, ν=0.30) [112] as well as those of the medullar tissue (1 MPa, ν=0.05) [144].

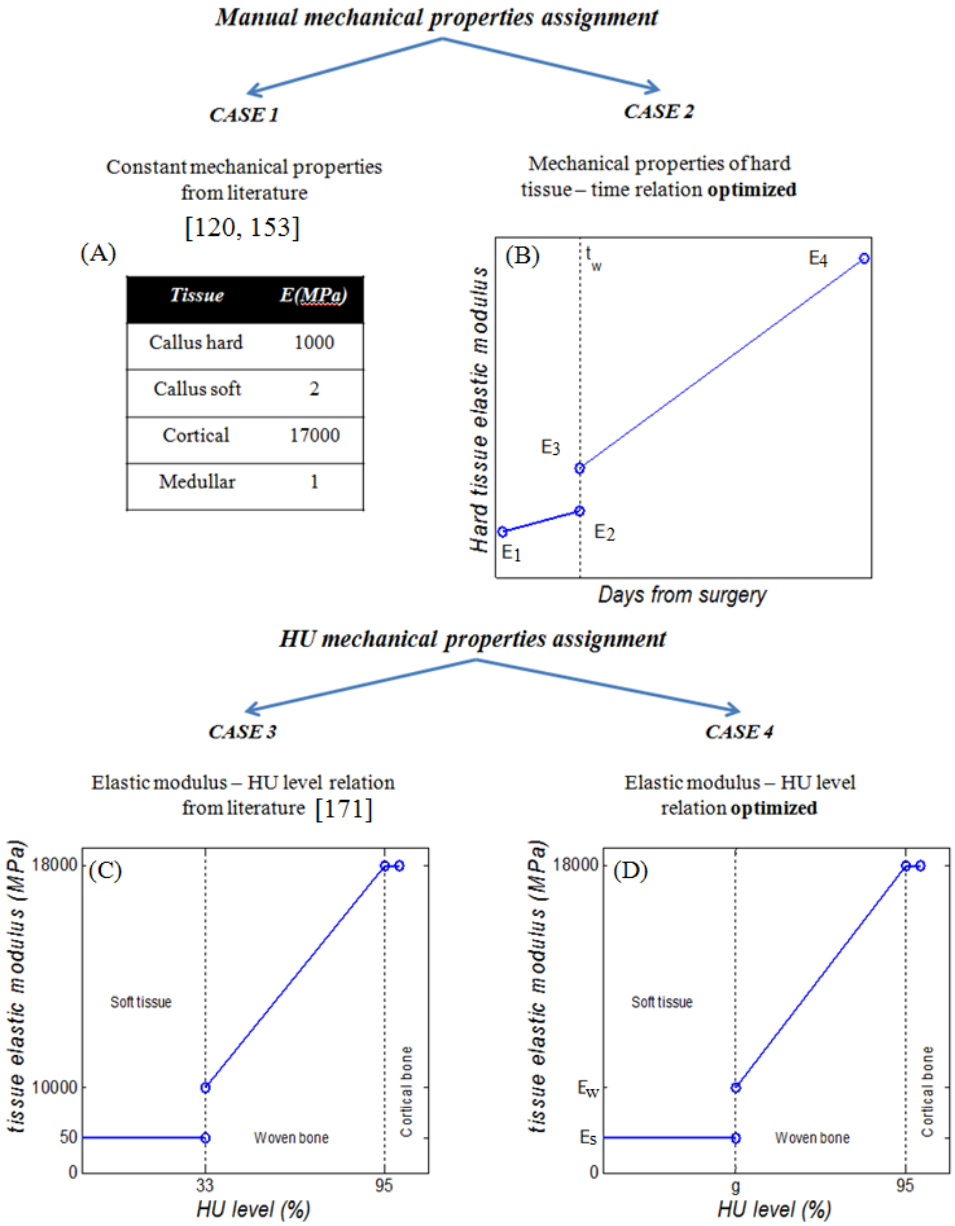

Figure 8.3: Scheme of the simulations carried out during this work. (A) Case 1: constant properties are assumed. (B) Case 2: relationship between days from surgery and hard callus tissue elastic modulus is optimized. (C) Case 3: relationship between the elastic modulus of the tissues and the level of HU according to Shefelbine et al. [161]. (D) Case 4: relationship between the elastic modulus of the tissues and the level of HU is optimized.

Case 2. In the second case, it was assumed the same constant values of elastic modulus for the soft and the medullar tissues. However, the elastic modulus of the hard tissue of the callus

and the cortical bone were taken according to previous nanoindentation tests obtained from the same experimental study (see Chapter 7). In this study, the woven bone elastic modulus was observed to vary with time during the process (see Chapter 7). It should be taken into account that the segmented volume corresponding to hard tissue involves both the trabeculae of woven bone and the spaces between them that contain tissue of very low stiffness. According to the maximum level of porosity of the hard tissue observed in these results (see Chapter 7, Fig. 7.10), it has been assumed that the hard tissue elements (woven bone and the space among trabeculae) could have a minimum elastic modulus of 50 MPa.

A simple bilinear evolution of the hard tissue elastic modulus with time was proposed (Fig. 8.3, case 2). This evolution depends on 5 parameters: E_1, E_2, E_3, E_4 and t_w (see Fig. 8.3, case 2). These parameters were chosen within a range in concordance with indentation results (see Chapter 7), from, the minimum value of 50 MPa considered above (maximum porosity and minimum elastic modulus of the woven bone) to the maximum value of 15000 MPa (no porosity and maximum elastic modulus of the woven bone). An optimization process was carried out to select the bilinear evolution of the hard tissue elastic modulus with time that minimizes the error between the callus stiffness predicted by the model and the callus stiffness measured *in vivo* [115]. A total of 328 cases were analyzed for different combinations of the E_1, E_2, E_3, E_4 and t_w possible values (Table 8.1). These values were chosen assuming that for each time point the value of elastic modulus of the hard tissue elements (woven bone and the space among trabeculae) may vary between the value corresponding to the maximum level of porosity and the value of the elastic modulus of the woven bone at this time point. E_1 is the elastic modulus of the hard tissue in the first days after surgery. According to experiments of this Thesis (Chapter 6, [105]), very small and porous amounts of hard tissue may be found until 21 days after surgery, therefore values from 50 MPa (the minimum established above) to 1000 MPa (minimum values obtained for woven bone in Chapter 7, 35 days after surgery, Fig. 7.7) were assumed for E_1. For E_4 absence of porosity was assumed, therefore the elastic modulus of the hard tissue should be the same as that measured in woven bone trabeculae at the end of the process, 15000 MPa (see Chapter 7). t_w represents a change of trend in the evolution of the elastic modulus of the hard tissue. This change of trend may be motivated by an increase of the woven bone elastic modulus (Fig. 7.7, Chapter 7) and a reduction of the porosity (Fig. 7.10). Values between 21 and 250 were used for t_w, according to the higher rates of increment of the elastic modulus of the woven bone and reduction of the porosity observed in Chapter 7. Values between E_1 and E_4 were assumed for E_2 and E_3 taking into account the possible values of t_w and the results of Chapter 7 (Fig. 7.7). For each combination of parameters, the callus stiffness was predicted for each time point. The values of callus stiffness predicted were correlated linearly with results *in vivo* until 80 days after surgery (Fig. 8.4 A). Best correlations were selected according to, firstly, the accuracy of the predictions (deviation from the ideal slope of the linear fit (m=1)) and secondly, how well is the data fit (coefficient of determination, R^2). Fig. 8.4 A shows the linear fits for the six cases with optimal values of deviation and coefficient of determination.

Table 8.1: Parameter values of the bilinear evolution of the hard callus tissue taken in the optimization process (case 2) in the manual segmentation.

Parameter	Values
E_1	50, 100, 150, 200, 500 and 1000 MPa
E_2	500, 700, 900, 1000 and 1500 MPa
E_3	E2, E2 x 2, 1000 and 5000 MPa
E_4	15000 MPa
t_w	21, 28, 30, 49, 70, 80, 100, 170 and 250 days

8.2.3 Mechanical properties assignment: HU segmentation

Also, two different cases were considered (see Fig. 8.3). First, the elastic modulus was linearly scaled to the HU level according to literature [161] (case 3). Second, the HU level - elastic modulus relationship was optimized based on the *in vivo* measurements of stiffness (see Chapter 6) (case 4).

Case 3. The relationship elastic modulus-gray value used by Shefelbine et al. [161] was adapted by extrapolating the gray values to HU (expressed as a percentage of the maximum HU level in each CT) (Fig. 8.3, case 3). Soft tissue (gray values $<$ 48, HU $<$ 36%) had a constant elastic modulus of 50 MPa. Hard tissue elastic modulus depends on the gray value/HU linearly, increasing from 50 MPa (gray value = 48, HU = 36%) to 18 GPa (gray value = 127, HU = 95%). In addition, to take into account the cortical bone (not modeled by Shefelbine et al. [161]), elements with HU level above 95% of the maximum HU level, were considered to be fully mineralized and were assigned the same elastic modulus as the the cortical bone (18 GPa).

Case 4. The following parameters were optimized (Fig. 8.3, case 4): elastic modulus of the soft tissue (E_s), the minimum elastic modulus of the hard tissue (E_w) and the percentage of the HU level that separates the soft tissue and the hard tissue (g). Like in the manual segmentation case, the optimization consisted of calculating the values of the different parameters and selecting the combination that provided the most accurate results compared to the *in vivo* measurements of stiffness (see Chapter 6 [115]). The optimization analyzed 336 combinations for the values in Table 8.2. These values were chosen according to experimental results. It has been shown in Chapter 5 [114] that the mean elastic modulus of the soft tissue within the callus during the distraction phase increases from 0 to 15 MPa; therefore, values between 1 and 20 MPa have been used for E_s in the optimization process. E_w values were between the assumed value of the elastic modulus corresponding to the maximum level of porosity, 50 MPa, and the minimum value of the elastic modulus of the woven bone according to Chapter 7, 5 GPa. An elastic modulus value according to nanoindentation experiments (Chapter 7) was used for the cortical bone (18 GPa) and was also considered the maximum elastic modulus of the hard tissue. Finally, a range of values was used also for g since, according to CT images, the HU level that separates the soft tissue and the hard tissue may vary between 18 and 36%. Fig. 8.4 B shows the linear fits for the six cases with optimal values of deviation and coefficient of determination.

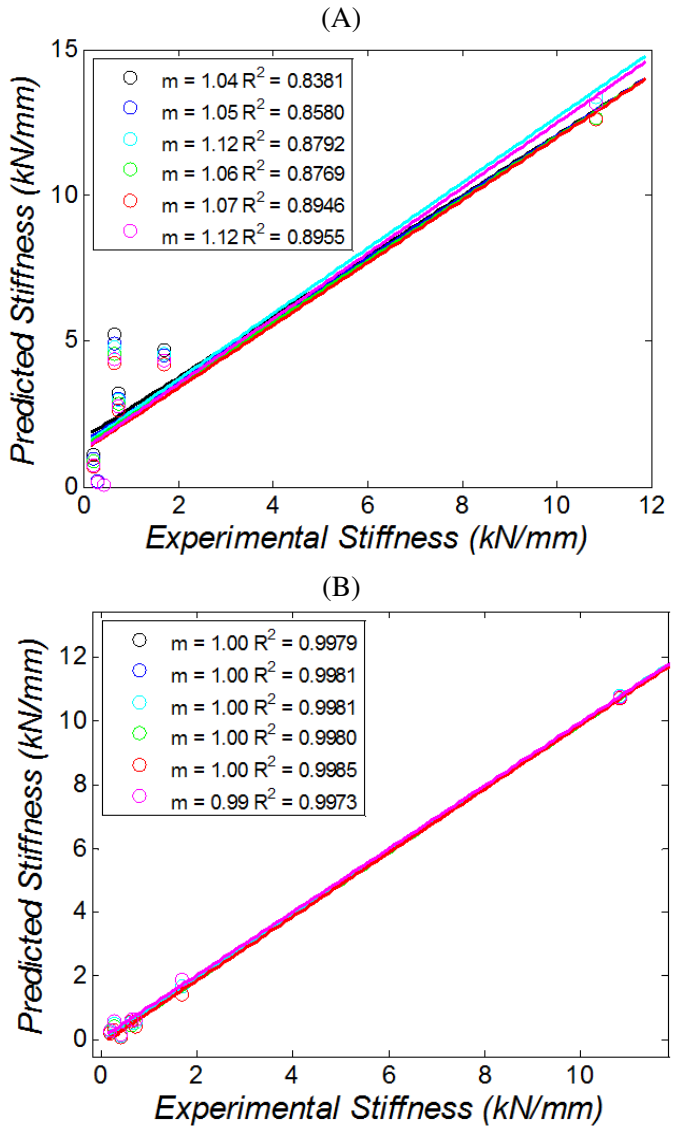

Figure 8.4: Predicted and experimental callus stiffness correlations with optimum values of slope (m) and coefficient of determination (R^2) in case 2 (A) and case 4 (B).

Table 8.2: Parameter values of the bilinear evolution of the hard callus tissue bone taken in the optimization process in the HU segmentation (case 4).

Parameter	Values
E_s	1, 5, 7.5, 10, 12.5, 15 and 20 MPa
E_w	100, 600, 800, 1000, 1200, 1400, 1600, 2500 and 5000 MPa
g	18, 20, 22, 24, 26, 28, 30, 31, 31.5, 32, 32.2, 32.5, 33, 34, 36 %

8.2.4 Loading and boundary conditions

Simulations were performed in Abaqus®. Boundary conditions of the model consisted of constraining the distal segment of the bone (Fig. 8.5 A). The loading conditions consisted of a force applied to the proximal segment according to the values measured experimentally *in vivo* in Chapter 6 for each day of the distraction process [115] (Fig. 8.5 B):

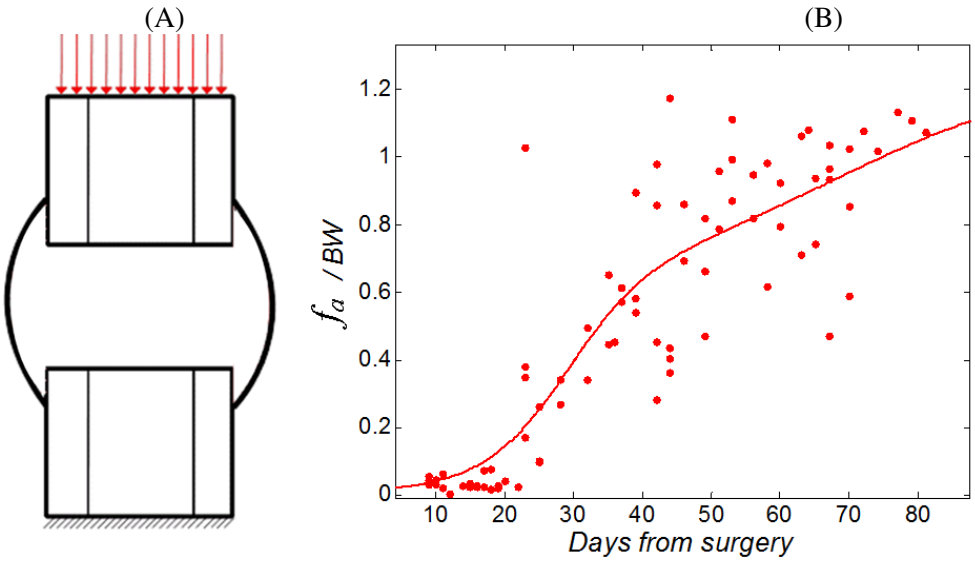

Figure 8.5: (A) Scheme of the loading and boundary conditions; (B) *In vivo* loading values versus time (in days) after surgery [115]. The points are experimental values of the force through the callus (f_a) with respect to the body weight (BW) and the line represents the fit of these values with time.

8.3 Results

In this section the predicted stiffness of the callus at different time points according to the four cases presented above is reported. The predicted callus stiffness until 80 days after surgery is compared with the *in vivo* values reported in Chapter 6 to evaluate the accuracy of each method. Finally the volume of the soft and hard tissues measured with the manual segmentations is also reported.

8.3.1 Mechanical properties assignment: manual

Case 1. The callus stiffness predicted assuming constant mechanical properties by this method for each CT image is shown in Fig. 8.6 A. Results predicted an increase of the callus stiffness from 0.5 to 70 KN/mm during the bone transport process. However, callus stiffness predictions values are not well correlated with *in vivo* experimental values measured until 80 days after surgery, $R^2 = 0.6255$ (Fig. 8.6 B).

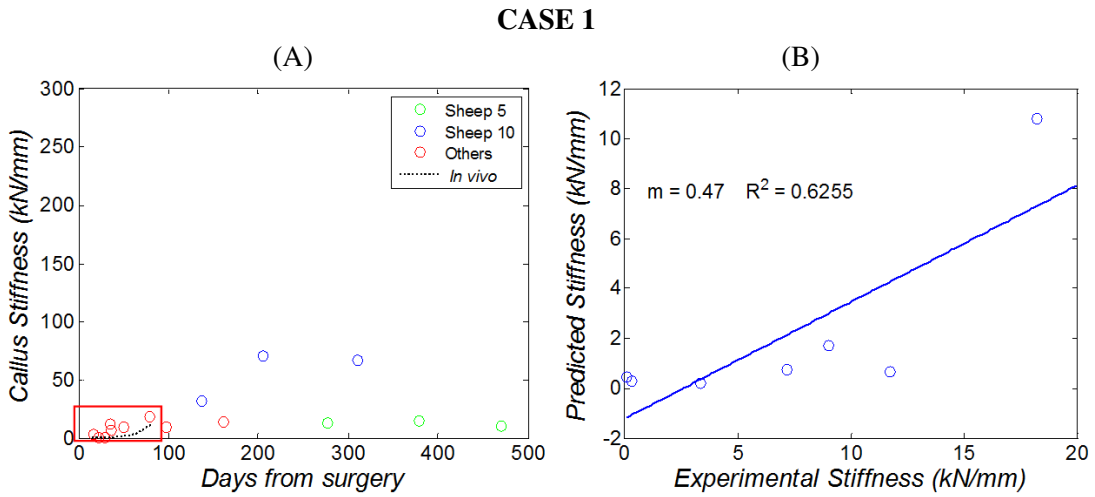

Figure 8.6: (A) Callus stiffness estimation from CT images based finite element using manual segmentation and the material properties used by Reina-Romo et al. [144] for each tissue type of the callus. The time points for each sheep are represented with a different color: sheep number 5 (green), sheep number 10 (blue) or the rest of the sheep which were evaluated at one time point (red). The callus stiffness values obtained from fitting the *in vivo* measurements are also represented by the dotted line. (B) Correlation between stiffness measurements *in vivo* and the stiffness predicted by the model until 80 days after surgery (data within the rectangle in (A)).

Case 2. For the method that considers mechanical properties of hard callus tissue variation with time and defines the properties by optimization, the best correlation was obtained for E_1 = 100 MPa, E_2 = E_3 = 700 MPa and E_4 = 15000 MPa and t_w = 80 days (See Fig 8.7 A). The callus stiffness values predicted by the model for the optimum material properties are shown in Fig. 8.7 B. In this case the model predicted that callus stiffness increases from 0.4 to 100-300 KN/mm after 300 days from surgery approximately. These predicted values are correlated with experimental values measured until 80 days after surgery (Fig. 8.7 C). The optimization process got slope of fit close to 1 (Fig. 8.7 C) and increased the determination coefficient value (R^2) from 0.6255, in case 1 (Fig. 8.6 B), to 0.8769 (Fig. 8.7 C).

8.3.2 Mechanical properties assignment: HU

Case 3. Fig. 8.8 A shows the predictions of callus stiffness values obtained using the HU - elastic modulus relation according to Shefelbine et al. [161]. Results predicted an increase of the callus stiffness from 0.4 - 1 kN/mm to 50-180 kN/mm during the bone transport process. Also, callus stiffness predictions values are well correlated with experimental values measured until 80 days after surgery, showing a slope close to 1 and a determination coefficient of 0.9719 (Fig. 8.8 B).

Case 4. After applying the optimization of the parameters that relate the elastic modulus of the different elements of the model with the HU level, the best correlation was obtained for

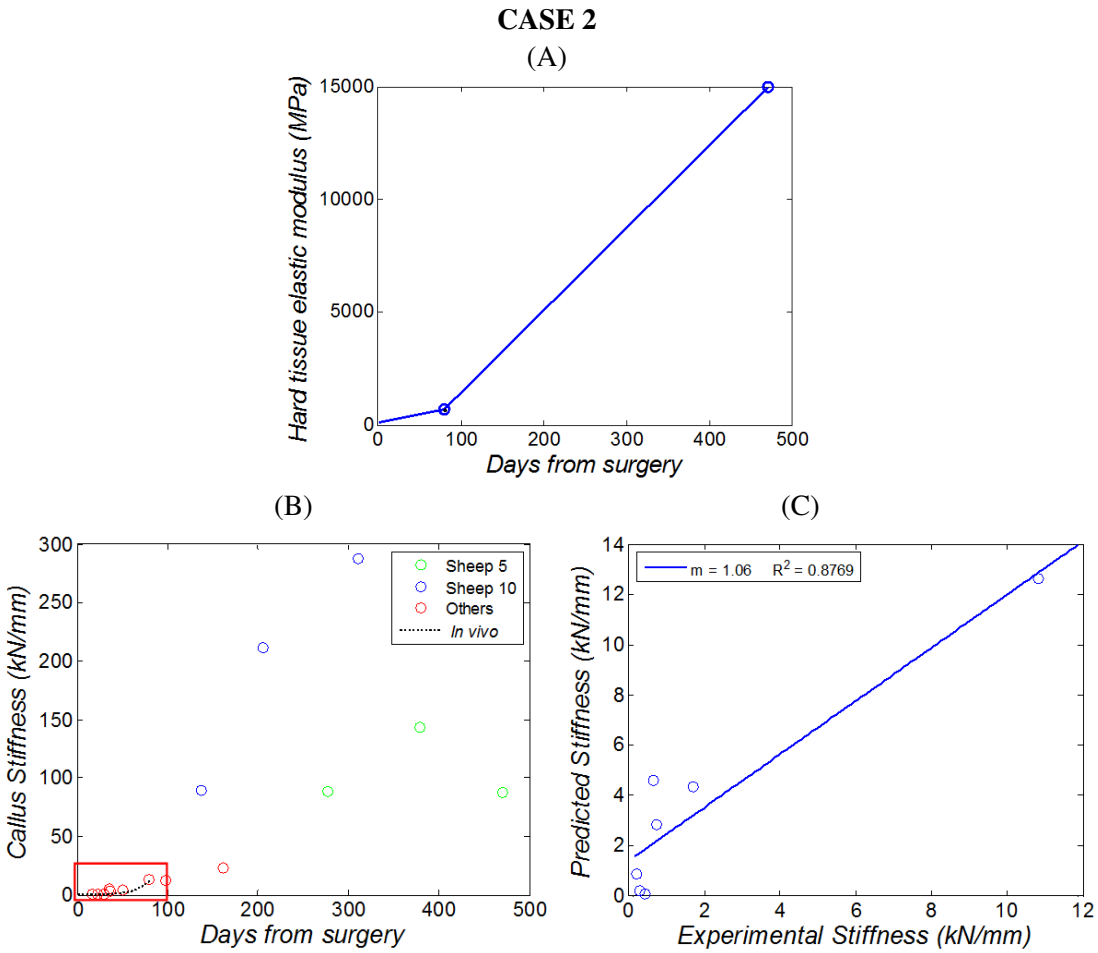

Figure 8.7: (A) Relationship between the hard callus tissue woven bone elastic modulus and the days from surgery after the optimization process in the manual segmentation; (B) Callus stiffness estimation from CT images based finite element after optimization of the mechanical properties of the callus tissue types. Each time point is represented with different colors depending on the sheep used for CT: sheep number 5 (green), sheep number 10 (blue) or the rest of the sheep which were evaluated at one time point (red). The callus stiffness values obtained from fitting of the *in vivo* measurements are also represented by the dotted line. (C) Correlation between stiffness measurements *in vivo* and the stiffness predicted by the model (data within the rectangle in (B)).

E_w = 12.5 MPa, E_s = 800 MPa and g = 31.5. The callus stiffness values predicted by the model for the optimum material properties are shown in Fig. 8.9 A. In this case the model predicted that callus stiffness increase from 0.1 - 0.2 to 140 - 150 kN/mm after 300 days from surgery approximately. These predicted values are correlated with experimental values measured until 80 days after surgery (Fig. 8.9 B). The optimization process increased the determination coefficient value from 0.9719 in case 3 (Fig. 8.8 B), to 0.9979 (Fig. 8.9 C) for values of stiffness

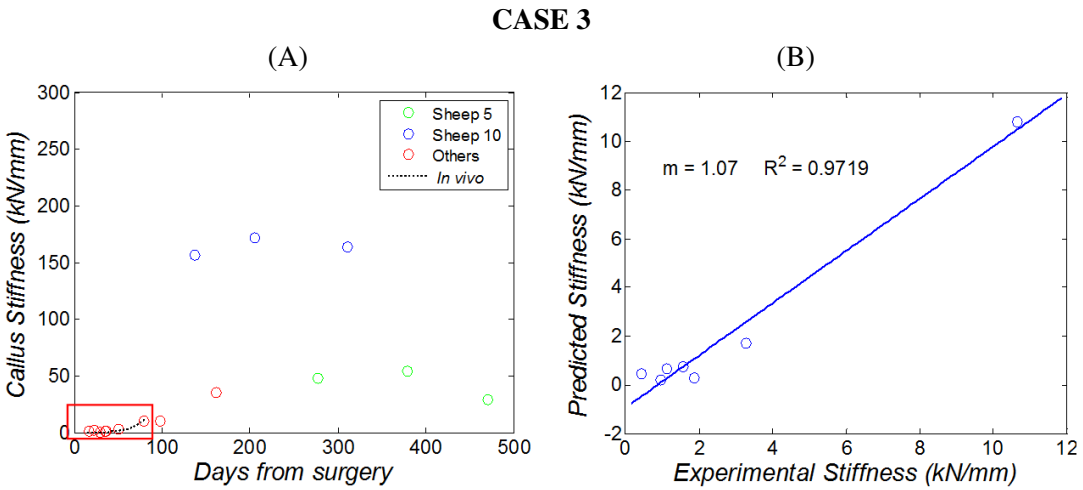

Figure 8.8: (A) Callus stiffness estimation from CT images based finite element using HU segmentation according to the elastic modulus of tissue - grey scale law proposed by Shefelbine et al. [161]. Each time point is represented with different colors depending on the sheep used for CT: sheep number 5 (green), sheep number 10 (blue) or the rest of the sheep which were evaluated at one time point (red). The callus stiffness values obtained from fitting of the *in vivo* measurements are also represented by the dotted line. (B) Correlation between stiffness measurements *in vivo* and the stiffness predicted by the model (data within the rectangle in (A)).

until 80 days after surgery.

8.3.3 Volume of soft and hard tissue within the callus

Fig. 8.10 shows the evolution of the callus tissue proportions (hard and soft tissue) from quantifying the manual segmentation volumes quantification. It may be seen that the percentage of hard tissue increased from approximately 50 - 60% at the end of the distraction process to 90-100% from 100 days after surgery. The opposite trend was followed by the soft tissue.

8.4 Discussion

In this work, the mechanical properties over time of the distraction callus have been evaluated *in silico* based on CT images. Two different approaches have been used to assign the mechanical properties to the tissues developed within the distracted callus: manual segmentation or based on the level of HU. Manual segmentation works with homogeneous sets of elements which represent the different tissue types: medullar tissue, cortical bone, soft and hard callus tissue. This approach has been traditionally used in mechanobiological studies of distraction osteogenesis and bone healing [59, 85, 140, 141, 145]. However, this is a strong assumption since tissue types within the callus may appear mixed and mechanical properties may vary significantly in the same tissue. Maps of elastic modulus determined in Chapter 7 show the

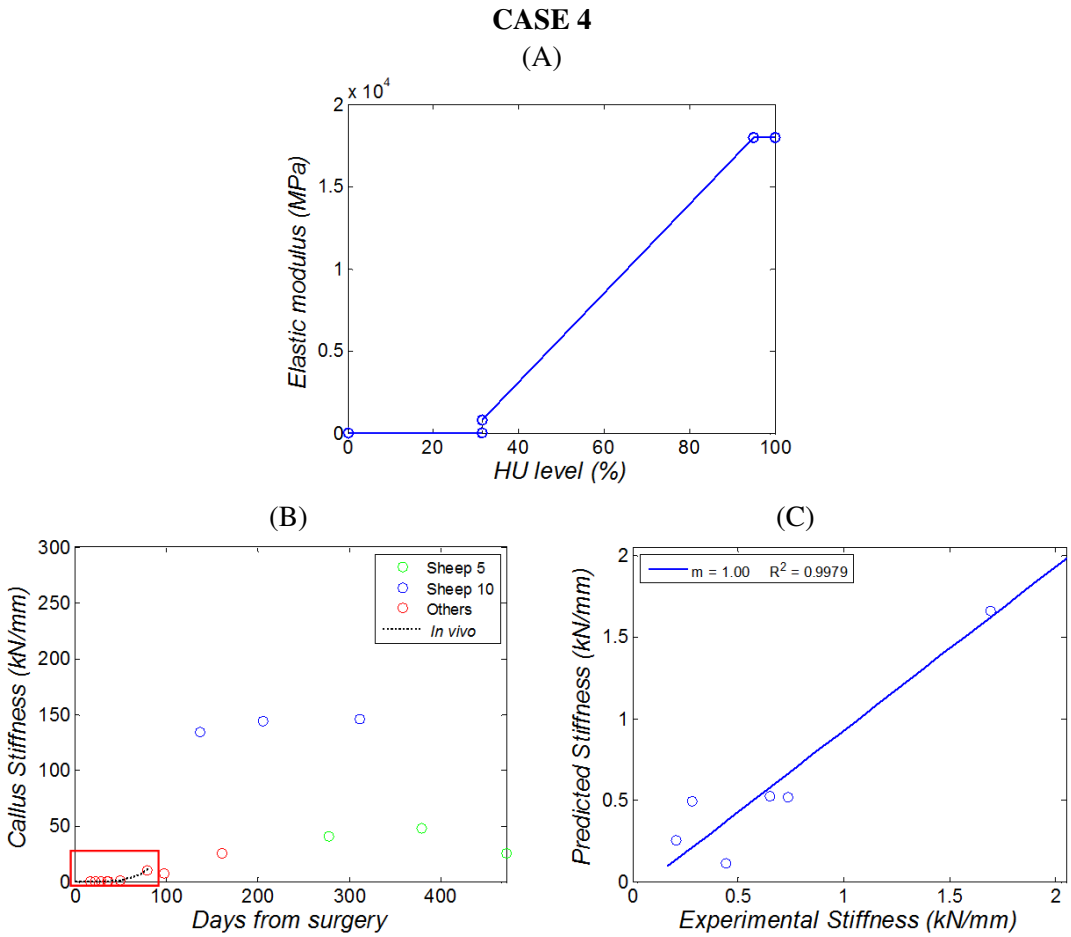

Figure 8.9: (A) Relationship between the hard callus tissue elastic modulus and the HU level after the optimization process; (B) Callus stiffness estimation from CT images based finite element after the optimization of the elastic modulus - HU level relation. Each time point is represented with different colors depending on the sheep used for CT: sheep number 5 (green), sheep number 10 (blue) or the rest of the sheep which were evaluated at one time point (red). The callus stiffness values obtained from the fit of the *in vivo* measurements are also represented by the dotted line. (C) Correlation between stiffness measurements *in vivo* and the stiffness predicted by the model (data within the rectangle in (B)).

heterogeneity of these tissues within the distracted callus at a given instant of the process. In addition, the mechanical properties of all tissue types within the callus increase during the distraction phase, as suggested previously [78, 114] (see Chapter 5). This drawback may be solved with the HU segmentation since this method allows assigning an elastic modulus to each element depending on its HU level and regardless its location. In addition, this method takes into account the variation of elastic modulus with time for all elements.

The results of callus stiffness using manual segmentation have shown acceptable level of

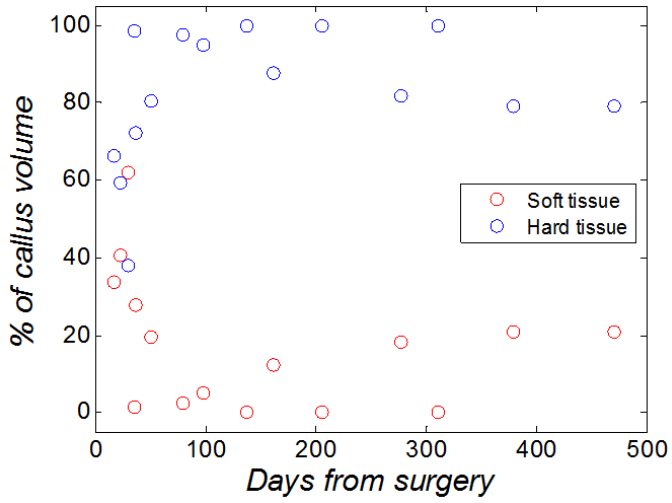

Figure 8.10: Proportion of soft and hard tissue within the callus from manual segmentation.

correlation if the elastic modulus of the hard tissue of the callus is considered variable with time, case 2 (Fig. 8.7 C). However, if constant properties for the callus tissues are assumed with time, results have low level of correlation, case 1 (Fig. 8.6 B). Also, in this case, stiffness values predicted at the end of the process for sheep n^{o}5 (277, 379 and 471 days after surgery) are similar to those obtained at the beginning of the process (Fig. 8.6 A).

Proportions of soft and hard tissue of the callus from manual segmentation (Fig. 8.10) are in concordance with histological results carried out with samples of the same study [105]. López-Pliego [105] provided the proportion of soft and hard callus tissue within the callus from quantification of the corresponding area in histological images (Fig. 8.11). According to both results the callus is 80-100% hard tissue since 100 days after surgery; however, the increase of stiffness continued until 200-400 days after surgery (Figs. 8.7 B, 8.8 A, 8.9 B). These results and the low level of correlation obtained if constant properties for the callus tissues are assumed, suggest that the hypothesis about the woven bone elastic modulus increment with time and reduction of the porosity of the hard tissue of the callus could be right.

Callus stiffness predictions using HU segmentation (cases 3 and 4) have shown more accurate results than using manual segmentation (cases 1 and 2) and the corresponding determination coefficient between numerical stiffness and *in vivo* measurements increases up to 0.9719 (Fig. 8.8 B) and 0.9979 (Fig. 8.9 C). Lower values of stiffness at the end of the process (50-180 kN/mm approximately) were obtained compared with predictions using manual segmentation (150-300 kN/mm). It can also be observed in all the cases studied that the stiffness decreases after achieving a peak value after at 200-400 days after surgery approximately (Figs. 8.6 A, 8.7 B, 8.8 A, 8.9 B). This has been suggested previously in other works in literature [10]. However, more time points after 471 days after surgery are necessary to consider this suggestion as a definitive result.

Results of the callus stiffness estimations show significant values of scatter for all the cases analyzed (Figs. 8.6 A, 8.7 B, 8.8 A, 8.9 B), especially at the end of the process. This scatter is

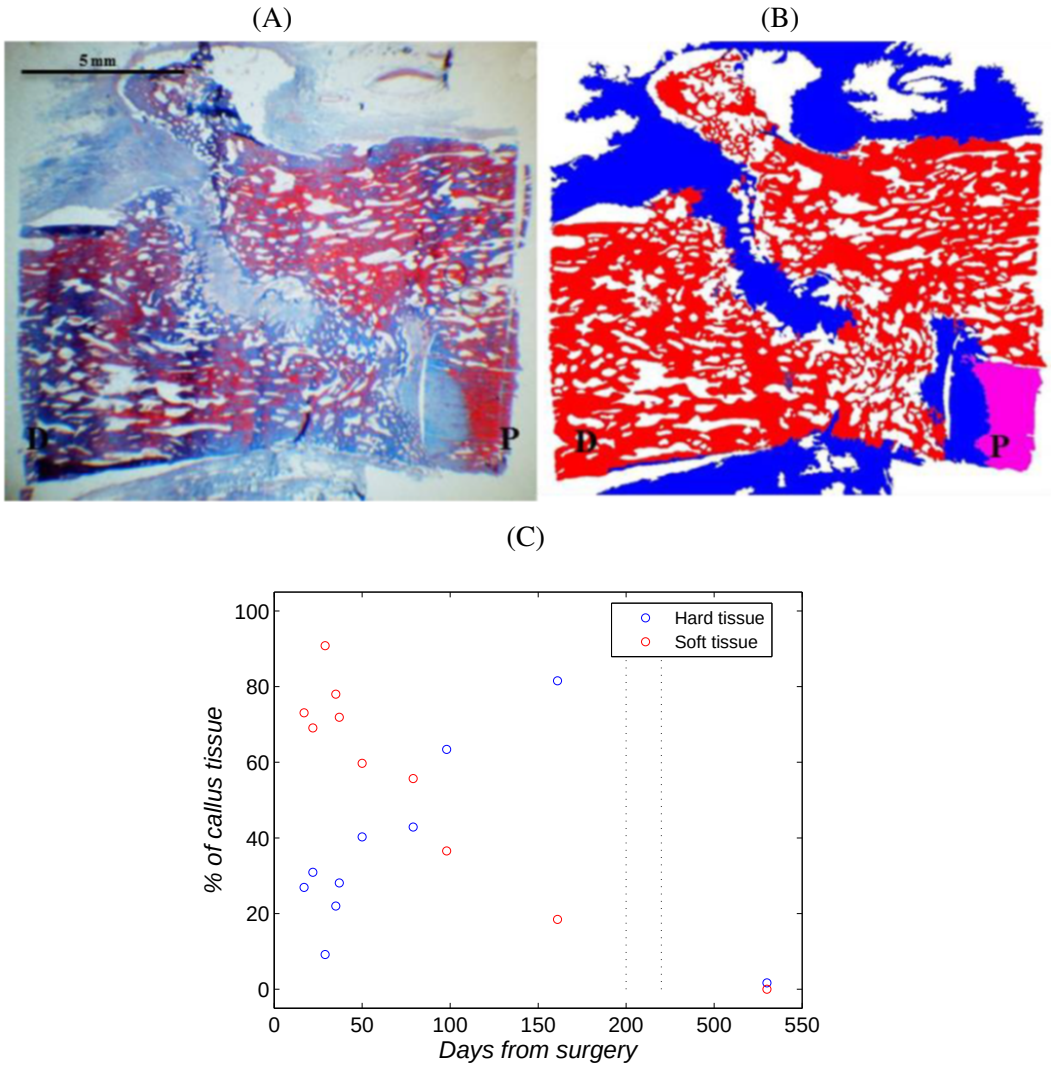

Figure 8.11: López-Pliego, [105]: (A) Histological image of the distraction callus 98 days after surgery, Masson trichrome, 10X. (B) Color map from (A) for quantification of the proportion of soft (blue) and hard (red) callus tissue. (C) Proportion of soft and hard tissue area within the callus from all the histological images carried out at different time points.

due to the inter-individual differences during the process. For example, Figs 8.6 A, 8.7 B, 8.8 A and 8.9 B show that the volume of the callus, for sheep n^o 10, is twice the callus volume of sheep n^o 5 around 300 days after surgery. Scatter between stiffness predictions for both sheep decreased considerably if the callus stiffness value is divided by the corresponding value of the average callus area (Figs. 8.12 A and 8.12 B).

Despite the experimental and computational results being similar, this work presents several limitations and assumptions that, at least, have to be revised in order to know their implications. Firstly, in the manual segmentation procedure, only four different tissue types have

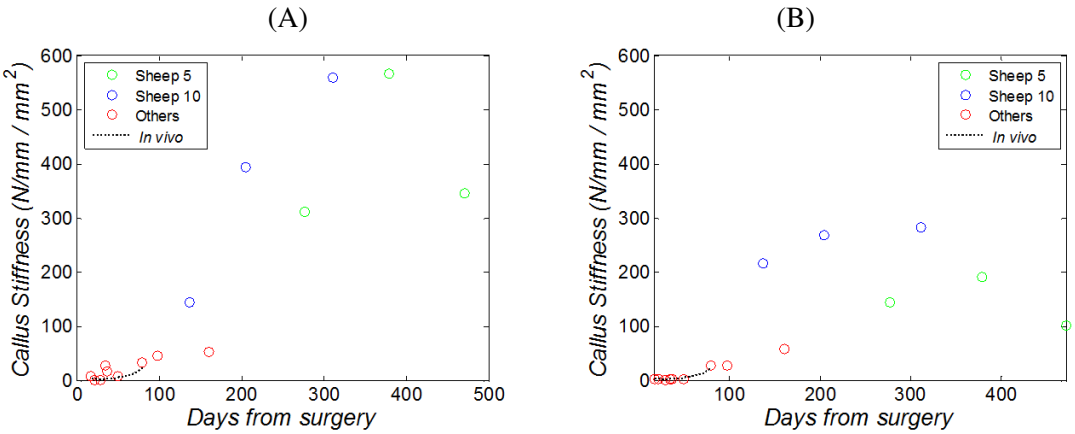

Figure 8.12: Callus stiffness estimation divided by the average area of the callus. Each time point is represented with different colors depending of the sheep used for CT: sheep number 5 (green), sheep number 10 (blue) or the rest of the sheep which were evaluated at one time point (red). The callus stiffness values obtained from the fit of the *in vivo* measurements divided by the fit of the average area measurements are also represented by the dotted line. (A) Manual segmentation; (B) HU approach.

been differentiated: the soft callus tissue, hard callus tissue, cortical bone and bone marrow. Secondly, all tissues were assumed to be linear, elastic and isotropic. Also, callus stiffness was evaluated under the small deformation assumption. Finally, numerical values have been compared against experimental data until day 80 after surgery.

As far as the author knows, this model is the first to evaluate the stiffness of the callus computationally during distraction osteogenesis. This can be very useful to improve current clinical protocols and for future *in silico* models.

Chapter 9

In vivo gait analysis during bone transport

The evolution of the gait conditions during the bone transport process are analyzed in this Chapter by means of measuring the ground reaction force during gait of intervened and healthy sheep from the surgery to more than one year later. The outcomes reported here are based on a published paper [116]: J Mora-Macías, E Reina-Romo, J Morgaz and J Domínguez. *In vivo* gait analysis during bone transport. *Annals of Biomedical Engineering*, 43(9):2090-100, 2015.

Chapter 10

Closure

10.1 Summary

The aim of this Thesis was to quantify and relate quantifiable biological parameters (the bone tissue volume and its distribution in the distraction callus, proportion of different tissue types...) with mechanical parameters (the force through the fixator and through the callus, the mechanical properties of the callus tissue during the process...) during the complete distraction osteogenesis process. Bone transport experiments were carried out in 11 sheep by an interdisciplinary team of mechanical engineers, orthopaedics surgeons and veterinarians. The experiments consisted of the implantation of the distractor in animals which followed the same distraction protocol: 7 days of latency after surgery, 15 days of distraction with a rate of 1 mm per day, the consolidation phase until the distraction callus was completely ossified and the remodeling phase. Different mechanical parameters were monitored *in vivo* by means of the instrumentation of the fixator. Each animal was sacrificed at different time points (17, 22, 29, 35, 37, 51, 79, 98, 161 and 525 days after surgery) to obtain samples for *ex vivo* experiments along the process.

The distractor used was designed, calibrated and tested in preliminary *in vivo* experiments. This distractor allowed measuring callus stiffness *in vivo* during the experiments at any time under real load conditions during the distraction and consolidation phases of the bone transport process. *In vivo* measurements during the distraction phase provided the force relaxation of the callus tissue and the contribution of the callus traction and the docking-site compression to the distraction force. In addition, an experimental band was provided for the residual force value after each step of distraction from models of mechanical behavior of the callus tissue. During the consolidation phase, the callus stiffness, the force through the callus and the volume of the callus were monitored. Moreover, nanoindentation experiments were carried out in the harvested samples completely ossified to assess the spatial and temporal evolution of the elastic modulus of the woven bone tissue generated during the bone transport process. Furthermore, a numerical analysis of the experimental results was also carried out. It consisted of a finite element analysis based on the computed tomographies for predicting the stiffness of the distraction callus. Finally, the gait conditions during bone transport were assessed by means of analyzing the ground reaction force measurements (peak force, mean force and impulse).

10.2 Discussion

A comparison among the evolution with time of the different mechanical parameters assessed during the bone transport process in the different Chapters of this Thesis follows. The experimental *in vivo* measurements of force through the callus and the callus stiffness, the woven bone volume of the callus (see Chapter 6), the woven bone volume production rate, the mean elastic modulus of the woven bone within the callus (see Chapter 7) and the gait symmetry based on the peak value of the ground reaction force (see Chapter 9) are represented together in Fig. 10.1. A correlation of the callus stiffness values obtained using finite element analysis based on computed tomography assigning the mechanical properties of the tissues within the distraction callus according to the level of Hounsfield Units (see Chapter 8) is also represented in Fig. 10.1. Parameters are normalized to allow comparison.

Table 10.1: Equations in which are based the curves in Fig. 10.1 which are the normalizations of these reported along the different Chapters of this work.

Woven bone volume within the distraction callus	$\frac{100}{1+e^{-0.065\cdot(t-42)}} - \frac{83.2}{1+e^{-0.007\cdot(t-320)}}$
Woven bone production rate	$\frac{416.7e^{-0.065\cdot(t-42)}}{(1+e^{-0.065\cdot(t-42)})^2} - \frac{37.0e^{-0.007\cdot(t-320)}}{(1+e^{-0.007\cdot(t-320)})^2}$
Callus stiffness (numerical results)	$\frac{100}{1+e^{-0.04\cdot(t-150)}}$
Callus stiffness (*in vivo* results)	$0.054e^{0.064t}$
Force through the callus	$\frac{50}{1+e^{-0.170(t-28.99)}} + \frac{50}{1+e^{-0.062\cdot(t-68.70)}}$
Mean elastic modulus of the woven bone	$100 - 56.04e^{-0.0024\cdot(t-21)}$
Gait symmetry	$100 - 41.23e^{-0.0059\cdot t}$

Fig. 10.1 shows that the force through the callus, the callus stiffness and the elastic modulus of the woven bone within the callus increased after the distraction phase following different rates and reaching the reference values for healthy animals after 90, 250 and 500 days from surgery respectively. The volume of the callus increased achieving a maximum value of approximately 5 times the volume of a similar section of metatarsus 90 - 150 days after surgery.

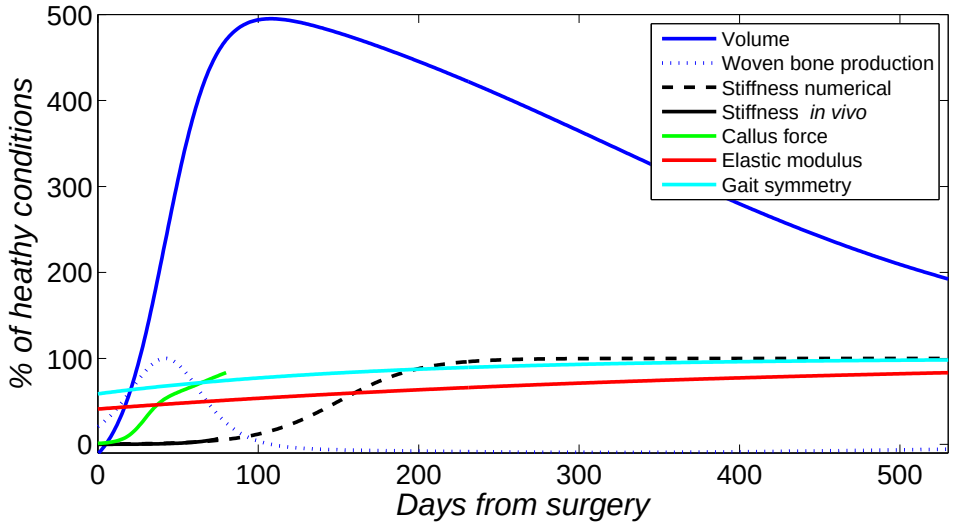

Figure 10.1: Evolution with time of the normalized values of the force through the callus, the callus stiffness (*in vivo* and numerical), the woven bone volume within the callus, the woven bone tissue production rate, the mean elastic modulus of the woven bone and the gait symmetry based on the peak value of the ground reaction force. The force through the callus was normalized to the mean value of the internal force that is the total force through the metatarsus (see Chapter 6), i.e. the sum of force through the distraction callus and through the fixator. The axial callus stiffness and woven bone volume were normalized to the values of a healthy segment of a metatarsus with the same length (see Chapter 6). The evolution with time of the reduced elastic modulus of the woven bone was normalized with the mean reduced elastic modulus of the cortical bone (18.2 GPa) (see Chapter 7). Since tissue production rate in healthy conditions is zero, their experimental values were normalized to the maximum value of tissue production rate. Finally the gait symmetry index values were scaled considering 100% as healthy conditions (see Chapter 9). The equations in which are based the curves of this figure, which are the normalizations of these reported along the different Chapters of this work, are included in Table 10.1

.

The maximum value of the woven bone production took place above 50 days after surgery. The recovery of the gait conditions was more progressive than other mechanical parameters analyzed. Gait conditions reached values close to healthy animals after 300 days from surgery. The analysis of all these mechanical parameters together allows obtaining additional information:

- It seems that the mechanical parameter that is related with the production of woven bone tissue during the consolidation phase is the force through the callus and not the callus stiffness or the elastic modulus of the woven bone. Maximum values of bone tissue production rate were achieved during the period of time when the force through the callus was below those produced in healthy conditions. Furthermore, the maximum callus volume was reached just after the total recovery of load bearing capacity and

after this moment it began to decrease. However, at the moment of maximum callus volume the callus stiffness was under 20% and the elastic modulus was far from the values of cortical bone. This fact means that the x-ray monitoring, which only provides information of the callus volume, must be used with caution in clinical applications.

- The contribution of the increase of the elastic modulus of the woven bone to the increase of the callus stiffness is low compared to the effect of the increase of the callus volume. It may be observed in Fig. 10.1 that just after the recovery of the stiffness in the intervened limb, the elastic modulus of the callus is over 65% of the elastic modulus of the cortical bone, only 20% more than at the beginning of the process. It was still 80% after 80 days from surgery. However, during the period of time in which the callus stiffness reached healthy values (0-200 days after surgery), the volume of the callus increased from zero to 4 o 5 times the value of a cortical bone segment of similar length.

- The reorganization of the woven bone structure and the reduction of the porosity have an important role in the increase of the callus stiffness, specially from 100 days after surgery. Once achieved the maximum value of the callus volume, approximately 100 days after surgery, the volume began to decrease. However, the callus stiffness continued increasing until approximately 250 - 300 days after surgery while the mean elastic modulus of the woven bone increased only 10%. On the other hand, from 250 - 300 days after surgery, the callus volume significantly decreased; however, the callus stiffness is approximately constant and the mean elastic modulus of the callus increased only approximately 20% in 200 days. These experimental facts may not be explained without the woven bone structure reorganization, the reduction of the porosity and/or the variation of the heterogeneity of the mechanical properties. In fact, it has been demonstrated that the variation of the heterogeneity of the material properties of the bone affects the mechanical properties [164].

- The recovery of the gait symmetry conditions took place after the stiffness recovery. It steps up the conclusion of the Chapter 9 about the possibility of using gait analysis as an alternative method to control distraction osteogenesis or bone healing. If gait symmetry conditions are recovered, it means that the stiffness of the leg has been recovered before. This fact makes the gait symmetry criterium a safer method compared to the observation of the callus volume in x-rays since it may be seen that the maximum level of callus volume is reached before the level of callus stiffness was recovered.

10.3 Conclusions

The major conclusions of this Thesis may be formulated as follows:

- The instrumented distractor developed and calibrated shown in Chapter 4, has allowed the mechanical characterization of the bone transport process by means of the experiments carried out in this Thesis. Devices with similar characteristics provide comprehensive control of the distraction osteogenesis applications since they allow monitoring

the force and the callus stiffness during the time that the distractor is implanted in the patients.

- An experimental band was provided for the relaxed forces values after each step of distraction from models of viscoelastic behavior of the callus tissue (see Chapter 5). According to these models, the residual force 24 hours after each distraction step reached a maximum value of 71.6 N, and the peak distraction force increased with days of distraction from 7-34 N to 41-246 N. The maximum residual force values that were predicted are much lower than those measured during bone lengthening in the literature [177]. These results may show the influence of the surrounding soft tissues during bone transport compared with bone lengthening cases of distraction osteogenesis. Moreover, experimental measurements showed that distraction force through the docking-site was negligible with respect to the distraction force through the callus at each step of distraction.

- During the consolidation phase of the bone transport process, the period of maximum ossification took place from 20 to 70 days after surgery, where the maximum bone tissue production rate was achieved and the volume of the woven bone within the callus increased from zero to 80% of their maximum values (see Chapter 6). This period also coincided with the recovery of load sustained by the intervened limb (from 3 to 12% to 60 to 70%). However, this period of maximum ossification corresponded to low callus stiffness values. The callus stiffness increased exponentially from the end of the distraction phase but did not achieved values above 10% of stiffness in healthy conditions until 70 days after surgery.

  Therefore, it can be concluded that callus volume is a good indicator of the load bearing capacity of the intervened limb but not of the stiffness. It means that usual examinations by means of radiographies may predict the load bearing capacity but not the recovery of stiffness in the intervened limb. The higher callus stiffness increase takes place after maximum callus volume is achieved and once load bearing capability is recovered (see Chapter 8), i.e. during the bone remodeling phase.

- Nanoindentation measurements in Chapter 7 showed that the mean elastic modulus of the woven bone generated during the bone transport process in the distraction and docking-site calluses increases with time (from 7 GPa, 35 days after surgery, to 14 GPa, 525 days after surgery approximately, which is 77% of mean elastic modulus of cortical bone). This increase was slower with time both in distraction and docking-site calluses (0.5 GPa per week to 0.05 GPa per week approximately). Woven bone generated during the bone transport process presented lower increments of elastic modulus with time than values reported for fracture healing cases [109]. During fracture healing the period of time needed to reach 95% of the mean value of elastic modulus of the cortical bone is approximately 20% relative to the same magnitude for the woven bone of the distraction callus and docking-site. It could be due to the absence of traction stimuli. Furthermore, different spatial variations of elastic modulus within the callus were found for different stages of the process.

- Finite element analysis based on computed tomographies are useful in predicting the callus stiffness during distraction osteogenesis (see Chapter 8). Results of the application of this technique using the level of Hounsfield Units to assign the mechanical properties of the tissues within the distraction callus have shown more accurate results than using manual segmentation. Manual segmentation studies with homogeneous sets of elements has been traditionally used in mechanobiological studies of distraction osteogenesis and bone healing [59, 85, 140, 141, 145]. Therefore, *in silico* models combined with computed tomographies images may be very useful to improve current clinical protocols and for future finite element models. Results reported the increase of the distraction callus stiffness from 0.1 - 0.2 to 140 - 150 kN/mm (which is in the order of stiffness of the healthy metatarsus) after 250 days from bone transport surgery approximately.

- Gait analysis could be used as an alternative method to control distraction osteogenesis or fracture healing evolution (see Chapter 9). Gait parameters obtained from ground reaction force measurements (peak force, mean force and impulse) decreased in the intervened limb and, most significantly, increases in the other limbs due to the intervention. During the consolidation, these gait parameters approached the normal values of healthy animals. By means of the evolution of these parameters the status of ossification within the callus could be estimated and the appropriate time to remove the fixator could be determined. Furthermore, gait analysis has advantages over other methods that allows mechanical assessment of the process because it provides quantitative data and does not require instrumented fixators.

10.4 Original Contributions

The main contributions of this Thesis are listed in the following points:

- A new instrumented distractor that allows force and callus stiffness monitoring during bone transport has been designed and calibrated.

- Two models of the distraction callus tissue viscoelastic behavior during the distraction phase of bone transport based in experiments *in vivo* were provided: assuming total force relaxation and assuming the existence of residual force. Experimental bounds were provided by these models for the force. It was shown that the distraction force due to the compression of the docking-site was negligible with respect to the distraction force due to the traction of the callus at each step of distraction.

- Experimental *in vivo* measurements of force, callus stiffness and callus volume during the consolidation phase of the bone transport process.

- Spatial and temporal variations of the elastic modulus in the woven bone generated during the bone transport process within the distraction and docking-site calluses.

- Estimation of the distraction callus stiffness by means of finite element analysis based on computed tomographies during bone transport. This technique was applied using the

level of Hounsfield Units to assign the mechanical properties of the tissues within the distraction callus and using manual segmentation.

- Monitoring of the recovery of the gait conditions (peak, mean and impulse of ground reaction force in the intervened limb) along the process of bone transport.
- Comparison of the evolution of the experimental data above said (force relaxation, forces through the callus, callus stiffness, callus volume, bone tissue production rate, elastic modulus of the woven bone within the callus and recovery of gait conditions), all of them obtained from the same bone transport experiment.

10.5 Future work

The possible improvements in the field of the distraction osteogenesis are innumerable since the mechanobiology of the process is not totally understood today. New findings will be necessary to provide instructions in clinical applications adaptable to the particularities of each case and not only based on the clinical experience. Computational models based on experimental data may contribute to make possible a tool able to predict the evolution of the process of distraction osteogenesis in different situations. Therefore, experimental and computational works should be developed in the next years and some of them could use the data provided in this Thesis as an extension of the work carried out. Some of the lines of research which could be developed follows:

1. Future experimental works:
    - This work provided data about the evolution of the local mechanical properties of the woven bone during distraction osteogenesis. Although, the force relaxation of the tissues within the callus during the distraction phase has been reported, the evolution of the local mechanical properties of each type of soft tissue within the distraction callus was not studied. More exhaustive mechanical characterization of the soft tissue within the distraction callus at different time points are needed to complete experimental database about distraction osteogenesis, specially during the distraction phase. For example, nanoindentation experiments like experiments carried out in the woven bone in this Thesis may be carried out.
    - Results of this Thesis showed that the tissues within the callus increase their mechanical properties with time. It means that for a different duration of the distraction phase, the tissues within the callus may have different mechanical properties than those here obtained and so may change the force boundary conditions. This fact could have consequences in the evolution of the ossification during the consolidation phase. Therefore, similar experiments to those performed in this Thesis, with longer distraction phase, could report interesting data, especially the study of the force relaxation after each step of distraction.
    - Although the outcomes of this work allowed comparing some mechanical parameters measured during bone transport with similar parameters measured in bone

lengthening experiments (e.g. the effects of the elongation of the surrounding soft tissues in the force through the callus), the varying conditions of the experiments in the literature make difficult to obtain more conclusions. Bone lengthening experiments which follow the same mechanical and animal conditions that the experiments carried out in this Thesis could provide useful information about the mechanical differences between the distraction osteogenesis process applied in bone lengthening or in bone transport.

- This work and others in the literature have focussed on the mechanic elastic properties of the woven bone; however, under certain conditions the mechanical behavior of the woven bone may not be assumed totally linear elastic, specially for young tissue. Therefore, future works focused on the evolution of the viscoelastic properties of the woven bone are necessary.
- More detailed and quantifiable experimental monitoring of the angiogenesis during the distraction osteogenesis process is necessary to determine how this process affects to the increase of the stiffness, the increase of the elastic modulus, the reduction of the porosity and the reorganization of the woven bone reported in this Thesis.

2. Future computational works:

   The conclusions of this Thesis and the experimental data obtained may be applied to improve computational works in distraction osteogenesis [85, 86, 141–144, 146] or to generate new models. Specifically, the aspects that could be studied or added in the new computational works follows:

   - Specific computational works about the distraction phase may be developed or improved incorporating experimental data of force relaxation provided in Chapter 5.
   - Chapter 8 shows that results of finite element models using heterogeneous material properties according to the level of Hounsfield Units are more accurate than those which use manual segmentation. New computational models in distraction osteogenesis should take into account the level of gray scale measured experimentally by means of monitoring with x-rays or computed tomographies to assign the mechanical properties of the callus.
   - Apart from the increase of the callus volume and the callus mechanical properties, results of this Tesis showed that the reorganization of the bone structure, the reduction of the porosity and/or variations of the heterogeneity of the woven bone contribute to the increase of the callus stiffness. Results of this Thesis may be used in the validation of models of the consolidation phase of the distraction osteogenesis which propose different hypothesis about the contribution of these factor in the distraction osteogenesis process.

Appendix A

Temporal variations of nanoscale mechanical properties in the same sample

The present Appendix studies the temporal variations during 60 days of the mechanical properties measured by nanoindentation tests performed at ambient and dry conditions in cortical bone and woven bone embedded and polished samples. This work was carried out to ensure that the duration of the experiments of the Chapter 7 does not affect the reliability of the data of woven bone elastic modulus measured. The outcomes presented in this Appendix come from a paper submitted for publication: J Mora-Macías, A Pajares, P Miranda, J Domínguez and E Reina-Romo. Time-dependence of nanoscale mechanical properties of cortical and woven bone.

A.1 Introduction

Ex vivo macro-mechanical experiments have been carried out to determine bone tissue mechanical properties both in mature bone [24, 187] and woven bone [47, 123]. More recently, nanoindentation was introduced to determine the mechanical properties of biological tissues [5, 21, 61, 97, 98, 104, 107, 109, 126, 127, 129, 147, 152, 152, 153, 164, 165, 168, 186]. This technique has also been widely used in bone tissue [5, 21, 97, 98, 107, 109, 126, 129, 147, 152, 152, 153, 164, 165] since it allows more versatility than conventional macro-mechanical experiments [24, 47, 123, 187].

Mechanical experiments with bone require sample preparation and manipulation during the duration of the experiments. During prolonged testing it is required to store the bone specimens, which can be made in different mineral solutions or ambient conditions. It has been determined that the elastic modulus of bone specimens soaked in normal saline significantly diminishes 2.4% after 10 days, whereas the elastic modulus of those soaked in calcium-buffered saline did not change significantly in four point bending test [64]. On the other hand, a 10% decrease in stiffness during the first 24 h post mortem was detected in compression test for samples at ambient conditions [100]. However, the influence in mechanical properties of bone

specimen storage time at ambient conditions during nanoindentation experiments has not been studied yet.

Nanoindentation in embedded and polished bone specimens have reported important information about the spatial and temporal variations of elastic modulus in bone healing [5, 109], bone permeability changes [154], variations due to age [147] or the influence of nanoscale heterogeneity in bone strength [164, 165]. Some of these nanoindentation tests can take hours or even days if the number of indentations is high. Some works in literature compared results of experiments under different conditions [21, 129, 153]. However some of the existing studies did not provide any data about the temporal variation of the mechanical properties of bone specimens in ambient conditions during the tests.

This study seeks to assess the temporal variations of bone mechanical properties (reduced elastic modulus and hardness) evaluated via nanoindentation at dry conditions in the same sample. Cortical and woven bone specimens prepared by embedding in epoxy resin and polishing have been used.

A.2 Material and methods

A.2.1 Sample preparation

The cortical bone specimen was obtained from the tibia mid-diaphysis of one of the sheep of the study (see Chapter 3) by cutting transversally. The woven bone sample came from the 15 mm distraction callus generated by bone transport in a sheep sacrificed 161 days after surgery [113, 115, 116]. See more details about the bone transport experiments in Chapter 3. All samples were preserved by freezing at -80 ^{o}C. After thawed and dried in ambient conditions, 2 mm width sheets were cut from the cortical and woven bone specimens, embedded in resin (Epofix®, Struers, California, US) and polished with carbide papers (P600 to P4000) and diamond slurry (from 3 to 0.25 μm). Colloidal silica slurry (0.04 μm) was used for the final polishing step. The samples were cleaned ultrasonically with distilled water between each polishing step. The total process of sample preparation took 3 days from thawing. Figs. A.1 and A.2 show optical micrographs (Epiphot 300, Nikon, Japan) of the sample surface and the location of the region where indentations were carried out, for cortical and woven bone respectively.

A.2.2 Nanoindentation measurements

Instrumented indentation (Nanotest, Micro Materials Ltd. Wrexham, UK) was performed to determine the reduced elastic modulus and hardness of the cortical and woven bones. The indentation tests were performed at ambient laboratory conditions using a Berkovich diamond indenter. The load was increased monotonically at a rate of 0.5 mN s^{-1} to a maximum load of 5 mN and held for 40 s before unloading at 0.5 mN s^{-1} rate. The load-depth data, after correction for the effects of machine compliance, were processed using Oliver and Pharr method [125] to determine the reduced elastic modulus and the hardness. The hardness (H) is determined from the peak load (P_{max}) and the projected contact area (A), obtained from the plastic depth and the indenter geometry, using the equation:

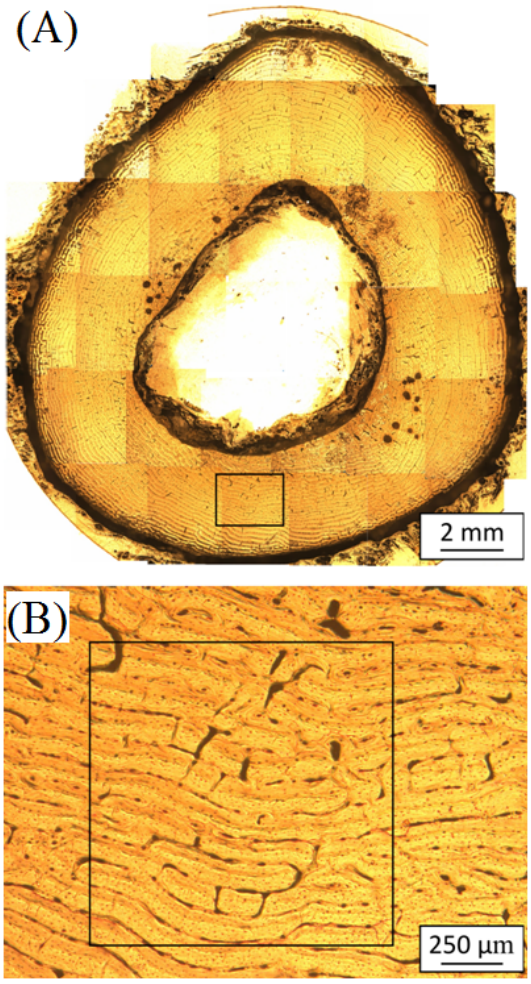

Figure A.1: Optical micrographs of (A) the complete cortical bone specimen (composite image) obtained from the cross section of the tibia; (B) a larger magnification of the region marked by a rectangle in (A) to show the indented area (square).

$$H = P_{max}/A. \tag{A.1}$$

The reduced elastic modulus is calculated from the expression:

$$E_r = \frac{S}{2}\sqrt{\frac{\pi}{A}}, \tag{A.2}$$

where S is the experimental stiffness of the contact (slope of unloading curve in the region between 20 and 95% of the maximum load) and E_r is the reduced modulus defined by:

$$\frac{1}{E_r} = \frac{1-\nu_s^2}{E_s} + \frac{1-\nu_i^2}{E_i}, \tag{A.3}$$

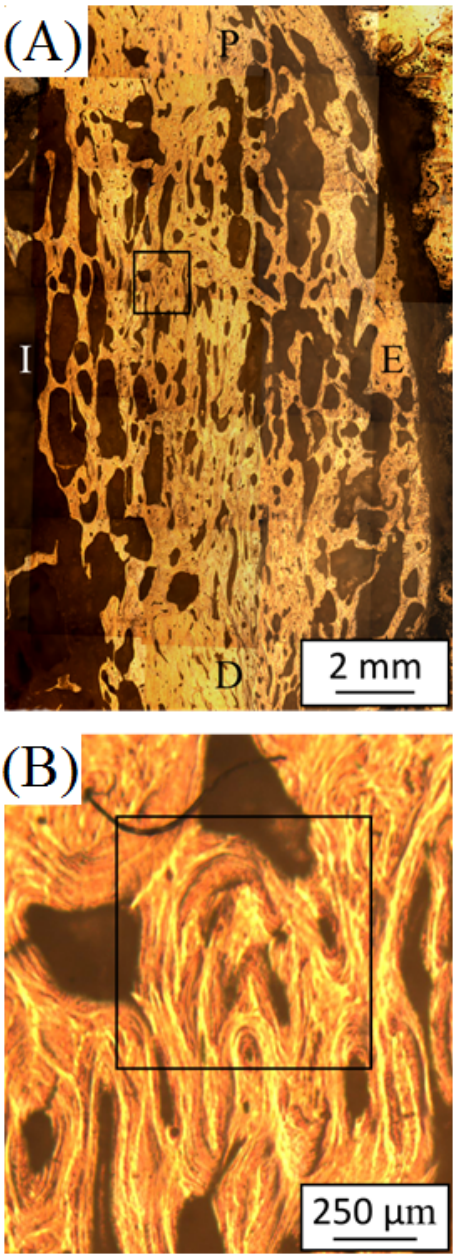

Figure A.2: Optical micrographs of (A) the complete specimen of the distraction callus and (B) high magnification of rectangular region in (A), with the indented region marked (square). The woven bone tissue was created between proximal (P) and distal (D) cortical bone segments. Half of the longitudinal section is represented, between the edge of the limb, internal callus (I), and the periosteal zone, external callus (E).

with E and ν Young's modulus and Poisson's ratio and the s and i subscripts denoting the specimen and indenter material respectively. Since the property of the bone is largely anisotropic,

the effective Young's modulus (E_s) cannot be derived in this experiment and therefore we report E_r here.

Nanoindentation measurements were carried out in the cortical bone specimens in the region shown in Fig. A.1 at five time points (1, 10, 20, 30 and 64 days). For each time point, a total of 100 indentations were performed in four matrices of 5 x 5 indentations and size 600 x 600 μm.

A total of 256 indentations were performed in the woven bone specimens in a 16x16 indentations matrix of size 750 x 750 μm for each time point. Four time points were assessed (1, 8, 37 and 67 days, periods between time points depended on availability of nanoindentation equipment) in the region shown in Fig. A.2.

Positions of indentation matrices were varied $\sim$25 μm from one time point to the next in order to avoid the plastic deformation areas generated in previous indentations. Samples were stored at room temperature between each time point.

To ascertain the accuracy of the nanoindentation equipment, before starting the indentation tests in the cortical of woven bone at each time point, a set of 6 indentations in the range 50-100 mN were performed in fused silica, whose mechanical properties are homogeneous and do not vary with time. Differences in these measurements were evaluated to be below $\pm$ 2 % for E_r and $\pm$ 4 % for H and the data did not evidence any drift of the measurements with time.

A.2.3 Data processing

The mean and the standard deviation of E_r and H of all indentations at each time point were evaluated in both specimens. The coefficient of variation of the results was obtained as the standard deviations divided by the corresponding mean value. The significance of the differences between data corresponding to each time point and the initial value was evaluated using Student's t-tests.

A.3 Results

Results of the nanoindentation experiments carried out in cortical bone specimen are shown in Fig. A.3. No clear dependence with time was observed for either E_r or H. For E_r, the mean values varied between 23.1 GPa and 25.2 GPa and the coefficient of variation for each time point was between 15 % and 20 %. The mean values of H varied between 0.84 GPa and 0.93 GPa and the coefficient of variation at each time point was between 19 % and 22 %. Results of the Student's t-tests performed to analyze the differences between the mean values at each time point and the mean value at the reference time point, day 1, are shown in Table A.1. Significant differences (p <0.05) were found between the values of E_r at 20 and 30 days and the values at the reference time point, but no between the values at 10 and 64 days and the reference. For H, no significant differences between the values at any time point and the initial value were found.

Results of the nanoindentation experiments carried out in woven bone specimen (Fig. A.4) presented greater values of the coefficient of variation, varying between 31 % and 46 % for E_r, and between 45 % and 81 % in the case of H. The mean values varied between 9.9 GPa and 12.1 GPa for E_r and between 0.42 GPa and 0.51 GPa for H and again no trend was apparent over time. For both E_r and H, significant differences ($p < 0.05$) were found in Student t-tests

(A)

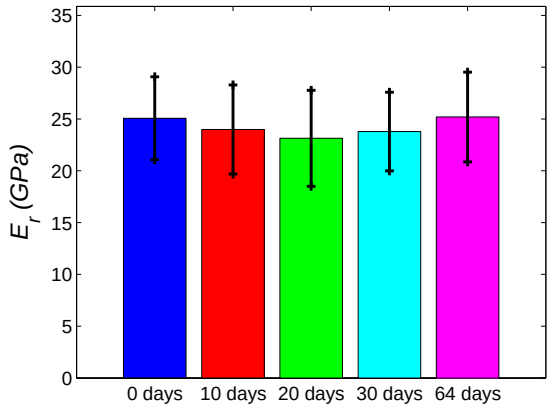

(B)

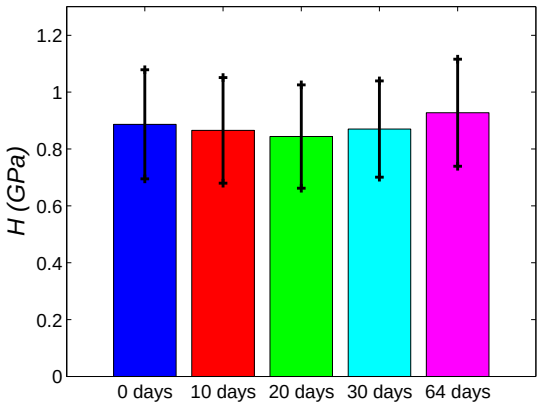

Figure A.3: Evolution with time of E_r (A) and H (B) in the cortical bone sample. The error bars indicate the mean value with standard deviation.

Table A.1: For the cortical bone specimen, p-values of the Student's t-tests performed to analyze the differences between the mean E_r and H at each time point and the corresponding value at reference time point, 1 day (*: p-values that correspond to significant differences).

Groups whose differences were analyzed	p value for E_r	p value for H
1 day - 10 days	0.0778	0.4460
1 day - 20 days	0.0028*	0.1206
1 day - 30 days	0.0267*	0.5378
1 day - 64 days	0.8388	0.1475

between the mean values at 8 and 67 days and the value at the reference time point (Table A.2). However, no significant differences were found between the mean values at 37 days and the

values at the reference time point.

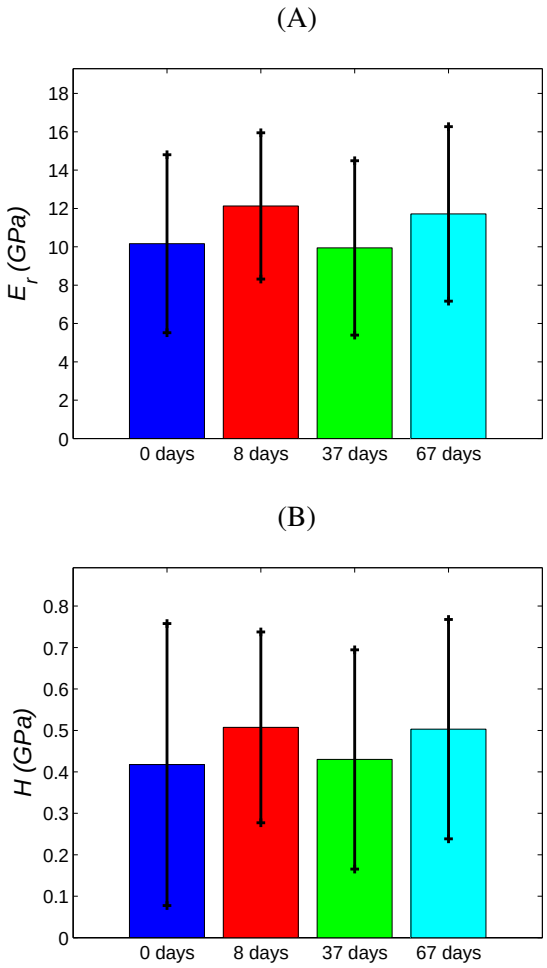

Figure A.4: Evolution with time of E_r (A) and H (B) in the woven bone sample. The error bars indicate the mean value with standard deviation.

Table A.2: For the woven bone specimen, p-values of the Student's t-tests performed to analyze the differences between the mean E_r and H at each time point and the corresponding value at reference time point, 1 day (*: p-values that correspond to significant differences).

Groups whose differences were analyzed	p value for E_r	p value for H
1 day - 8 days	0.0000*	0.0034*
1 day - 37 days	0.6494	0.6989
1 day - 67 days	0.0002*	0.0031*

A.4 Discussion

The results of this study allow one to assess variations in nanoscale mechanical properties (E_r and H) with time of cortical and woven bone specimens prepared by means of embedding and polishing in dry conditions.

The results of this work are in good accord with reported values in literature. Rodriguez-Florez et al. [153] obtained similar values for E_r of mouse bone tissue using similar sample preparation and measurement techniques that were used in this work. The mean E_r reported was 20.1 GPa with a coefficient of variation of 19.4 % and the mean H was 0.74 GPa with 26.5% of coefficient of variation. Results for cortical bone show mean values of E_r of 23-25 GPa with a coefficient of variation of 13-20 % (Fig. A.3 A) and mean values of H of 0.85-0.95 GPa with a coefficient of variation of 19-22 % (Fig. A.3 B). On the other hand, Manjubala et al. [109], assessed E_r and H for woven bone during bone healing in sheep. After 9 weeks of consolidation, they reported a mean E_r of 11.5 GPa with a coefficient of variation of 29.2 % and a mean H of 0.45 GPa with a coefficient of variation of 32.5%. For the woven bone specimen studied here, 20 weeks after the end of the distraction process, the mean values of E_r were 10-12 GPa with a coefficient of variation of 32-49 % (Fig. A.4 A) and the mean values of H were 0.42-0.51 GPa with a coefficient of variation of 45-80 % (Fig. A.4 B).

The mean values of E_r and H for the different time points spanning two months did not vary more than 10% for cortical bone and 20% for woven bone specimens. These variations are not significant compared with the levels of the coefficient of variation of the results arising from the heterogeneity of the cortical bone tissue (13-20% coefficient of variation for E_r and 19-22% for H) and, specially, the woven bone tissue (32-49% coefficient of variation for E_r and 45-80% for H). In addition, although in a few cases Student's t-tests indicated significant differences (Tables A.1 and A.2), no apparent trends could be observed with time for neither E_r or H in any of the specimens analyzed (Figs. A.3 and A.4). Therefore, the variations observed are deemed to be random and not due to a mechanical properties temporal variation. These random differences are attributed mainly to tissue heterogeneity. Small variations in the test conditions such as temperature or humidity could also influence the results, although these variations are considered secondary. These are the same sources of the data scattering for a specific time point.

To the best of the author knowledge, the temporal variation of nanoscale mechanical properties in bone and woven bone embedded and polished specimens had not been evaluated. At the macroscale level, Linde and Sorensen [100] reported that the stiffness of the bone evaluated by compression tests decreased 10% after 24 hours post-mortem. The first time-point evaluated in this study took place 3 days after specimens thawing and temporal variations of mechanical properties was not detected. Therefore, it could be concluded that the decrease in stiffness reported by Linden and Sorensen does not continue after 3 days post-mortem or does not take place at the nanoscale level.

Works in literature which used embedded and polished samples of bone [153, 154, 164, 165] and woven bone [5, 109] did not report the duration of the indentation tests. The outcomes of this study do not show time-dependence of E_r and H during these experiments in dry conditions up to 60 days. Time for mapping areas by nanoindentation may be high depending on the examinations that need to be carried out. Taking into account the outcome of this

study, larger maps of E_r and H could be safely performed in future experiments in embedded-polished specimens and dry conditions since the increased duration of a greater number of indentations should not affect the outcome. Such a study would provide more details about the bone microstructure mechanical properties in larger regions, which could be beneficial to improve statistical significance of data, and also to better characterize the heterogeneity of the bone tissue.

A.5 Conclusions

The results reported in this study demonstrate that mean E_r and H of dry embedded-polished cortical and woven bone specimens measured via nanoindentation do not show appreciable trend with time for more than 60 days after the 3 days sample preparation. Variations found were random and due to the material heterogeneity. This finding justifies the validity of results from nanoindentation experiments in the literature requiring long data gathering time which attribute differences in E_r and H to material heterogeneity. Furthermore, results obtained suggest that it should be possible to increase the duration of nanoindentation experiments further in order to map larger areas of bone and woven bone, or a given area with a greater level of detail, without sacrificing reliability.

Bibliography

[1] GT Aarnes, H Steen, LP Kristiansen, E Festø, and P Ludvigsen. Optimum loading mode for axial stiffness testing in limb lengthening. *Journal of Orthopaedic Research*, 24(3):348–354, 2006.

[2] GT Aarnes, H Steen, LP Kristiansen, P Ludvigsen, and O Reikeras. Tissue response during monofocal and bifocal leg lengthening in patients. *Journal of Orthopaedic Research*, 20(1):137–141, 2002.

[3] GT Aarnes, H Steen, P Ludvigsen, LP Kristiansen, and O Reikeras. High frequency distraction improves tissue adaptation during leg lengthening in humans. *Journal of Orthopaedic Research*, 20(4):789–792, 2002.

[4] GT Aarnes, H Steen, P Ludvigsen, NA Waanders, R Huiskes, and SA Goldstein. In *vivo* assessment of regenerate axial stiffness in distraction osteogenesis. *Journal of Orthopaedic Research*, 23(2):494–498, 2005.

[5] N Amanata, LH He, MV Swain, and DG Little. The effect of zoledronic acid on the intrinsic material properties of healing bone: an indentation study. *Medical Engineering & Physics*, 30(7):843–7, 2008.

[6] C Ament and EP Hofer. On the importance of the osteogenic and vasculative factors in callus healing. In *Proceedings of the 5^{th} Meeting of the International Society for Fracture Repair*, 1996.

[7] J Aronson. Temporal and spatial increases in blood flow during distraction osteogenesis. *Clinical Orthopaedics and Related Research*, (301)(301):124–131, 1994.

[8] J Aronson and JH Harp. Mechanical forces as predictors of healing during tibial lengthening by distraction osteogenesis. *Clinical Orthopaedics and Related Research*, (301)(301):73–79, 1994.

[9] J Aronson, BH Harrison, CL Stewart, and JH Harp Jr. The histology of distraction osteogenesis using different external fixators. *Clinical Orthopaedics and Related Research*, (241)(241):106–116, 1989.

[10] J Aronson, WR Hogue, CM Flahiff, GG Gao, XC Shen, RA Skinner, TM Badger, and CK Lumpkin. Development of tensile strength during distraction osteogenesis in a rat model. *Journal of Orthopaedic Research*, 19(1):64–9, 2001.

[11] J Aronson, XC Shen, RA Skinner, WR Hogue, TM Badger, and CK Lumpkin Jr. Rat model of distraction osteogenesis. *Journal of Orthopaedic Research*, 15(2):221–226, 1997.

[12] P Augat, J Merk, HK Genant, and L Claes. Quantitative assessment of experimental fracture repair by peripheral computed tomography. *Calcified Tissue International*, 60(2):194–9, 1997.

[13] A Bailón-Plaza and MC van der Meulen. A mathematical framework to study the effects of growth factor influences on fracture healing. *Journal of Theoretical Biology*, 212(2):191–209, 2001.

[14] CM Barone, M Ferder, DF Jimenez, L Grossman, C Hall, B Strauch, and RV Argamaso. Distraction of the frontal bone outside the cranial plane: a rabbit model. *The Journal of Craniofacial Surgery*, 4(3):177–81, 1993.

[15] A Boccaccio, L Lamberti, C Pappalettere, A Carano, and M Cozzani. Mechanical behavior of an osteotomized mandible with distraction orthodontic devices. *Journal of Biomechanics*, 39(15):2907–2918, 2006.

[16] A Boccaccio, C Pappalettere, and DJ Kelly. The influence of expansion rates on mandibular distraction osteogenesis: a computational analysis. *Annals of Biomedical Engineering*, 35(11):1940–1960, 2007.

[17] A Boccaccio, PJ Prendergast, C Pappalettere, and DJ Kelly. Tissue differentiation and bone regeneration in an osteotomized mandible: a computational analysis of the latency period. *Medical & Biological Engineering & Computing*, 46(3):283–298, 2008.

[18] AS Bonnet, G Dubois, P Lipinski, and T Schouman. In vivo study of human mandibular distraction osteogenesis. Part I: bone transport force determination. *Acta of Bioengineering and Biomechanics*, 14(4):3–14, 2012.

[19] AS Bonnet, G Dubois, P Lipinski, and T Schouman. In vivo study of human mandibular distraction osteogenesis. Part II: Determination of callus mechanical properties. *Acta of Bioengineering and Biomechanics*, 15(1):11–18, 2013.

[20] UH Brunner, J Cordey, L Schweiberer, and SM Perren. Force required for bone segment transport in the treatment of large bone defects using medullary nail fixation. *Clinical Orthopaedics and Related Research*, (301)(301):147–155, 1994.

[21] AJ Bushby, VL Ferguson, and A Boyde. Nanoindentation of bone: Comparison of specimens tested in liquid and embedded in polymethylmethacrylate. *Journal of Materials Research*, 19(01):249–259, 2011.

[22] DR Carter. Mechanical loading history and skeletal biology. *Journal of Biomechanics*, 20(11-12):1095–1109, 1987.

[23] DR Carter, GS Beaupré, NJ Giori, and JA Helms. Mechanobiology of Skeletal Regeneration. *Clinical Orthopaedics and Related Research*, 355S:S41–S55, 1998.

[24] DR Carter and DM Spengler. Mechanical properties and composition of cortical bone. *Clinical Orthopaedics and Related Research*, (135):192–217, 1978.

[25] MA Catagni, F Guerreschi, JA Holman, and R Cattaneo. Distraction osteogenesis in the treatment of stiff hypertrophic nonunions using the Ilizarov apparatus. *Clinical Orthopaedics and Related Research*, (301):159–63, 1994.

[26] Paolo M Cattaneo, T Kofod, M Dalstra, and B Melsen. Using the finite element method to model the biomechanics of the asymmetric mandible before, during and after skeletal correction by distraction osteogenesis. *Computer Methods in Biomechanics and Biomedical Engineering*, 8(3):157–65, 2005.

[27] PM Cattaneo, M Dalstra, and LH Frich. A three-dimensional finite element model from computed tomography data: a semi-automated method. *Proceedings of the Institution of Mechanical Engineers. Part H, Journal of Engineering in Medicine*, 215(2):203–13, 2001.

[28] LE Claes, P Augat, S Schorlemmer, C Konrads, A Ignatius, and C Ehrnthaller. Temporary distraction and compression of a diaphyseal osteotomy accelerates bone healing. *Journal of Orthopaedic Research*, 26(6):772–7, 2008.

[29] LE Claes, R Grass, T Schmickal, B Kisse, C Eggers, H Gerngross, W Mutschler, M Arand, T Wintermeyer, and A Wentzensen. Monitoring and healing analysis of 100 tibial shaft fractures. *Langenbeck's Archives of Surgery*, 387(3-4):146–152, 2002.

[30] LE Claes and CA Heigele. Magnitudes of local stress and strain along bony surfaces predict the course and type of fracture healing. *Journal of Biomechanics*, 32(3):255–266, 1999.

[31] LE Claes, J Laule, K Wenger, G Suger, U Liener, and L Kinzl. The influence of stiffness of the fixator on maturation of callus after segmental transport. *The Journal of Bone and Joint Surgery. British Volume*, 82(1):142–148, 2000.

[32] LE Claes, A Veeser, M Göckelmann, D Horvath, L Dürselen, and A Ignatius. A novel method for lateral callus distraction and its importance for the mechano-biology of bone formation. *Bone*, 47(4):712–7, 2010.

[33] A Codivilla. On the means of lengthening, in the lower limbs, the muscles and tissues which are shortened through deformity. *American Journal of Orthopedic Surgery*, 2:353, 1905.

[34] JM Converse, PJ Coccaro, M Becker, and D Wood-Smith. On hemifacial microsomia: the first and second branchial arch syndrome. *Plastic and Reconstructive Surgery*, pages 268–79.

[35] SC Cowin. Structural Change in Living Tissues. *Meccanica*, 34(5):379–398, 1999.

[36] JL Cunningham, J Kenwright, and CJ Kershaw. Biomechanical measurement of fracture healing. *Journal of Medical Engineering & Technology*, 14(3):92–101, 1990.

[37] F de la Huerta. Correction of the neglected clubfoot by the Ilizarov method. *Clinical Orthopaedics and Related Research*, (301):89–93, 1994.

[38] J de Pablos Jr and J Canadell. Experimental physeal distraction in immature sheep. *Clinical Orthopaedics and Related Research*, (250)(250):73–80, 1990.

[39] C Delloye, G Delefortrie, L Coutelier, and A Vincent. Bone regenerate formation in cortical bone during distraction lengthening. An experimental study. *Clinical Orthopaedics and Related Research*, (250)(250):34–42, 1990.

[40] M Doblaré and JM García-Aznar. On numerical modelling of growth, differentiation and damage in structural living tissues. *Archives of Computational Methods in Engineering*, 13(4):471–513, 2006.

[41] ER Draper, RK Strachan, SP Hughes, AC Nicol, and JP Paul. The design and performance of an experimental external fixator with variable axial stiffness and a compressive force transducer. *Medical Engineering & Physics*, 19(8):690–5, 1997.

[42] GN Duda, K Eckert-Hubner, R Sokiranski, A Kreutner, R Miller, and LE Claes. Analysis of inter-fragmentary movement as a function of musculoskeletal loading conditions in sheep. *Journal of Biomechanics*, 31(3):201–210, 1998.

[43] JS Dwyer, PJ Owen, GA Evans, JH Kuiper, and JB Richardson. Stiffness measurements to assess healing during leg lengthening. A preliminary report. *The Journal of Bone and Joint Surgery. British Volume*, 78(2):286–289, 1996.

[44] DH Enlow. *Facial growth*. SPCK Publishing, 1990.

[45] B Fink, C Pollnau, M Vogel, R Skripitz, and A Enderle. Histomorphometry of distraction osteogenesis during experimental tibial lengthening. *Journal of Orthopaedic Trauma*, 17(2):113–8, 2003.

[46] T Floerkemeier, W Aljuneidi, J Reifenrath, N Angrisani, D Rittershaus, D Gottschalk, S Besdo, A Meyer-Lindenberg, H Windhagen, and F Thorey. Telemetric in vivo measurement of compressive forces during consolidation in a rabbit model. *Technology and Health Care*, 19(3):173–183, 2011.

[47] T Floerkemeier, F Thorey, C Hurschler, M Wellmann, F Witte, and H Windhagen. Stiffness of callus tissue during distraction osteogenesis. *Orthopaedics & Traumatology Surgery & Research*, 96(2):155–160, 2010.

[48] ScientificAmerican. New Limb-Lengthening Tech May Reduce Complications for Sufferers of Crippling Deformities [Slide Show]. http://www.scientificamerican.com/article/limb-lengthening-technology/.

[49] F Forriol, L Denaro, UG Longo, H Taira, N Maffulli, and V Denaro. Bone lengthening osteogenesis, a combination of intramembranous and endochondral ossification: an experimental study in sheep. *Strategies in Trauma and Limb Reconstruction*, 5(2):71–78, 2010.

[50] TM Ganey, DW Klotch, J Sasse, JA Ogden, and T Garcia. Basement membrane of blood vessels during distraction osteogenesis. *Clinical Orthopaedics and Related Research*, (301):132–8, 1994.

[51] FL Garcia, CH Picado, and SB Garcia. Histology of the regenerate and docking site in bone transport. *Archives of Orthopaedic and Trauma Surgery*, 129(4):549–58, 2009.

[52] JM García-Aznar, JH Kuiper, MJ Gómez-Benito, M Doblaré, and JB Richardson. Computational simulation of fracture healing: influence of interfragmentary movement on the callus growth. *Journal of Biomechanics*, 40(7):1467–76, 2007.

[53] J Garcia-Rodriguez. *Modelo de remodelación de callo óseo de fractura de fémur humano*. PhD thesis, University of Seville, 2014.

[54] TN Gardner, M Evans, AH Simpson, PJ Kyberd, and J Kenwright. A method of examining the magnitude and origin of "soft" and "hard" tissue forces resisting limb lengthening. *Medical Engineering & Physics*, 19(5):405–411, 1997.

[55] TN Gardner, M Evans, H Simpson, and J Kenwright. Force-displacement behaviour of biological tissue during distraction osteogenesis. *Medical Engineering & Physics*, 20(9):708–715, 1998.

[56] L Geris, A Gerisch, C Maes, G Carmeliet, R Weiner, J Vander Sloten, and H Van Oosterwyck. Mathematical modeling of fracture healing in mice: comparison between experimental data and numerical simulation results. *Medical & Biological Engineering & Computing*, 44(4):280–9, 2006.

[57] L Geris, A Gerisch, J Vander Sloten, R Weiner, and H Van Oosterwyck. Angiogenesis in bone fracture healing: a bioregulatory model. *Journal of Theoretical Biology*, 251(1):137–58, 2008.

[58] LC Gerstenfeld. Fracture healing as a post-natal developmental process: Molecular, spatial, and temporal aspects of its regulation. *Journal of Cellular Biochemistry*, (5):873–84, 2003.

[59] MJ Gómez-Benito, JM García-Aznar, JH Kuiper, and M Doblaré. Influence of fracture gap size on the pattern of long bone healing: a computational study. *Journal of Theoretical Biology*, 235(1):105–19, 2005.

[60] AD Grant, D Atar, and WB Lehman. The Ilizarov technique in correction of complex foot deformities. *Clinical Orthopaedics and Related Research*, (280):94–103, 1992.

[61] CA Grant, NH Thomson, MD Savage, HW Woon, and D Greig. Surface characterisation and biomechanical analysis of the sclera by atomic force microscopy. *Journal of the Mechanical Behavior of Biomedical Materials*, 4(4):535–40, 2011.

[62] J Grasa, MJ Gomez-Benito, LA Gonzalez-Torres, D Asiain, F Quero, and JM Garcia-Aznar. Monitoring in vivo load transmission through an external fixator. *Annals of Biomedical Engineering*, 38(3):605–612, 2010.

[63] S Gupta, FCT Van der Helm, JC Sterk, F Van Keulen, and B L Kaptein. Development and experimental validation of a three-dimensional finite element model of the human scapula. *Proceedings of the Institution of Mechanical Engineers. Part H, Journal of Engineering in Medicine*, 218(2):127–42, 2004.

[64] MB Gustafson, RB Martin, V Gibson, DH Storms, SM Stover, J Gibeling, and L Griffin. Calcium buffering is required to maintain bone stiffness in saline solution. *Journal of Biomechanics*, 29(9):1191–4, 1996.

[65] G Hägglund, U Rydholm, and G Sundén. Ilizarov Technique in the Correction of Knee Flexion Contracture: Report of Four Cases. *Journal of Pediatric Orthopaedics B*, 2(2):103–197, 1993.

[66] JH Harp, J Aronson, and M Hollis. Noninvasive determination of bone stiffness for distraction osteogenesis by quantitative computed tomography scans. *Clinical Orthopaedics and Related Research*, (301):42–8, 1994.

[67] RK Harshwal, Sohan S Sankhala, and D Jalan. Management of nonunion of lower-extremity long bones using mono-lateral external fixator–report of 37 cases. *Injury*, 45(3):560–7, 2014.

[68] R Hente, J Cordey, and SM Perren. In vivo measurement of bending stiffness in fracture healing. *Biomedical Engineering Online*, 28:2–8, 2003.

[69] D Hertling and RM Kessler. *Management of Common Musculoskeletal Disorders: Physical Therapy Principles and Methods*. Lippincott Williams & Wilkins, 2006.

[70] OxfordWeb. Limb Reconstruction Oxford University Hospitals. http://www.ouh.nhs.uk/limbreconstruction/, 2015.

[71] Short Persons Support: Health : Cosmetic Leg Lengthening : Hospitals. http://www.shortsupport.org/health/leg-lengthening/hospitals.html.

[72] A Hyodo, H Kotschi, H Kambic, and G Muschler. Bone transport using intramedullary fixation and a single flexible traction cable. *Clinical Orthopaedics and Related Research*, (325):256–268, 1996.

[73] C Iacobellis, A Berizzi, and R Aldegheri. Bone transport using the Ilizarov method: a review of complications in 100 consecutive cases. *Strategies in Trauma and Limb Reconstruction*, 5(1):17–22, 2010.

[74] NI Ibrahim, MF Khamis, MF Mod Yunoh, S Abdullah, N Mohamed, and AN Shuid. Targeted delivery of lovastatin and tocotrienol to fracture site promotes fracture healing in osteoporosis model: micro-computed tomography and biomechanical evaluation. *Plos One*, 9(12):e115595, 2014.

[75] S Idelsohn, JA Planell, FJ Gil, and D Lacroix. Development of a dynamic mechano-regulation model based on shear strain and fluid flow to optimize distraction osteogenesis. *Journal of Biomechanics*, 39:S9–S10, jan 2006.

[76] GA Ilizarov. Basic principles of transosseous compression and distraction osteosynthesis. *Ortopediia Travmatologiia i Protezirovanie*, 32(11):7–15, 1971.

[77] GA Ilizarov. The principles of the Ilizarov method. *Bulletin of the Hospital for Joint Diseases Orthopaedic Institute*, 48(1):1–11, 1988.

[78] GA Ilizarov. The tension-stress effect on the genesis and growth of tissues. Part I. The influence of stability of fixation and soft-tissue preservation. *Clinical Orthopaedics and Related Research*, (238):249–281, 1989.

[79] GA Ilizarov. The tension-stress effect on the genesis and growth of tissues: Part II. The influence of the rate and frequency of distraction. *Clinical Orthopaedics and Related Research*, (239):263–285, 1989.

[80] GA Ilizarov. Clinical application of the tension-stress effect for limb lengthening. *Clinical Orthopaedics and Related Research*, 250:8–26, 1990.

[81] GA Ilizarov and VI Gracheva. Bloodless treatment of congenital pseudarthrosis of the crus with simultaneous elimination of shortening using dosed distraction. *Ortopediia Travmatologiia i Protezirovanie*, 32(2):42–6, 1971.

[82] GA Ilizarov, AG Kaplunov, VE Degtiarev, and VI Lediaev. Treatment of pseudarthroses and ununited fractures, complicated by purulent infection, by the method of compression-distraction osteosynthesis. *Ortopediia Travmatologiia i Protezirovanie*, 33(11):10–4, 1972.

[83] GA Ilizarov, VI Lediaev, and VE Degtiarev. Operative and bloodless methods of repairing defects of the long tubular bones in osteomyelitis. *Vestnik khirurgii Imeni I. I. Grekova*, 110(5):55–9, 1973.

[84] GA Ilizarov and VI Ledyaev. The Replacement of Long Tubular Bone Defects by Lengthening Distraction Osteotomy of One of the Fragments. *Clinical Orthopaedics and Related Research*, 280:7–10, 1992.

[85] H Isaksson, O Comas, CC van Donkelaar, J Mediavilla, W Wilson, R Huiskes, and K Ito. Bone regeneration during distraction osteogenesis: mechano-regulation by shear strain and fluid velocity. *Journal of Biomechanics*, 40(9):2002–2011, 2007.

[86] H Isaksson, CC Van Donkelaar, R Huiskes, and K Ito. A mechano-regulatory bone-healing model incorporating cell-phenotype specific activity. *Journal of Theoretical Biology*, 252(2):230–46, 2008.

[87] KA Jacobsen, ZS Al-Aql, C Wan, JL Fitch, SN Stapleton, ZD Mason, RM Cole, SR Gilbert, TL Clemens, EF Morgan, TA Einhorn, and LC Gerstenfeld. Bone formation during distraction osteogenesis is dependent on both VEGFR1 and VEGFR2 signaling. *Journal of Bone and Mineral Research*, 23(5):596–609, 2008.

[88] T Jensen. *Alveolar Distraction Osteogenesis*. Quintessence, 2002.

[89] LCU Junqueira and J Carneiro. *Basic Histology: Text & Atlas*. McGraw-Hill, 2005.

[90] TJ Kallio, MV Vauhkonen, JI Peltonen, and EO Karaharju. Early bone matrix formation during distraction. A biochemical study in sheep. *Acta Orthopaedica Scandinavica*, 65(4):467–71, 1994.

[91] T Kofod, PM Cattaneo, and B Melsen. Three-dimensional finite element analysis of the mandible and temporomandibular joint on simulated occlusal forces before and after vertical ramus elongation by distraction osteogenesis. *The Journal of Craniofacial Surgery*, 16(3):421–9, 2005.

[92] H Kojimoto, N Yasui, T Goto, S Matsuda, and Y Shimomura. Bone lengthening in rabbits by callus distraction. The role of periosteum and endosteum. *The Journal of Bone and Joint Surgery. British Volume*, 70(4):543–549, 1988.

[93] E Kontogiorgos, ME Elsalanty, U Zapata, I Zakhary, WW Nagy, PC Dechow, and LA Opperman. Three-dimensional evaluation of mandibular bone regenerated by bone transport distraction osteogenesis. *Calcified Tissue International*, 89(1):43–52, 2011.

[94] J Lammens, Z Liu, J Aerssens, J Dequeker, and G Fabry. Distraction bone healing versus osteotomy healing: a comparative biochemical analysis. *Journal of Bone and Mineral Research*, 13(2):279–86, 1998.

[95] LE Lanyon. Functional strain in bone tissue as an objective, and controlling stimulus for adaptive bone remodelling. *Journal of Biomechanics*, 20(11-12):1083–1093, 1987.

[96] MT Lauterburg, GU Exner, and HA Jacob. Forces involved in lower limb lengthening: an in vivo biomechanical study. *Journal of Orthopaedic Research*, 24(9):1815–1822, 2006.

[97] PL Leong and EF Morgan. Measurement of fracture callus material properties via nanoindentation. *Acta Biomaterialia*, 4(5):1569–1575, 2008.

[98] PL Leong and EF Morgan. Correlations between indentation modulus and mineral density in bone-fracture calluses. *Integrative and Comparative Biology*, 49(1):59–68, 2009.

[99] JR Lieberman and GE Friedlaender, editors. *Bone Regeneration and Repair*. Humana Press, Totowa, NJ, 2005.

[100] F Linde and HC Sørensen. The effect of different storage methods on the mechanical properties of trabecular bone. *Journal of Biomechanics*, 26(10):1249–52, 1993.

[101] XS Liu, XH Zhang, CS Rajapakse, MJ Wald, J Magland, KK Sekhon, MF Adam, P Sajda, FW Wehrli, and XE Guo. Accuracy of high-resolution in vivo micro magnetic resonance imaging for measurements of microstructural and mechanical properties of human distal tibial bone. *Journal of Bone and Mineral Research*, 25(9):2039–2050, 2010.

[102] EG Loboa, TD Fang, DW Parker, SM Warren, KD Fong, MT Longaker, and DR Carter. Mechanobiology of mandibular distraction osteogenesis: finite element analyses with a rat model. *Journal of Orthopaedic Research*, 23(3):663–70, 2005.

[103] AE Loiselle, EM Paul, GS Lewis, and HJ Donahue. Osteoblast and osteocyte-specific loss of Connexin43 results in delayed bone formation and healing during murine fracture healing. *Journal of Orthopaedic Research*, 31(1):147–54, 2013.

[104] M Loparic, D Wirz, AU Daniels, R Raiteri, MR Vanlandingham, G Guex, I Martin, U Aebi, and M Stolz. Micro- and nanomechanical analysis of articular cartilage by indentation-type atomic force microscopy: validation with a gel-microfiber composite. *Biophysical Journal*, 98(11):2731–40, 2010.

[105] EM López-Pliego. *Osteogénesis por distracción con mantenimiento de la actividad motriz: Estudio histológico de la estructura del callo y el Docking Site*. PhD thesis, University of Seville, 2016.

[106] HW Losken, MP Mooney, J Zoldos, A Tschakaloff, AM Burrows, TD Smith, GM Cooper, MR Kapucu, and MI Siegel. Internal calvarial bone distraction in rabbits with delayed-onset coronal suture synostosis. *Plastic and Reconstructive Surgery*, 102(4):1109–19; discussion 1120–1, 1998.

[107] R Lucchini, D Carnelli, M Ponzoni, E Bertarelli, D Gastaldi, and P Vena. Role of damage mechanics in nanoindentation of lamellar bone at multiple sizes: experiments and numerical modeling. *Journal of the Mechanical Behavior of Biomedical Materials*, 4(8):1852–63, 2011.

[108] F Macri, LF Marques, RC Backer, MJ Santos, and WD Belangero. Validation of a standardised gait score to predict the healing of tibial fractures. *The Journal of Bone and Joint Surgery. British Volume*, 94(4):544–548, 2012.

[109] I Manjubala, Y Liu, DR Epari, P Roschger, H Schell, P Fratzl, and GN Duda. Spatial and temporal variations of mechanical properties and mineral content of the external callus during bone healing. *Bone*, 45(2):185–192, 2009.

[110] EN Marieb and K Hoehn. *Human Anatomy & Physiology*. Pearson Benjamin Cummings, 2007.

[111] DR Marsh, S Shah, J Elliott, and N Kurdy. The Ilizarov method in nonunion, malunion and infection of fractures. *The Journal of Bone and Joint Surgery. British Volume*, 79(2):273–9, 1997.

[112] RB Martin, DB Burr, and NA Sharkey. *Skeletal Tissue Mechanics*. 1998.

[113] J Mora-Macías, E Reina-Romo, and J Domínguez. Distraction osteogenesis device to estimate the axial stiffness of the callus in Vivo. *Medical Engineering & Physics*, 37(10):969–78, 2015.

[114] J Mora-Macías, E Reina-Romo, and J Domínguez. Model of the distraction callus tissue behavior during bone transport based in experiments in vivo. *Journal of the Mechanical Behavior of Biomedical Materials*, 15(61):419–430, 2016.

[115] J Mora-Macías, E Reina-Romo, M López-Pliego, M A Giráldez-Sánchez, and J Domínguez. In Vivo Mechanical Characterization of the Distraction Callus During Bone Consolidation. *Annals of Biomedical Engineering*, 43(11):2663–74, 2015.

[116] J Mora-Macías, E Reina-Romo, J Morgaz, and J Domínguez. In vivo gait analysis during bone transport. *Annals of Biomedical Engineering*, 43(9):2090–100, 2015.

[117] EF Morgan, AI Hussein, BA Al-Awadhi, DE Hogan, H Matsubara, Z Al-Alq, J Fitch, B Andre, K Hosur, and LC Gerstenfeld. Vascular development during distraction osteogenesis proceeds by sequential intramuscular arteriogenesis followed by intraosteal angiogenesis. *Bone*, 51(3):535–45, 2012.

[118] EF Morgan, MT Longaker, and DR Carter. Relationships between tissue dilatation and differentiation in distraction osteogenesis. *Matrix Biology*, 25(2):94–103, 2006.

[119] R Müller and P Rüegsegger. Three-dimensional finite element modelling of non-invasively assessed trabecular bone structures. *Medical Engineering & Physics*, 17(2):126–33, 1995.

[120] JH Murray and RD Fitch. Distraction histiogenesis: principles and indications. *The Journal of the American Academy of Orthopaedic Surgeons*, 4(6):317–327, 1996.

[121] DC Newitt, S Majumdar, B Van Rietbergen, G von Ingersleben, ST Harris, HK Genant, C Chesnut, P Garnero, and B MacDonald. In vivo assessment of architecture and micro-finite element analysis derived indices of mechanical properties of trabecular bone in the radius. *Osteoporosis International*, 13(1):6–17, 2002.

[122] I Ohnishi, T Kurokawa, W Sato, and K Nakamura. Measurement of the tensile forces during bone lengthening. *Clinical Biomechanics*, 20(4):421–7, 2005.

[123] M Ohyama, Y Miyasaka, M Sakurai, AT Yokobori Jr, and S Sasaki. The mechanical behavior and morphological structure of callus in experimental callotasis. *Biomedical Materials and Engineering*, 4(4):273–281, 1994.

[124] H Okazaki, T Kurokawa, K Nakamura, T Matsushita, K Mamada, and H Kawaguchi. Stimulation of bone formation by recombinant fibroblast growth factor-2 in callotasis bone lengthening of rabbits. *Calcified Tissue International*, 64(6):542–546, 1999.

[125] WC Oliver and GM Pharr. An improved technique for determining hardness and elastic modulus using load and displacement sensing indentation experiments. *Journal of Materials Research*, 7(6):1564–1583, 1992.

[126] ML Oyen. Nanoindentation hardness of mineralized tissues. *Journal of Biomechanics*, 39(14):2699–702, 2006.

[127] ML Oyen. *Handbook of nanoindentation: with biological applications*. Pan Stanford, 2010.

[128] J de Pablos and C Barrios. Large experimental segmental bone defects treated by bone transportation with monolateral external distractors. *Clinical Orthopaedic and Related Research*, 298:259–65, 1994.

[129] RC Paietta, SE Campbell, and VL Ferguson. Influences of spherical tip radius, contact depth, and contact area on nanoindentation properties of bone. *Journal of Biomechanics*, 44(2):285–90, 2011.

[130] D Paley. The correction of complex foot deformities using Ilizarov's distraction osteotomies. *Clinical Orthopaedics and Related Research*, (293):97–111, 1993.

[131] D Paley, M Catagni, F Argnani, J Prevot, D Bell, and P Armstrong. Treatment of congenital pseudoarthrosis of the tibia using the Ilizarov technique. *Clinical orthopaedics and Related Research*, (280):81–93, 1992.

[132] MM Panjabi, RW Lindsey, SD Walter, and AA White 3^{rd}. The clinician's ability to evaluate the strength of healing fractures from plain radiographs. *Journal of Orthopaedic Trauma*, 3(1):29–32, 1989.

[133] MM Panjabi, SD Walter, M Karuda, AA White, and JP Lawson. Correlations of radiographic analysis of healing fractures with strength: a statistical analysis of experimental osteotomies. *Journal of Orthopaedic Research*, 3(2):212–218, 1985.

[134] LF Peltier. *Fractures: a history and iconography of their treatment*. Norman Publishing, 1990.

[135] SM Perren. Physical and biological aspects of fracture healing with special reference to internal fixation. *Clinical Orthopaedics and Related Research*, (138)(138):175–196, 1979.

[136] SM Perren and J Cordey. *The concept of interfragmentary strain pp. 63- 77. Current concepts of internal fixation of fractures.* Springer-Verlarg, Berlin, 1980.

[137] M Pombo-Arias and J Argemí. *Tratado de endocrinología pediátrica*. Díaz de Santos, 1997.

[138] PJ Prendergast, R Huiskes, and K Søballe. Biophysical stimuli on cells during tissue differentiation at implant interfaces. *Journal of Biomechanics. ESB Research Award 1996*, 30(6):539–48, 1997.

[139] K Raum, I Leguerney, F Chandelier, E Bossy, M Talmant, A Saied, F Peyrin, and P Laugier. Bone microstructure and elastic tissue properties are reflected in QUS axial transmission measurements. *Ultrasound in Medicine & Biology*, 31(9):1225–1235, 2005.

[140] E Reina-Romo, MJ Gomez-Benito, J Dominguez, and JM Garcia-Aznar. A lattice-based approach to model distraction osteogenesis. *Journal of Biomechanics*, 45(16):2736–2742, 2012.

[141] E Reina-Romo, MJ Gomez-Benito, J Dominguez, F Niemeyer, T Wehner, U Simon, and LE Claes. Effect of the fixator stiffness on the young regenerate bone after bone transport: computational approach. *Journal of Biomechanics*, 44(5):917–923, 2011.

[142] E Reina-Romo, MJ Gomez-Benito, JM Garcia-Aznar, J Dominguez, and M Doblare. Modeling distraction osteogenesis: analysis of the distraction rate. *Biomechanics and Modeling in Mechanobiology*, 8(4):323–335, 2009.

[143] E Reina-Romo, MJ Gomez-Benito, JM Garcia-Aznar, J Dominguez, and M Doblare. An interspecies computational study on limb lengthening. *Proceedings of the Institution of Mechanical Engineers. Part H, Journal of Engineering in Medicine*, 224(11):1245–1256, 2010.

[144] E Reina-Romo, MJ Gomez-Benito, JM Garcia-Aznar, J Dominguez, and M Doblare. Growth mixture model of distraction osteogenesis: effect of pre-traction stresses. *Biomechanics and Modeling in Mechanobiology*, 9(1):103–115, 2010.

[145] E Reina-Romo, MJ Gomez-Benito, A Sampietro-Fuentes, J Dominguez, and JM Garcia-Aznar. Three-dimensional simulation of mandibular distraction osteogenesis: mechanobiological analysis. *Annals of Biomedical Engineering*, 39(1):35–43, 2011.

[146] Esther Reina-Romo. *Distraction osteogenesis: mechanobiological modeling and numerical applications*. PhD thesis, University of Seville, 2009.

[147] JY Rho, P Zioupos, JD Currey, and GM Pharr. Microstructural elasticity and regional heterogeneity in human femoral bone of various ages examined by nano-indentation. *Journal of Biomechanics*, 35(2):189–98, 2002.

[148] M Richards, JA Goulet, MB Schaffler, and SA Goldstein. Temporal and spatial characterization of regenerate bone in the lengthened rabbit tibia. *Journal of Bone and Mineral Research*, 14(11):1978–1986, 1999.

[149] JB Richardson, JL Cunningham, AE Goodship, BT O'Connor, and J Kenwright. Measuring stiffness can define healing of tibial fractures. *The Journal of Bone and Joint Surgery. British Volume*, 76(3):389–394, 1994.

[150] RC Riddle and HJ Donahue. From streaming-potentials to shear stress: 25 years of bone cell mechanotransduction. *Journal of Orthopaedic Research*, 27(2):143–149, 2009.

[151] AG Robling, AB Castillo, and Charles H Turner. Biomechanical and molecular regulation of bone remodeling. *Annual Review of Biomedical Engineering*, 8:455–98, 2006.

[152] N Rodriguez-Florez, E Garcia-Tunon, Q Mukadam, E Saiz, KJ Oldknow, C Farquharson, JL Millán, A Boyde, and SJ Shefelbine. An investigation of the mineral in ductile

and brittle cortical mouse bone. *Journal of Bone and Mineral Research*, 30(5):786–95, 2015.

[153] N Rodriguez-Florez, ML Oyen, and SJ Shefelbine. Insight into differences in nanoindentation properties of bone. *Journal of the Mechanical Behavior of Biomedical Materials*, 18:90–99, 2013.

[154] N Rodriguez-Florez, ML Oyen, and SJ Shefelbine. Age-related changes in mouse bone permeability. *Journal of Biomechanics*, 47(5):1110–6, 2014.

[155] SR Rozbruch. Correction of tibial deformity with use of the Ilizarov-Taylor spatial frame. *The Journal of Bone and Joint Surgery. American*, 88(suppl 4):156–74, 2006.

[156] ML Samchukov. *Craniofacial Distraction Osteogenesis*. 2001.

[157] ML Samchukov, JB Cope, RP Harper, and JD Ross. Biomechanical considerations of mandibular lengthening and widening by gradual distraction using a computer model. *Journal of Oral and Maxillofacial Surgery*, 56(1):51–9, 1998.

[158] RK Schenk and A Gatchter. Bone Formation and repair. In *Bone Formation and repair*, chapter 27. American Academy of Orthopaedic Surgeons, 1994.

[159] P Seebeck, MS Thompson, A Parwani, WR Taylor, H Schell, and GN Duda. Gait evaluation: a tool to monitor bone healing? *Clinical Biomechanics*, 20(9):883–891, 2005.

[160] JR Shearer, HI Roach, and SW Parsons. Histology of a lengthened human tibia. *The Journal of Bone and Joint Surgery. British Volume*, 74(1):39–44, 1992.

[161] SJ Shefelbine, U Simon, LE Claes, A Gold, Y Gabet, I Bab, R Müller, and P Augat. Prediction of fracture callus mechanical properties using micro-CT images and voxel-based finite element analysis. *Bone*, 36(3):480–8, 2005.

[162] U Simon, P Augat, A Ignatius, and LE Claes. Influence of the stiffness of bone defect implants on the mechanical conditions at the interface–a finite element analysis with contact. *Journal of Biomechanics*, 36(8):1079–86, 2003.

[163] F Taddei, M Viceconti, M Manfrini, and A Toni. Mechanical strength of a femoral reconstruction in paediatric oncology: a finite element study. *Proceedings of the Institution of Mechanical Engineers. Part H, Journal of Engineering in Medicine*, 217(2):111–9, 2003.

[164] K Tai, M Dao, S Suresh, A Palazoglu, and C Ortiz. Nanoscale heterogeneity promotes energy dissipation in bone. *Nature Materials*, 6(6):454–62, 2007.

[165] K Tai, FJ Ulm, and C Ortiz. Nanogranular origins of the strength of bone. *Nano Letters*, 6(11):2520–5, 2006.

[166] KF Taylor, B Rafiee, N Inoue, KA McHale, RS Howard, and EY Chao. Linear increase in axial stiffness of regenerate callus during limb lengthening. *Clinical Orthopaedics and Related Research*, (435):239–244, 2005.

[167] KF Taylor, B Rafiee, JE Tis, and N Inoue. Low-intensity pulsed ultrasound does not enhance distraction callus in a rabbit model. *Clinical Orthopaedics and related research*, 459:237–45, 2007.

[168] P Tracqui, A Broisat, J Toczek, N Mesnier, J Ohayon, and L Riou. Mapping elasticity moduli of atherosclerotic plaque in situ via atomic force microscopy. *Journal of Structural Biology*, 174(1):115–23, 2011.

[169] B Van Rietbergen, H Weinans, R Huiskes, and A Odgaard. A new method to determine trabecular bone elastic properties and loading using micromechanical finite-element models. *Journal of Biomechanics*, 28(1):69–81, 1995.

[170] B Vargas-Barreto, J Caton, Z Merabet, JC Panisset, and JP Pracros. Complications of Ilizarov leg lengthening: a comparative study between patients with leg length discrepancy and short stature. *International Orthopaedics*, 31(5):587–591, 2006.

[171] CR Verlinden, SE Van de Vijfeijken, DB Tuinzing, AG Becking, and GR Swennen. Complications of mandibular distraction osteogenesis for acquired deformities: a systematic review of the literature. *International Journal of Oral and Maxillofacial Surgery*, 44(8):956–64, 2015.

[172] NA Waanders, M Richards, H Steen, JL Kuhn, SA Goldstein, and JA Goulet. Evaluation of the mechanical environment during distraction osteogenesis. *Clinical Orthopaedics and Related Research*, (349):225–234, 1998.

[173] NA Waanders, LE Senunas, H Steen, JA Goulet, J Bonadio, and SA Goldstein. In *Proceedings of 40th Annual Meeting of the Orthopedic Research Society*, volume 40, pages 20–24. 1994.

[174] H Wagner. Operative beinverlangerung. *Chirurg.*, 42:260, 1971.

[175] WR Walsh, RC Hamdy, and MG Ehrlich. Biomechanical and physical properties of lengthened bone in a canine model. *Clinical Orthopaedics and Related Research*, (306):230–8, 1994.

[176] J Webb, G Herling, T Gardner, J Kenwright, and AH Simpson. Manual assessment of fracture stiffness. *Injury*, 27(5):319–320, 1996.

[177] J Wee, T Rahman, RE Akins, R Seliktar, DG Levine, DW Richardson, GR Dodge, AM Thabet, L Holmes, and WG Mackenzie. Using distraction forces to drive an autodistractor during limb lengthening. *Medical Engineering & Physics*, 33(8):1001–1007, 2011.

[178] SH White and J Kenwright. The timing of distraction of an osteotomy. *The Journal of Bone and Joint Surgery. British Volume*, 72(3):356–61, 1990.

[179] SH White and J Kenwright. The importance of delay in distraction of osteotomies. *The Orthopedic Clinics of North America*, 22(4):569–79, 1991.

[180] H Windhagen, H Bail, A Schmeling, S Kolbeck, A Weiler, and M Raschke. A new device to quantify regenerate torsional stiffness in distraction osteogenesis. *Journal of Biomechanics*, 32(8):857–860, 1999.

[181] H Windhagen, S Kolbeck, H Bail, A Schmeling, and M Raschke. Quantitative assessment of in vivo bone regeneration consolidation in distraction osteogenesis. *Journal of Orthopaedic Research*, 18(6):912–919, 2000.

[182] N Yasui, H Kojimoto, K Sasaki, A Kitada, H Shimizu, and Y Shimomura. Factors affecting callus distraction in limb lengthening. *Clinical Orthopaedics and Related Research*, (293):55–60, 1993.

[183] N Yasui, H Kojimoto, H Shimizu, and Y Shimomura. The effect of distraction upon bone, muscle, and periosteum. *The Orthopedic Clinics of North America*, 22(4):563–567, 1991.

[184] AS Younger. *The biomechanical properties of distraction callus created during Ilizarov tibial lengthening in sheep*. PhD thesis, Aberdeen University, 1997.

[185] AS Younger, WG Mackenzie, and JB Morrison. Femoral forces during limb lengthening in children. *Clinical Orthopaedics and Related Research*, (301):55–63, 1994.

[186] PA Yuya, EK Amborn, MW Beatty, and JA Turner. Evaluating anisotropic properties in the porcine temporomandibular joint disc using nanoindentation. *Annals of Biomedical Engineering*, 38(7):2428–37, 2010.

[187] H Zilch, A Rohlmann, G Bergmann, and R Kölbel. Material properties of femoral cancellous bone in axial loading. Part II: Time dependent properties. *Archives of Orthopaedic and Traumatic Surgery*, 97(4):257–62, 1980.

List of Figures

El vasto mundo: un grano de polvo en el espacio.
Toda la ciencia de los hombres: palabras.
Los pueblos, las bestias y las flores de los siete climas: sombras.
El resultado de tu meditación perpetua: nada.

Omar Khayyam